

**Computer Assisted Human Pharmacokinetics: Non-compartmental,  
Deconvolution, Physiologically Based, Intestinal Absorption, Non-Linear**

David G. Levitt, M.D., Ph. D.

Department of Physiology, University of Minnesota, Emeritus

[levit001@umn.edu](mailto:levit001@umn.edu)

May 12, 2017

## Table of Contents

1. Introduction, Physiologically Based Pharmacokinetics and PKQuest .....	5
1.1 Summary of the material covered in each book section.....	7
1.2 PKQuest Example: PBPK modeling of labeled water. ....	10
1.3 References .....	16
2. Compartment Modeling: Clearance and Volume of Distribution .....	17
2.1 Two-compartment models.....	19
2.2 Multicompartment, Mammillary models. ....	23
2.3 PKQuest Example: Human endogenous albumin pharmacokinetics. ....	24
2.4 References. ....	29
3. Non-compartmental PK: Steady state clearance ( $Cl_{ss}$ ), volume of distribution ( $V_{ss}$ ) and bioavailability. ....	30
3.1 Bioavailability, first pass metabolism. ....	32
3.2 PKQuest Example 1: Estimation of $Cl_{ss}$ and $V_{ss}$ for albumin. ....	34
3.3 PKQuest Example 2. Amoxicillin: comparison of non-compartmental and PBPK estimates of $V_{ss}$ and $Cl_{ss}$ .....	35
3.4 Exercise 1: Morphine-6-Glucuronide pharmacokinetics. ....	38
3.5 Derivation of the $Cl_{ss}$ relation. ....	42
3.6 Derivation of the $V_{ss}$ relation. ....	44
3.7 References .....	46
4. Physiologically based pharmacokinetics (PBPK): Tissue/blood partition coefficient; toxicological and other applications. ....	47
4.1 Tissue/blood ( $K_B^i$ ) or tissue/plasma ( $K_P^i$ ) solute partition coefficient. ....	50
4.2 Toxicological and other PBPK applications. ....	53
4.3 PBPK Software. ....	54
4.4 PKQuest Example: PBPK model for thiopental, a weak acid requiring input of tissue/partition ( $K_B^i$ ) parameters. ....	55
4.5 PKQuest Example: Rat PBPK model for antipyrine.....	56
4.6 PKQuest Example: PBPK model for Amoxicillin oral input.....	57
4.7 PKQuest Example: Amoxicillin PBPK model for 6 times/day oral dose. ....	59
4.8 References: .....	60
5. Extracellular Solutes: The pharmacokinetics of the interstitial space. ....	63

5.1	PKQuest Example: amoxicillin.....	65
5.2	References.....	66
6.	Capillary Permeability Limitation.....	67
6.1	PKQuest Example: Dicloxacillin, a highly protein bound, diffusion limited $\beta$ -lactam antibiotic.....	70
6.2	References.....	72
7.	Highly lipid soluble solutes (HLS): Pharmacokinetics of volatile anesthetics, persistent organic pollutants, cannabinoids, etc.....	73
7.1	Volatile anesthetics.....	77
7.2	PKQuest Example: Short term PK of volatile anesthetics.....	78
7.3	PKQuest Example: Adipose tissue perfusion heterogeneity and time dependent PBPK calculations.....	80
7.4	PKQuest Example: Cannabinol – Non-volatile highly lipid soluble solute.....	83
7.5	References.....	83
8.	Persistent organic pollutants (POP): why are they “persistent”?.....	85
8.1	POP metabolism limited kinetics.....	85
8.2	POP diffusion limited adipose tissue exchange.....	89
8.3	PKQuest Example: Determine the apparent rat adipose perfusion rate ( $F_{Ad}^{ap}$ ) and adipose/blood partition ( $K_B^{Ad}$ ) for POPs.....	92
8.4	References.....	94
9.	Deconvolution: a powerful, underutilized tool.....	96
9.1	PKQuest Example: Determination of nitrendipine absorption rate by deconvolution... ..	98
9.2	PKQuest Example: Fentanyl dermal patch.....	105
9.3	PKQuest Example: Amoxicillin.....	106
9.4	Exercise: Propranolol.....	108
9.5	References.....	109
10.	Intestinal absorption rate and permeability, the “Averaged Model” and first pass metabolism.....	110
10.1	Derivation of the “Averaged Model” (AM).....	111
10.2	Small intestinal permeability: correlation with $P_{oct/W}$ , Caco-2 monolayer permeability and fraction absorbed.....	115
10.3	PKQuest Example: Propranolol intestinal permeability.....	119

10.4	PKQuest Example: Acetaminophen – very rapid, unstirred layer limited, intestinal permeability. ....	121
10.5	PKQuest Example: Risedronate – very low permeability drug, absorption limited by small intestinal transit time. ....	123
10.6	PKQuest Example: Acetylcysteine – weak acid absorbed only in the proximal region of small intestine. ....	124
10.7	References. ....	126
11.	Non-linear pharmacokinetics - Ethanol first pass metabolism. ....	128
11.1	PKQuest Example: PBPK model of IV ethanol input. ....	134
11.2	PKQuest Example: PBPK model of oral ethanol in fasting subject. ....	135
11.3	PKQuest Example: PBPK model of oral ethanol with a meal. ....	136
11.4	References ....	137

## 1. Introduction, Physiologically Based Pharmacokinetics and PKQuest

Pharmacokinetics (PK) is defined as “The quantitative relationship between the administered doses and dosing regimens and the plasma and tissue concentrations of the drug.” That is, what is the time course of the drug in the blood and different tissues following one or multiple doses? The time course obviously depends on the site of the administration (intravenous, oral, subcutaneous, etc.) and one aspect of this subject is predicting, for example, the oral (i.e. intestinal) absorption rate of a drug.

Pharmacokinetics is the simplest and most focused branch of the general area of pharmaceutical science, which also includes pharmacodynamics (relationship between drug concentration and pharmacological effect), drug metabolism, toxicokinetics, and drug formulation. Pharmacokinetics is unique in that it is basically a mathematical and physical description of drug kinetics and, unlike nearly all other areas of medical science, is independent of the complex biochemical machinery. Because of this, it is a relatively self-contained mature subject that is not altered by the incredible pace of advances occurring in cellular medicine.

A unique aspect of this textbook is that it is closely integrated with the pharmacokinetic software program PKQuest. PKQuest is a freely distributed, Java based, program that provides detailed quantitative and graphical results for all the subjects discussed in this book. The program PKQuest, instructions for its installation and a large set of specific drug example files that are used in this book are available on the website [www.pkquest.com](http://www.pkquest.com). In addition, a detailed tutorial is provided that covers many of the examples discussed in this book. A great deal of effort has gone into the design of PKQuest to make it both user friendly and yet still be general enough to be applicable to most clinical pharmacokinetic questions. In addition to the numerical output, it has a flexible graphical output that is useful for illustrating the pharmacokinetic results. It is expected that the reader will download and install PKQuest and use it to follow the detailed examples that are provided in the text. This is an important component of the book. These PKQuest examples provide a more detailed and focused look at the topics covered in the different sections. In addition, and probably more important, familiarization with PKQuest and these example applications will allow the reader to apply PKQuest to their own research or clinical questions. The different PKQuest applications can be used as templates in which to substitute their own specific data. In addition, some exercises have been included that require the student to use PKQuest to answer specific questions.

An important aspect of PKQuest is its implementation of Physiologically Based Pharmacokinetic modeling (PBPK). In PBPK, the drug kinetics in each of the major organs of the body are directly modeled as shown in Figure 1-1 with each organ characterized by a set of parameters (blood flow, volume, protein binding, etc.). The set of differential equations describing each organ is then solved to determine each organ's drug concentration as a function

of time. For example, the venous concentration is simply equal to the drug concentration in the organ “vein”.

PBPK modeling is usually treated as a specialized advanced topic and is not even mentioned in some PK textbooks,. In this book, PBPK modeling is used heuristically even when discussing more standard simple approaches, such as compartmental modeling. Comparisons of the “exact” PBPK model with the simplifying assumptions of other models provide measures of their accuracy. Also, it is valuable for the student to understand how physiological factors such as fat or muscle blood flow (see example below) play important roles in determining the PK of drugs.

The complete PBPK model is characterized by 30 or more parameters (organ volumes, blood flows, serum and tissue protein binding, etc.) that, because they cannot be directly measured in the human, become, in effect, adjustable parameters. Since the actual human PK measurements can usually be accurately characterized by only 4 parameters (ie, two compartments, see Compartment Modeling), it is obvious that one cannot determine these 30 PBPK parameters simply by fitting the human PK data. A unique feature of PKQuest is that a “standard” resting human PBPK parameter set has been developed from the application of PKQuest to more than 100 different drugs with varying properties. For example, drugs with very high lipid solubility are used to determine the parameters of the human adipose tissues. The fact that the exact same set of standard parameters provides good fits to the PK of 100 drugs with markedly different properties gives one confidence in the validity of the parameters. It is a unique advantage of PKQuest that this standard parameter set is built in, allowing the user to ignore this aspect. (PKQuest also allows the option of changing these parameters, if necessary.) In applying the standard PBPK module of PKQuest to a specific PK data set, the user needs to first input the body weight and an estimate of the percent body fat (which can be estimated from the BMI). Then, there are some additional input parameters that specifically characterize the drug (e.g. lipid solubility, albumin binding). These will be discussed in detail in the chapters focused on the different drug classes.

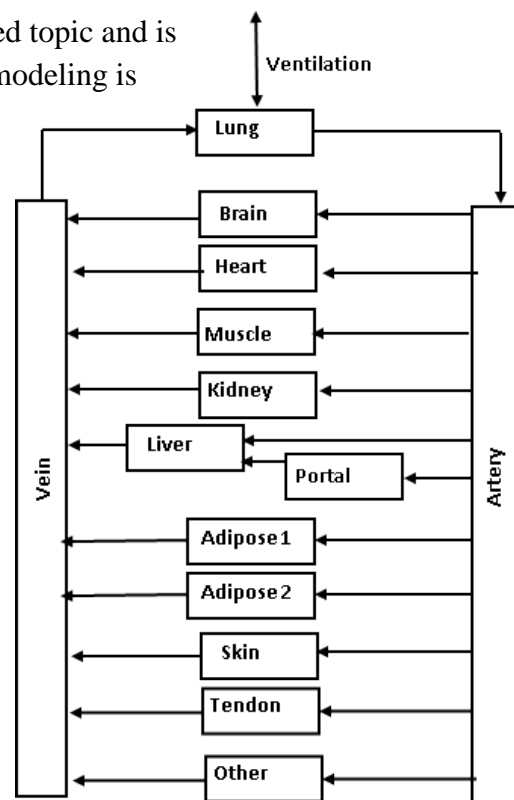


Figure 1-1

Pharmacokinetics is a subject that is highly weighted towards clinical applications and PK textbooks usually follow a standard format. After chapters covering the basic results, the focus turns to various clinical drugs and examples that are of interest to the author. This book is also idiosyncratic in that its focus is primarily on topics and publications in which PKQuest has been applied. However, as is illustrated in the following Summary, this is not that limiting and most of the important areas of PK are covered. The only major modern PK subject that is not

discussed is Population Based Pharmacokinetics since this has its own well developed proprietary software (NONMEM) [1]. In addition, while some textbooks combine PK with pharmacodynamics (PK/PD) [2], no pharmacodynamics applications will be discussed here.

### **1.1 Summary of the material covered in each book section.**

Each of the following Sections are relatively self-contained and can be read as independent topics, for example, as a supplement to material in a PK course. Some of the material is at a general introductory level that should be useful to a student with a limited background, while other material is more advanced and primarily of interest only to research investigators. In the following, a brief synopsis of each section is presented.

**Section 2. Compartment Modeling: Clearance and Volume of Distribution.** This provides a general introduction to the use of simple PK compartment modeling. It begins with an introductory level discussion of material that should be fundamental for anyone studying PK. This approach is then illustrated by a specific, and clinically important, PKQuest example of using a 2-compartment model to determine the human endogenous albumin synthesis rate and the total amount of albumin in the blood and whole body compartment. This example is highly quantitative and could be skipped by general readers.

**Section 3. Non-compartmental PK: Steady state clearance ( $Cl_{ss}$ ), volume of distribution ( $V_{ss}$ ) and bioavailability.** This section describes material that represents the essence of the subject of pharmacokinetics. The discussion is at a level that is somewhat more quantitative than the typical textbook with a focus on the assumptions required for the validity of the fundamental  $Cl_{ss}$  and  $V_{ss}$  relationships – areas that are skipped in some textbooks. For example, the  $V_{ss}$  relation is only strictly valid if the blood is sampled from the artery. A rigorous derivation of the  $Cl_{ss}$  and  $V_{ss}$  relations is also provided. Two examples using PKQuest to determine  $Cl_{ss}$  and  $V_{ss}$  with actual clinical data (albumin and amoxicillin) are discussed. These examples help to flesh out some of the subtleties and limitations of these relations and should be of value to the beginning student. The PKQuest example files also provide a template that allows the student to easily substitute their own PK data and determine  $Cl_{ss}$  and  $V_{ss}$ . The amoxicillin example uses a PBPK model to estimate the error in the  $V_{ss}$  estimate if the antecubital vein is used as the sample site versus arterial sampling (the theoretically required sample site). The section concludes with a detailed, step by step exercise for determining the PK of morphine-6-glucuronide. It emphasizes the practical problems that are presented when using real clinical data that has limited precision.

**Section 4. Physiologically based pharmacokinetics (PBPK): Tissue/blood partition coefficient; toxicological and other applications.** This section provides a general introduction to the PBPK modeling approach. It describes the mathematical blood/tissue exchange model, its assumptions, and how the body tissue organs are combined to produce a complete whole animal model. It directs special attention to the difficult problem of accurately estimating the tissue/blood partition coefficient ( $K_B$ ) and how this limits the applicability of the PBPK approach

for the great majority of drugs that are weak acids or bases with partition coefficients that cannot be accurately predicted, a priori. There are two drug classes that are exceptions to this rule: the extracellular solutes and the highly lipid soluble solutes. The  $K_B$  for these two classes can be predicted a priori and their PBPK analyses are described in separate sections. It provides a brief overview of the PBPK software routines that are available. This material does not require any special background and it is intended to provide students an introduction to the PBPK modeling approach and its strengths and weaknesses. These concepts are then illustrated with 4 specific PBPK examples using PKQuest that cover the gamut of experimental situations that students might face: Example 1) PBPK modeling of human thiopental PK, a weak acid that requires input of previous measurements (rat) of the  $K_B$  of each of the PBPK model organs. Example 2) PBPK model of rat antipyrine PK. Although the focus in this book is on human PK, this example describes the modifications required to apply PKQuest to non-humans. Example 3) Describes how the user can model the intestinal input to a PBPK model, in this case, for amoxicillin. Example 4) Once a PBPK model is developed, one can determine blood concentrations for arbitrary inputs, in this case, oral amoxicillin, 3 times/day.

**Section 5. Extracellular Solutes: The pharmacokinetics of the interstitial space.** Because this drug class cannot enter cells, the primary tissue binding that determines the tissue/blood partition coefficient ( $K_B$ ) is the binding to interstitial and plasma albumin. Since this can be directly predicted from the known interstitial and plasma albumin concentrations and the drug albumin binding constant (determined from the plasma “free fraction”), its  $K_B$  can be accurately predicted. Thus, the PK of this drug class can be accurately modeled using the PBPK approach with only one or two adjustable parameters. This section begins with a brief review of the PK of extracellular drugs, including a table summarizing the extracellular volume and albumin concentration of the different organs. It ends with a PKQuest example describing the PBPK modeling of amoxicillin.

**Section 6. Capillary Permeability Limitation.** This is a specialized topic that is probably not of interest to introductory students. It focuses on a subject that is almost never discussed in PK textbooks: the capillary permeability limitation of tissue/blood exchange. The section begins with a discussion of the highly protein (albumin) bound extracellular solutes and describes why they are permeability limited. It ends with a PKQuest PBPK example for Dicloxacillin, using human PK data, quantifying the permeability limitation and its clinical importance.

**Section 7. Highly lipid soluble solutes (HLS): Pharmacokinetics of volatile anesthetics, persistent organic pollutants, cannabinoids, etc.** This is the other drug class for which the tissue/blood partition coefficient ( $K_B$ ) can be predicted from first principles, allowing successful PBPK modeling with a minimum of adjustable parameters. The  $K_B$  of these drugs is dominated by the tissue/blood lipid partition, which can be predicted from measurements of tissue and blood lipid and the drug’s oil/water partition ( $P_{L/W}$ ). The section describes how PKQuest can be used to accurately describe human volatile anesthetics PK, with **no** adjustable parameters (their clearance can be predicted from alveolar ventilation). This discussion of how the PK of



anesthetics can be predicted just using their water/air, olive oil/air, and blood/air partition coefficients should be of particular interest to students with an interest in these drugs (eg, nurse anesthetists, anesthesiology fellows, etc.). This PBPK method is both more general and more accurate with fewer adjustable parameters than the compartmental modeling approach that is the standard in the anesthesiology field. Since the PBPK model depends crucially on the value(s) of the adipose blood flow, special attention is devoted to describing how PKQuest was used to determine what is, currently, the best available measurement of the heterogeneity of human adipose blood flow. The section ends with three PKQuest examples: Example 1) the short term (3 hours) human PK of isoflurane, sevoflurane and desflurane. Example 2) the long term (5 days) human PK of isoflurane, sevoflurane and desflurane. During these long term experimental measurements, the PBPK parameters change as the patients wake up from the anesthesia and become ambulatory, and this section describes how PKQuest can be used to accommodate changing parameters. Example 3) applies this same model to cannabiniol, a non-volatile, highly lipid soluble drug.

**Section 8. Persistent organic pollutants (POP): why are they “persistent”?** The POPs (eg, dioxins, PCBs, DDT) represent a special class of the highly lipid soluble drugs discussed in the previous section. They are of interest to students in a large range of fields and most of this section is written at a general introductory level. Pharmacokinetic modeling and prediction is especially important for these compounds because experimental human PK measurements are limited because of their long lifetimes (years). For such an important drug class, there is a surprising lack of coverage in the standard PK textbook and what is available is inaccurate. This section looks in detail at the question of why these POPs have such long lifetimes? It explains that the usual explanation (high lipid partition) is incorrect and, instead, it results simply from their very low metabolic rates. There is a detailed PKQuest example illustrating that, as the metabolic rate falls to very low values, the human PK can be accurately described by a simple 1-compartment model characterized just by its volume and clearance and the details of the peripheral PBPK tissue-blood exchange become irrelevant. There is also a PKQuest example that describes in detail the quantitative measurement of the previously unrecognized adipose/blood diffusion limitation that develops for the POPs with very high lipid partition. This last example is of interest only for a limited set of investigators.

**Section 9. Deconvolution: a powerful, underutilized tool.** Deconvolution is a general PK approach that is discussed only briefly in most PK textbooks. It provides, for most drugs, the best approach for quantitating PK inputs such as the intestinal absorption of oral drugs or from dermal patches. Most of this section could serve as a stand-alone introduction to this topic. The most limiting aspect of the subject is that, without the appropriate software, it has no practical value. PKQuest has been designed to make deconvolution simple and versatile, with 6 different deconvolution routines that can be selected. The strengths and weaknesses of the different routines are explained and illustrated with three PKQuest examples using clinical human PK data (oral absorption of amoxicillin and nitrendipine and fentanyl absorption from a dermal patch). It

ends with an exercise that takes the student through the individual steps for determining the intestinal absorption of propranolol.

**Section 10. Intestinal absorption rate and permeability, the “Averaged Model” and first pass metabolism.** This section describes a specialized application of the deconvolution technique that provides a direct estimate of the human intestinal epithelial permeability of drugs. It uses a new approach (“Averaged model”) that I recently developed and applied to 90 drugs with a wide range of PK properties.[3] The first part of this section is focused on the details of the “Averaged model” approach, and could be skipped by most students. However, the remainder of this section discusses a large range of topics related to intestinal absorption (bioavailability, first pass metabolism, mucosal permeability, dependence on octanol/water partition, caco-2 monolayer measurements, etc.) that could serve as an in depth introduction to intestinal drug absorption. It concludes with four PKQuest examples that illustrate different aspects of intestinal absorption: Example 1) Propranolol, a drug with a very high first pass metabolism. Example 2) Acetaminophen, a drug with a very high absorption rate that is limited by luminal unstirred layer diffusion. Example 3) Risedronate, a drug with a very low absorption rate that is limited by the small intestinal transit time. Example 4) Acetylcysteine, a weak acid that is absorbed only in the proximal small intestine which has relatively acid pH.

**Section 11. Non-linear pharmacokinetics - Ethanol first pass metabolism.** Although this is a topic that is rarely addressed in PK textbooks, students should be aware of the importance of the standard, and usually unrecognized, assumption that the PK are linear. This is dramatically illustrated by the set of publications by Lieber and colleagues that they interpreted as indicating that there was a large first pass gastric ethanol metabolism that was clinically important in determining human blood alcohol levels and was widely covered by the popular press. In fact, as was first pointed out by Levitt and Levitt [4], gastric ethanol metabolism is negligible and this conclusion is an artifact of erroneously assuming that ethanol PK is linear. The classical PK clearance is not a valid descriptor of the PK if it is non-linear. PBPK modeling is probably the best approach for handling this situation, allowing direct modeling of the nonlinearity. This section focuses on the concept of “bioavailability” (the main emphasis of Lieber and colleagues) and illustrates that the usual definition is not applicable to the non-linear situation. A new and rigorous definition of the non-linear bioavailability has been implemented in PKQuest and applied to oral ethanol.[5] The first part of this section provides a general introduction to non-linear PK that should be of interest to students. The four PKQuest examples provide detailed analyses of human experimental ethanol PK and are of interest primarily to investigators with a specific concern with ethanol.

## 1.2 PKQuest Example: PBPK modeling of labeled water.

The PBPK of labeled water ( $D_2O$ ) will be discussed here to provide an introduction to the PKQuest interface and its value as a teaching tool.  $D_2O$  is the “drug” with the simplest possible

PK since it simply distributes freely in the body water, is not metabolized and its excretion rate is negligible for the time course of most kinetic studies. For PBPK modeling, one only needs to know the organ blood flows and water volumes. It is assumed that the reader has now installed PKQuest. **(This is an essential aspect of this textbook)**. A D<sub>2</sub>O PK study is the default background program in PKQuest that is performed when no other PK drug files are specified. Start PKQuest (double click pkquest.jar). One should see the following window open (Figure 1-2). (Note: one limitation of the current version of PKQuest is that it does not adjust to the computer screen size and cannot be used on small laptops).

PKQuest (Copyright David G. Levitt, 2008)

---

**Model Parameters**

Weight  Fat fr

☐ Liver Fr. Clear  ☐ Vm or Intrinsic clr  ☐ Km  ☐ Renal Clr

☐ Extracellular Plasma fr. free  ECF  Cap perm

☐ Volatile Kbair  Kwair  Kfwat  Blood fat fr

Vent  Vol  Perf/vent stdF  stdV

☐ Fat/water partition Kfwat  free plasma fr  Blood fat fr

☐ Partition Bld/plasma   freepl  Bind C  Scatch

---

**Input**

☐ Amount u...  ☐ Find In...

---

**Non-compartment PK; Deconvolution; Experimental Blood Conc**

☐ NonPK ☐ Fit Vein ☐ Const N Exp  Wt

☐ Deconvolution  Est. Dose  Method

Smoothing  FitTime  Lag Time   Tgi

---

**Plot**

☒ Absolute

☐ FreeWat   ☐ Semilog

**Time Dependent**

☐ Time Dep...

---

**Minimize**

Comments

Title

Figure 1-2

This default module is used for the PBPK modeling of the Schloerb et. al. [6] experimental arterial D<sub>2</sub>O PK results (reference details in the “Comments” block of PKQuest). The experimental results are for subject JO following a 15 second IV injection of 69 ml of D<sub>2</sub>O. This example illustrates the parameters that are required to specify any PK study, even one with this simplicity. The top section of the PKQuest module (Figure 1-2) specifies the PBPK model parameters. For this case only the weight of subject JO and estimated fat fraction are required and the other checkboxes are not required. Their use will be explained and illustrated in later examples. The second section specifies the details of the drug input. **In PKQuest, the time is**

**always in minutes, the volume in liters and the weight in kg.** The amount unit is arbitrary and is specified by the input string in the “Amount unit” box. This string is only used in the plots and does not affect the calculations. In the Schloerb et. al. experiment, the arterial concentration was measured in units of vol% of D<sub>2</sub>O in the blood water and, since the volume must be in liters, this corresponds to a concentration of “centiliters” per liter. The “N input” box specifies the number of inputs, which in this case is 1. Clicking the “Regimen” button opens a table specifying the details of each input. In this case it is a constant input (“Type”=1) of a total amount of 6.9 centiliters D<sub>2</sub>O starting at time = 0 and ending at time = 0.25 minutes (=15 sec) into the vein (“Site” = 0). (The other two boxes (“N Hill” and “Duration” are ignored for a constant input). The third section (“Non-compartment PK”) is ignored for this example. The fourth section (“Plot”) specifies the plotting and the experimental data. Clicking the “Organs” button opens a table specifying the organs that are plotted and their concentration units. In this case only the “artery” is plotted with units of amount/liter of arterial blood water (“Conc. Unit” = 3, and amount in centiliters). The “Exp S...” box specifies the number of experimental data sets plotted which in this case is 1. Clicking the “Exp Data 1” button opens a table in which the Schloerb et. al. experimental **arterial** D<sub>2</sub>O concentration measurement (in units of vol% = centiliter/liter) are input. The “Absolute” and “Semilog” radio buttons specify whether the plot is semilog or absolute. The “Start” and “End” inputs specify the time of the output plot. This completes the characterization of this D<sub>2</sub>O PBPK model.

It may seem a little off putting that all of these details must be input just to specify this simple example. One of the main advantages of PBPK analysis is that one is directly confronted with what is required to correctly describe a PK experiment. The details of the input (total amount, time course, etc.), the concentration units and whether it is the concentration, eg, in whole blood, or plasma or blood water, are essential features of any experiment.

If one clicks the “Run” button in the PKQuest module one gets the following graphical output (Figure 1-3).

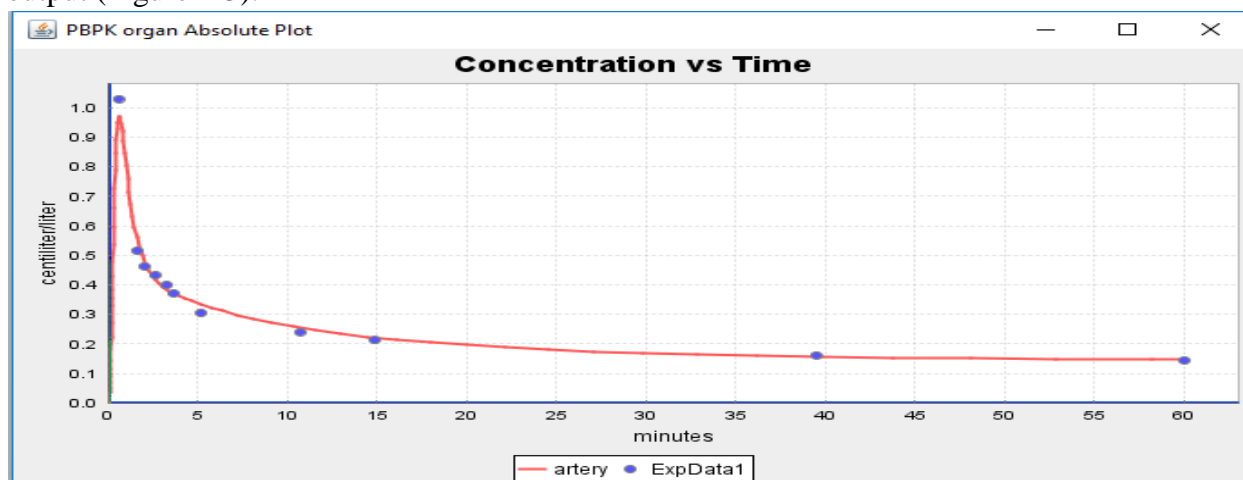


Figure 1-3

It shows a plot of the PBPK D<sub>2</sub>O arterial concentration (red line) vs the experimental arterial measurements (blue solid circles) of Schloerb et. al. This is the type of physiological data that is used to determine the PBPK model parameters. The equilibrium D<sub>2</sub>O concentration at long time provides a direct measurement of the dilution volume of the injected D<sub>2</sub>O, i.e. the total human water volume. The time course of the arterial concentration (red line), although influenced by all the PBPK parameters, is dominated by the muscle blood flow because it has such a large water volume and relatively low resting blood flow. This can be illustrated by observing the change in the D<sub>2</sub>O kinetics with changes in the muscle blood flow. Clicking the “Organ Par” button opens a table listing the adjustable PBPK organ parameters. The values in this table are those for the **Standard 70 kg, 21% fat subject**. They are adjusted for the “Weight” and “Fat fr” that are input for the specific run. Note that the standard muscle “Perfusion” rate is 0.0225 lit/min/kg. Change the muscle perfusion to half this value (0.0112) and clicking “Run” again yields Figure 1-4 in which the arterial concentration decays more slowly than the experimental data. PKQuest has an option that automatically finds the optimal organ blood flow. Click on the “Parameters” button in the “Minimize” module at the bottom of the PKQuest screen and then check the “muscle” “flow” box in the “Parameter Adjusted” table and “Run” PKQuest again. After finding the muscle perfusion rate that provides the best fit to the experimental data, the new plot is output.

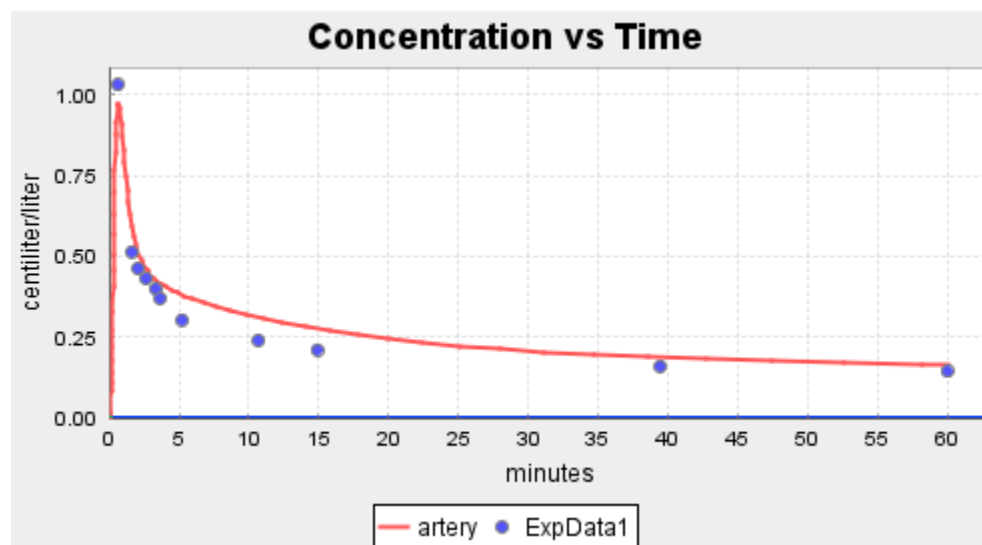


Figure 1-4 D<sub>2</sub>O PBPK model results for muscle blood flow of half normal.

Close PKQuest (click on the “X” in upper left) and rerun again to get the standard PBPK model. Click on the “Organs” button in the “Plot” section and check the “muscle” and “antecubital” button. Note that the default “Conc Unit” for muscle (=5) is “F/liter tissue water” where “F = free (unbound) amount”. For D<sub>2</sub>O which, by definition, is unbound, “Conc Unit” 3 and 5 are identical. Rerun PKQuest, getting the output shown in Figure 1-5.

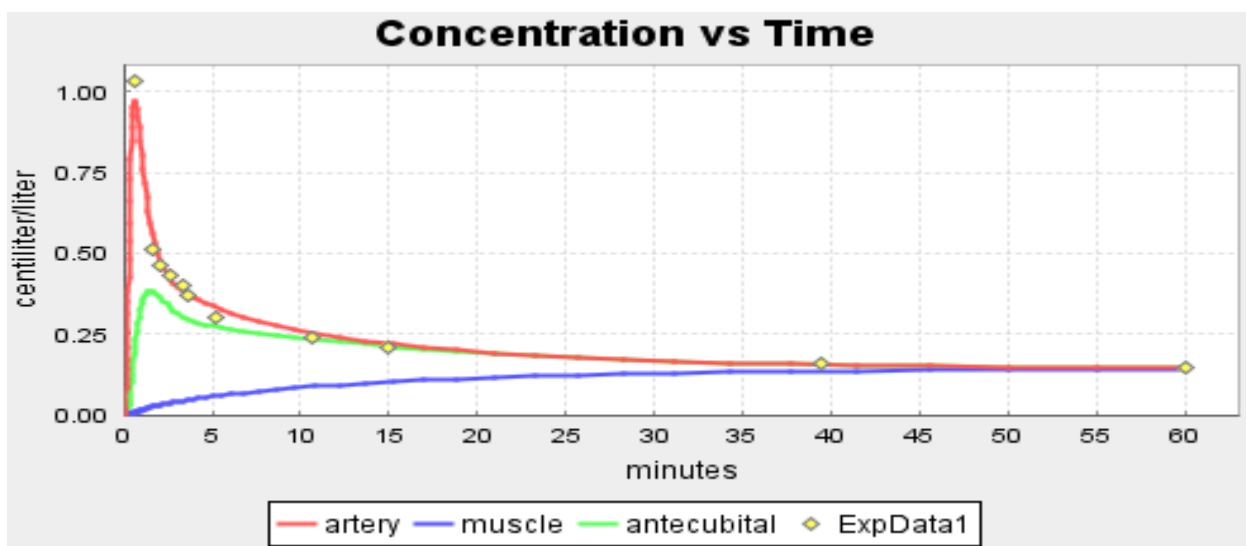


Figure 1-5 PKQuest PBPK mode I of D<sub>2</sub>O concentration in artery (red), antecubital (green) and muscle tissue water (blue).

The slow rise of the muscle D<sub>2</sub>O water concentration (blue line) to the equilibrium arterial concentration is the primary factor determining the arterial kinetics. Of particular interest is the green line, which is the concentration for blood sampled from the antecubital vein ( $C_{ac}$ ). The antecubital vein is dominated by blood draining the hand and forearm and the  $C_{ac}$  at early times differs markedly from the arterial or central venous concentrations. Although this is not widely recognized, it is important because the antecubital vein is the sample site in the great majority of PK studies. This ability to output the antecubital vein concentration is a novel feature that was first developed for PKQuest [7].

This completes the initial introduction to PKQuest. It is hoped that this example has convinced the reader of the potential value of PKQuest as a tool in understanding pharmacokinetics. Only a few of PKQuest’s features were used here and subsequent chapters will elucidate many more useful qualities. When the reader has finished this book, he/she should be fluent in the use of PKQuest as an aid in addressing most PK questions and be able to apply it to his/her own problems. There is an inherent tension in the use of software tools such as PKQuest between the ability to “calculate” a result versus an in depth understanding of the equations and ideas underlying the calculation. This is addressed in this book by providing a rigorous

description of the underlying theory. In particular, more attention is paid to the assumptions and limitations of theoretical PK concepts (e.g. volume of distribution, clearance, etc.) than the typical PK textbook. However, even the simplest situations can be computationally complex and there seems little benefit for the student to reinvent, for example using Matlab, numerical solutions that are already available in PKQuest (or other PK software packages).

### 1.3 References

1. Owen JS, Fiedler-Kelly J: **Introduction to population pharmacokinetic/pharmacodynamic analysis with nonlinear mixed effects models.** Hoboken, New Jersey: John Wiley & Sons; 2014.
2. Gabrielsson J, Weiner D: **Pharmacokinetic and Pharmacodynamic Data Analysis: Concepts and Applications, Fourth Edition:** Taylor & Francis; 2007.
3. Levitt DG: **Quantitation of small intestinal permeability during normal human drug absorption.** *BMC Pharmacol Toxicol* 2013, **14**:34.
4. Levitt MD, Levitt DG: **The critical role of the rate of ethanol absorption in the interpretation of studies purporting to demonstrate gastric metabolism of ethanol.** *J Pharmacol Exp Ther* 1994, **269**(1):297-304.
5. Levitt DG: **PKQuest: measurement of intestinal absorption and first pass metabolism - application to human ethanol pharmacokinetics.** *BMC Clin Pharmacol* 2002, **2**:4.
6. Schloerb PR, Friis-Hansen BJ, Edelman IS, Solomon AK, Moore FD: **The measurement of total body water in the human subject by deuterium oxide dilution; with a consideration of the dynamics of deuterium distribution.** *J Clin Invest* 1950, **29**(10):1296-1310.
7. Levitt DG: **Physiologically based pharmacokinetic modeling of arterial - antecubital vein concentration difference.** *BMC Clin Pharmacol* 2004, **4**:2.



## 2. Compartment Modeling: Clearance and Volume of Distribution

Historically, compartmental models were the original approach to PK analysis and, although this approach has been partially supplanted by non-compartment modeling (see Section 3), it is still important and should be regarded as basic required PK background material. The simplest one compartment model (Figure 2-1) introduces the fundamental PK concepts of “clearance” and “volume of distribution”.

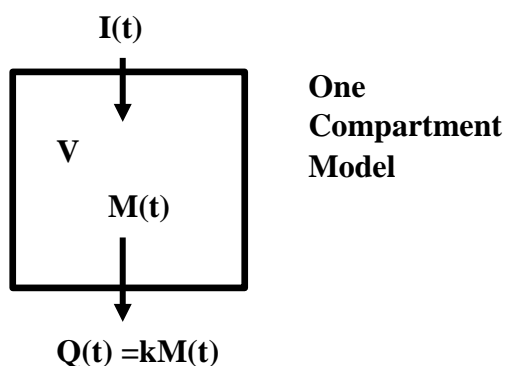


**Figure 2-1**

$I(t)$  is the time dependent input to the compartment and  $M(t)$  is the total amount of solute in the compartment. The solute leaves the compartment (e.g., excreted, metabolized) at rate  $Q(t)$  that is proportional to  $M(t)$  with a rate constant  $k$ . Experimentally, one cannot directly measure  $M(t)$ , but only the concentration  $C(t)$  in some sample of the compartment. Thus, one needs to add an auxiliary derived parameter  $V$ , the volume or “volume of distribution” of the compartment, which is defined as:

$$(2.1) \quad V = M(t) / C(t)$$

It is important to recognize that  $V$  depends on the definition of the concentration  $C$ . For example, suppose that the one compartment corresponds to the total blood volume and that the solute is dissolved in the blood water and also binds to the red cells and plasma albumin, and the solute distribute rapidly between these different components. One could define, at least, 3 different concentrations: 1) the unbound water concentration  $C_W(t)$ ; 2) the plasma concentration  $C_P(t)$  which includes albumin bound solute; and 3) the whole blood concentration  $C_B(t)$ . These concentrations would then define 3 different volumes ( $V_W$ ,  $V_P$ ,  $V_B$ ):

$$(2.2) \quad M(t) = V_W C_W(t) = V_P C_P(t) = V_B C_B(t)$$

Only  $V_B$  would correspond to the actual physical volume of the blood compartment. If the drug was tightly bound to albumin so that only 1% of the total solute was free in the water ( $C_W = 0.01 C_B$ ),  $V_W$  would be 100 times larger than  $V_B$ .

The other derived parameter, the clearance (Cl), also depends on the definition of the concentration:

$$(2.3) \quad \begin{aligned} \text{Excretion Rate} &= Q(t) = Cl C(t) \\ \text{Clearance} = Cl &= Q(t) / C(t) = kM(t) / C(t) = kV \end{aligned}$$

The clearance corresponds to the volume that is cleared of solute per unit time and has units in PKQuest of liters/minute. It also depends on the definition of the concentration. For example, at steady state after a long time constant input  $I_{ss}$ , the input equals the excretion rate and one has the following relationship between the “Whole Blood” clearance ( $Cl_{WB}$ ) and “Plasma” clearance ( $Cl_P$ ):

$$(2.4) \quad I_{ss} = \text{Excretion Rate} = Cl_P C_P(t) = Cl_{WB} C_{WB}(t)$$

The plasma concentration (obtained by centrifuging down the red cells) is the standard concentration that is used in most PK measurements, although the whole blood concentration is occasionally used. The “serum” concentration, obtained after removal of the coagulated component, is, in most cases identical to the plasma concentration.

For the special case where the input  $I(t)$  in Figure 2-1 is an instantaneous bolus input of amount  $D$  at  $t=0$ , the time course is described by the differential equation:

$$(2.5) \quad \frac{dC(t)}{dt} = -k C(t) \quad C(t=0) = C_0 = D/V$$

which has the solution:

$$(2.6) \quad C(t) = C_0 e^{-kt}$$

This can be expressed in terms of the volume of distribution and clearance:

$$(2.7) \quad C(t) = (D/V) e^{-(Cl/V)t}$$

The most elegant approach to handling the case of an arbitrary input  $I(t)$  is via the concept of convolution, which will be introduced here and used in subsequent chapters. One can approximate  $I(t)$  as a series of infinitesimal bolus inputs of varying amounts at continuous time points, with each input producing expressions of the form of eq. (2.6) with the total result the sum of these expressions. This leads to the following mathematical relationship:

$$(2.8) \quad C(t) = \int_0^t I(\tau) h(t-\tau) d\tau = \int_0^t I(t-\tau) h(\tau) d\tau$$

where  $h(t)$  is the “system unit response function” defined as the response of the system to a bolus input of a dose  $D = 1$ . For the 1-compartment model, with  $D=1$  in eq. (2.6):

$$(2.9) \quad h(t) = (1/V) e^{-kt}$$

A fundamental assumption of eq. (2.8) is that the system is linear. There is a simple experimental test of linearity: a) input dose  $D$  and measure the response; b) input dose  $2 \times D$  - if the response is exactly twice that of the  $1 D$  dose, then the system is linear. Whatever system you are studying, this should be the first question you ask. If it is non-linear, then the classic concepts of clearance and volume of distribution breakdown. The PK of the vast majority of clinically important drugs are linear. Investigators are so accustomed to the drugs with linear PK that, when faced with a non-linear drug, confusion can result. This will be illustrated in Section 11 which focuses on ethanol PK, a classic example of a non-linear solute.

A typical PK input is a constant infusion (rate=  $R_{in}$ ) for a finite time  $T_{in}$ :

$$(2.10) \quad \begin{aligned} I(t) &= R_{in} & 0 \leq t \leq T_{in} \\ &= 0 & t > T_{in} \end{aligned}$$

Substituting eq. (2.10) into eq. (2.8) and using eq. (2.9) for  $h(t)$ :

$$(2.11) \quad \begin{aligned} C(t) &= (R_{in}/V) \int_0^t e^{-k(t-\tau)} d\tau & t \leq T_{in} \\ &= (R_{in}/V) \int_0^{T_{in}} e^{-k(t-\tau)} d\tau & t > T_{in} \end{aligned}$$

Integrating:

$$(2.12) \quad \begin{aligned} C(t) &= \frac{R_{in}}{kV} (1 - e^{-kt}) & t \leq T_{in} \\ &= \frac{R_{in}}{kV} (e^{kT_{in}} - 1) e^{-kt} & t > T_{in} \end{aligned}$$

## 2.1 Two-compartment models.

There are two limiting 2-compartment cases, differing in the site of metabolism or excretion (Figure 2-2).

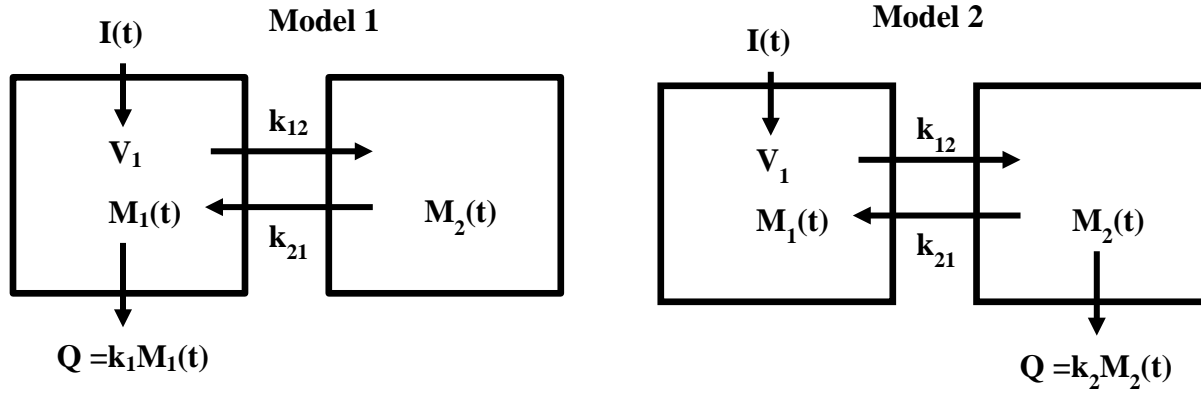


Figure 2-2 Two different 2-compartment models, differing in the site of excretion.

Compartment 1, which receives the input  $I(t)$  is referred to as the “central” (e.g. blood) compartment, while compartment 2 is the “peripheral” or tissue compartment. Model 1 is described by the following two differential equations:

$$(2.13) \quad \begin{aligned} \frac{dM_1}{dt} &= I_1(t) + k_{21}M_2 - k_1M_1 - k_{12}M_1 \\ \frac{dM_2}{dt} &= k_{12}M_1 - k_{21}M_2 \end{aligned}$$

Solving eq. (2.13) for the case where  $I(t)$  is a bolus input of amount  $D$ :

$$(2.14) \quad \begin{aligned} \text{Model 1:} \\ M_1(t) / D &= A_1 e^{-a_1 t} + A_2 e^{-a_2 t} \\ A_1 &= (B - k_1 - k_{12} + k_{21}) / (2B) \quad A_2 = (B + k_1 + k_{12} - k_{21}) / (2B) \\ a_1 &= (k_1 + k_{12} + k_{21} - B) / 2 \quad a_2 = (k_1 + k_{12} + k_{21} + B) / 2 \\ B &= \sqrt{k_1^2 + 2k_1k_{12} - 2k_1k_{21} + k_{12}^2 + 2k_{12}k_{21} + k_{21}^2} \end{aligned}$$

The corresponding differential equation and solution for Model 2 is:

$$(2.15) \quad \begin{aligned} \frac{dM_1}{dt} &= I_1(t) + k_{21}M_2 - k_{12}M_1 \\ \frac{dM_2}{dt} &= k_{12}M_1 - k_{21}M_2 - k_2M_2 \end{aligned}$$

*Model 2 :*

$$\begin{aligned}
 (2.16) \quad & M_1(t) / D = A_1 e^{-a_1 t} + A_2 e^{-a_2 t} \\
 & A_1 = [1/2 + (k_2 + k_{21} - k_{12}) / (2B)] \quad A_2 = [(1/2 + (k_{12} - k_{21} - k_2) / (2B)] \\
 & a_1 = (k_2 + k_{12} + k_{21} - B) / 2 \quad a_2 = (k_2 + k_{12} + k_{21} + B) / 2 \\
 & B = \sqrt{k_2^2 + 2k_2 k_{21} - 2k_2 k_{12} + k_{12}^2 + 2k_{12} k_{21} + k_{21}^2}
 \end{aligned}$$

In order to relate  $M_1(t)$  to the experimentally measured concentration  $C_1(t)$  it is necessary to define the parameter  $V_1$ :

$$\begin{aligned}
 (2.17) \quad & C_1(t) = M_1(t) / V_1 = (D / V_1)(A_1 e^{-a_1 t} + A_2 e^{-a_2 t}) \\
 & = A e^{-\alpha t} + B e^{-\beta t}
 \end{aligned}$$

where in the second line  $C_1(t)$  has been written as the sum of two exponentials using the conventional notation.

The two compartmental model is characterized by the two time dependent functions  $C_1(t)$  ( $=M_1(t)/V_1$ ) and  $M_2(t)$  and the four parameters ( $V_1$ ,  $k_1$ ,  $k_{12}$  and  $k_{21}$ ). There is another parameter convention that, in place of  $M_2(t)$  uses  $C_2(t)$  and a corresponding volume  $V_2 = M_2(t)/C_2(t)$  where  $C_2(t)$  and  $V_2$  are defined by the condition that if excretion is turned off ( $k_1=0$ ) (ie, equilibrium) the following condition is required:

$$\begin{aligned}
 (2.18) \quad & \text{At equilibrium: } C_1 = C_2 = C \text{ and } k_{12} M_1 = k_{21} M_2 \\
 & \Rightarrow k_{12} C V_1 = k_{21} C V_2 \Rightarrow V_2 = \frac{k_{12}}{k_{21}} V_1 \\
 & \Rightarrow k_{12} V_1 = k_{21} V_2 = Cl_d
 \end{aligned}$$

where  $Cl_d$  is the clearance for the intercompartmental exchange. For example, if the rate of exchange between the two compartments is by passive diffusion ( $J = PS(C_1 - C_2)$ ) where  $PS$  is the permeability surface area product, then  $Cl_d = PS$ . Using this alternative convention, the 2 compartment model time dependent functions  $C_1(t)$  and  $C_2(t)$  are characterized by the 4 parameters:  $V_1$ ,  $V_2 (=k_{12} V_1 / k_{21})$ ,  $Cl_1 (=k_1 V_1)$  and  $Cl_d (=k_{12} V_1)$ .

For multicompartmental models, one can extend the above one compartmental definition of clearance:

$$\begin{aligned}
 (2.19) \quad & \text{Total Clearance} = Cl = Q(t) / C_1(t) \\
 & = k_1 V_1 \quad \text{for Model 1} \\
 & = k_2 M_2(t) / C_1(t) = k_2 V_2 C_2(t) / C_1(t) \quad \text{for Model 2}
 \end{aligned}$$

It can be seen from eq. (2.19) that the clearance does not depend on time for Model 1. This is also true for the general case of an arbitrary number of compartments as long as the clearance (ie,

metabolism) is from the central compartment. For this case (clearance constant, not time dependent), for an arbitray input  $I(t)$  of dose  $D$ :

$$(2.20) \quad D = \int_0^{\infty} Q(t) dt = \int_0^{\infty} Cl C_1(t) dt = Cl \int_0^{\infty} C_1(t) dt$$

$$Cl = D / \int_0^{\infty} C_1(t) dt$$

The last expression provides a simple, direct and nearly universally used experimental definition of clearance. It will be shown in Section 3 that a slight variation on this relation is valid even if the solute is metabolized in a peripheral compartment and is time dependent.

One can define a total system “volume of distribution” as an extension of the one compartment volume:

$$(2.21) \quad \text{Volume of distribution} = V = (M_1(t) + M_2(t)) / C_1(t)$$

$$= V_1 + V_2 C_2(t) / C_1(t)$$

For both model 1 and 2 the volume of distribution is time dependent and, therefore, is not a useful PK parameter. One possiblity is to use the “Equililbruim Volume of Distribution” defined by turning off the metabolism ( $k_1=0$  for Model 1 or  $k_2=0$  for Model 2) and determining the total volume of distribution of a dose  $D$  after the system has come to equilibrium. Since there is no excretion,  $D$  is equal to the total amount in the system ( $=M_1 + M_2$ ):

$$(2.22) \quad V_{eq} = D / C_{eq} = (M_1 + M_2) / C_{eq} = \frac{M_1}{C_{eq}} (1 + \frac{k_{12}}{k_{21}})$$

$$= V_1 (1 + \frac{k_{12}}{k_{21}})$$

where  $k_{12}/k_{21}$  is relation between  $M_1$  and  $M_2$  at equilibrium ( $dM/dt=0$ ; eq. (2.13)).

Although in some animal studies it is possible to approximate the equilibrium situation by, for example, nephrectomy for a solute that is only excreted by the kidney,  $V_{eq}$  is usually not a useful PK paramers. A better descriptor is the “steady state” clearance ( $Cl_{ss}$ ) and volume of distribution ( $V_{ss}$ ):

$$(2.23) \quad Cl_{ss} = Q_{ss} / C_1^{ss} = I_{ss} / C_1^{ss}$$

$$V_{ss} = (M_1^{ss} + M_2^{ss}) / C_1^{ss}$$

where “ss” referes to the concentration after a steady state is established, e.g., at long times after a constant infusion ( $I(t) = I_{ss}$ ). (In the steady state, the excretion rate  $Q$  equals the infusion rate  $I_{ss}$ ). For model 1, the clearance is, in general, time independent so that, from eq. (2.19):

$$(2.24) \quad Cl_{ss} = Cl = k_1 V_1$$

For Model 1, from the second equation in eq. (2.13), at steady state ( $dM_1/dt=0$ ):

$$(2.25) \quad M_2^{ss} = (k_{12} / k_{21}) M_1^{ss}$$

Thus, from eq.(2.23), for Model 1:

$$(2.26) \quad V_{ss} = M_1^{ss} (1 + k_{12} / k_{21}) / C_1^{ss} = V_1 (1 + k_{12} / k_{21}) = V_{eq}$$

For Model 1,  $V_{ss} = V_{eq}$  (eq.(2.22)). This is a general result: if the excretion is from the central compartment then  $V_{ss} = V_{eq}$ . For Model 2:

$$(2.27) \quad M_2^{ss} = \frac{k_{12}}{k_{21} + k_2} V_1 C_1^{ss}$$

$$Cl_{ss} = \frac{k_2 k_{12}}{k_{21} + k_2} V_1 \quad V_{ss} = V_1 (1 + \frac{k_{12}}{k_{21} + k_2}) \neq V_{eq}$$

The usual site of drug metabolism is the liver, not the central (i.e. blood) compartment, and Model 1 is not strictly correct. However, because the liver equilibrates very rapidly with the blood ( $k_2 \ll k_{21}$ ), in most situations it can be regarded as part of the central compartment and Model 1 is a good approximation. In order to estimate  $V_{ss}$  for an arbitrary input  $I(t)$ , one would first determine the two exponential fit to  $C(t)$ , solve for the compartmental rate constants and then determine  $V_{ss}$  from eq. (2.26) or (2.27).

## 2.2 Multicompartment, Mammillary models.

The compartmental model can, of course, be extended to an arbitrary number (N) compartments. It is usually assumed that compartments have a “mammillary” arrangement with a central compartment (e.g. blood) from which the clearance occurs and N-1 peripheral compartments (tissue) that exchange only with this central compartment (Figure 2-3):

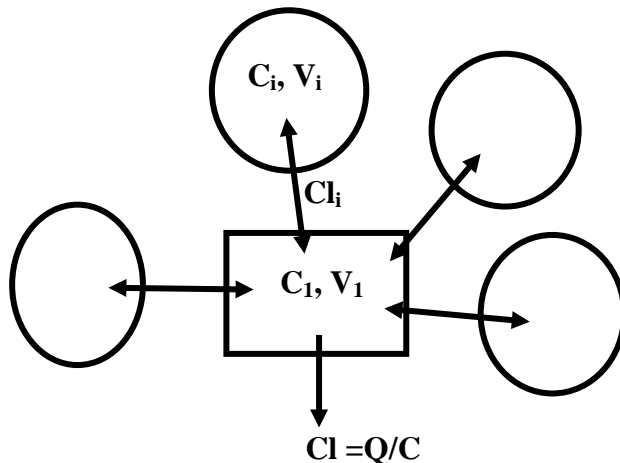


Figure 2-3 Mammillary compartment model.

The N compartment model is described by 2N parameters: the N volumes for each compartment, the clearance from the central compartment ( $Cl=k_1V_1$ , see eq. (2.19)) which is the total system clearance (metabolism, excretion) and the N-1 clearances ( $Cl_j, j=2..N$ ) representing the "exchange" between the central compartment (#1) and each peripheral compartment j. It can be shown that the concentration in the central compartment ( $C(t)$ ) following a bolus input is equal to a sum of N exponentials:

$$(2.28) \quad C(t) = A_1 e^{-\alpha_1 t} + A_2 e^{-\alpha_2 t} + \dots + A_n e^{-\alpha_n t}$$

The concentration for an arbitrary input  $I(t)$  is obtained from a convolution (eq. (2.8)). The general procedure that is followed when describing the PK with this model is to use a non-linear routine to fit eq. (2.28) (or its convolution) to the experimental  $C(t)$  data, then determine the 2N exponential terms ( $A_i, \alpha_i$ ) and solve for the model parameters ( $V_i, Cl, Cl_j$ ) using model equations similar to those of eq. (2.14) for the 2 compartment model. In practice, this procedure becomes unreliable for more than 3 compartments (6 parameters). One cannot accurately distinguish more than 3 exponential terms and, in most cases, just 2 exponentials (4 parameters) are adequate to fit the experimental PK data.

### 2.3 PKQuest Example: Human endogenous albumin pharmacokinetics.

As mentioned above, compartmental modeling has now been largely supplanted by the non-compartmental approach discussed in the next section. In the early literature (pre 1960), estimates of clearance and volume of distribution were based on this compartmental approach. We will examine one of these older calculations in detail because, although now old fashioned, it is straight forward and relatively robust and clearly has educational value. This analysis provides a measurement of the human endogenous albumin synthesis rate and the total body albumin. The 2-compartment Model 1 will be used in the following calculations, although this is not a strict requirement for the validity of the final result.

The human albumin steady state endogenous rate of synthesis ( $I_{ss}$ ) and volume of distribution ( $V_{ss}$ ) will be determined from the PK of a bolus IV injection of an albumin tracer. The tracer kinetics is measured over a long time period, roughly equal to the albumin half-time ( $\approx 17$  days). In eq. (2.14)  $a_2$  is larger than  $a_1$  because the B ( $>0$ ) term has a minus sign in  $a_1$  and a plus sign in  $a_2$ . Thus, at long times the second exponential becomes negligible relative to the first and the 2-compartment tracer concentration can be approximated by:

$$(2.29) \quad C_1(t) = M_1(t) / V_1 \xrightarrow{t \rightarrow \infty} (D / V_1) A_1 e^{-a_1 t}$$

This calculation also assumes that the inter-compartmental exchange rate is fast compared to the metabolic rate,  $k_1 \ll k_{12}$  (Model 1). This is a good approximation for albumin where the exchange time constant ( $=1/k_{12}$ ) is about 1 day and the metabolic time constant ( $=1/k_1$ ) is about 20 days.[1] Using this assumption, the expression for B in eq. (2.14) can be approximated by:



$$(2.30) \quad B \approx \sqrt{(k_{12} + k_{21})^2 + 2k_1(k_{12} - k_{21})} = (k_{12} + k_{21}) \sqrt{1 + 2k_1(k_{12} - k_{21}) / (k_{12} + k_{21})}$$

$$\approx k_{12} + k_{21} + \frac{k_1(k_{12} - k_{21})}{k_{12} + k_{21}}$$

Substituting this approximation for B into the Model 1 expression for  $a_1$  (eq. (2.14)) and using the expressions for  $Cl_{ss}$  (eq. (2.24) and  $V_{ss}$  (2.26):

$$(2.31) \quad a_1 \approx \frac{k_1 k_{21}}{k_{12} + k_{21}} = Cl_{ss} / V_{ss}$$

Substituting this approximation to B in the Model 1 expression for  $A_1$  (eq.(2.14)) and assuming  $k_1 \ll k_{12}$ :

$$(2.32) \quad A_1 \approx k_{21} / (k_{12} + k_{21}) = V_1 / V_{ss}$$

Finally, substituting these expressions for  $a_1$  and  $A_1$  into eq.(2.29):

$$(2.33) \quad C_1(t) \xrightarrow[t \rightarrow \infty; k_1 \ll k_{12}]{} C_0 e^{-\alpha t} \quad C_0 = D / V_{ss} \quad \alpha = Cl_{ss} / V_{ss} = 1/T$$

where T is excretion time constant. That is, in a semi-log plot of the tracer albumin concentration at long times, the slope =  $Cl_{ss}/V_{ss}$  and the intercept at  $t=0$  is  $D/V_{ss}$ .

Using this value of  $Cl_{ss}$  determined from the bolus tracer input, one can determine the normal human endogenous steady state rate of albumin synthesis  $I_{ss}$  (= rate of metabolism). From eq. (2.23), the albumin synthesis rate is described by (the central compartment concentration =  $C_1$  = plasma concentration =  $C_p$ ):

$$(2.34) \quad \text{Albumin synthesis rate} = I_{ss} = Cl_{ss} C_p^{ss}$$

where  $C_p^{ss}$  is the normal plasma steady state albumin concentration. This approach of estimating the  $Cl_{ss}$  and  $V_{ss}$  from the long time exponential decay was a common practice in the early literature (pre 1960). The essential assumption that the inter-compartmental exchange rate is fast compared to the excretion was not usually explicitly stated and may be only approximately satisfied.

This albumin PK analysis will be illustrated by applying PKQuest to the experimental  $^{131}\text{I}$  PK data of Takeda and Reeve [2] for a normal subject. Start PKQuest, click “Read”, click “Select File”, move to the folder where the “Example files” that were downloaded with the textbook are stored, select the file “Albumin I131 PK.xls” and click “Open”. Note that the 5 most recent files are remembered, so that the next time you click “Read”, you can immediately select this file. This selects the parameters and experimental data for the  $^{131}\text{I}$  PK analysis. Note that, in the third panel (“Non-compartmental PK”), the “NonPK” box is checked. This indicates

that one only wants to use PKQuest to find the non-compartment  $Cl_{ss}$  and  $V_{ss}$  using the techniques described in the next section 3 and not to do any PBPK modeling. Also, the “N EXP” has been selected to use 2 exponentials (i.e. 2 compartments) to fit the data. The experimental radioactive  $^{131}\text{I}$  plasma concentrations have been scaled proportional to the total radioactive  $^{131}\text{I}$  dose, so that the “Amount” and “Amount unit” both equal 1. Clicking the “Regimen” button in the second panel, specifies an input “Amount” = 1, given as a constant 1 minute IV input. The “Amount unit” is set =1 (dimensionless). Clicking the “Vein Conc1” button in the third panel, one can see the 17 experimental plasma  $^{131}\text{I}$  concentration measurements, ranging from 15 minutes to 24 hours (=34,560 minutes). (Remember, in PKQuest, time is in minutes, volume in liters, weight in kg). In the “Plot” panel, since there is no PBPK analysis, only the “Vein” concentration is, by default, optimized to fit the experimental data. (Note: in non-compartmental analysis one just wants to fit whatever data is input, and this is arbitrarily assigned to “vein”). The data is plotted from the first data point (15 min) to the last (34560 min). One can plot either the “Absolute” or “Semilog” output. Click the “Semilog” radio button. That is all the input that is needed.

Clicking “Run”, brings up the following semi-log graphical output (Figure 2-4)

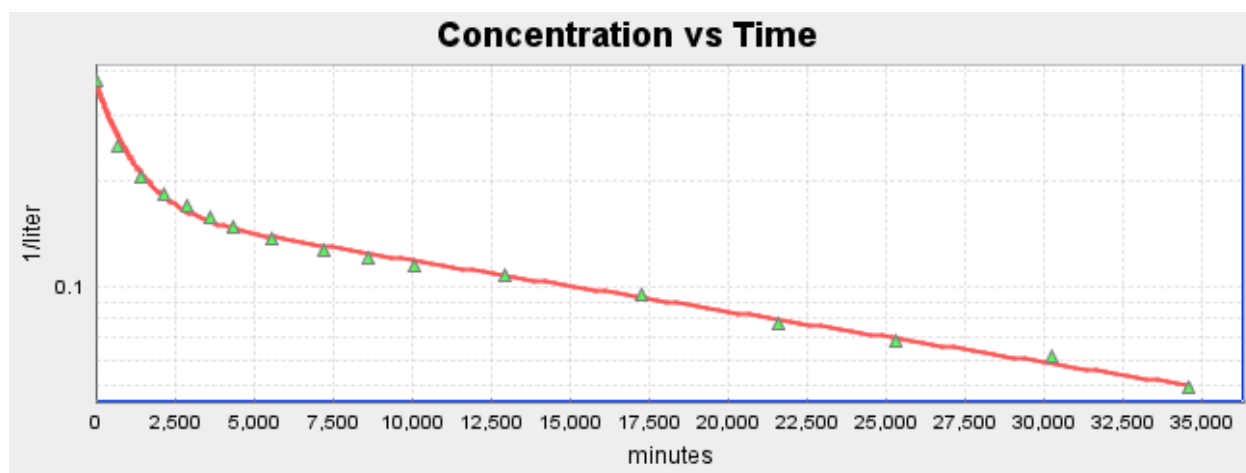


Figure 2-4 Two compartment exponential fit to the  $^{131}\text{I}$ -albumin concentration.

The green triangles are the experimental  $^{131}\text{I}$ -albumin concentration and the red line is the 2-exponential fit. (Actually, it is the convolution of the 2-exponential transfer function  $h(t)$  and the constant 1 minute input  $I(t)$ , eq. (2.8)). For this calculation, finding the 2-exponential function that provides the optimal fit to the experimental data requires non-linear minimization, a complex subject with a variety of numerical approaches. The numerical analysis methods used in PKQuest are not the focus of this book. There is some subjectivity in this fitting, in particular how one weights the different experimental points. The PKQuest default is to minimize the error function:

$$(2.35) \quad \text{Error} = \sum_{i=1}^N \frac{[\text{Model}(t_i) - \text{Exp}(t_i)]^2}{[\text{Model}(t_i) + \text{del}]^2}$$

where  $\text{Model}(t_i)$  is the 2-exponential convolution concentration and  $\text{Exp}(t_i)$  is the experimental value at  $t_i$  and the sum is over all the experimental data points. If  $\text{del}$  in eq. (2.35) is zero, the sum is over the square of the fractional error for each time point. Since the long time data points likely have low concentrations, there is, presumably, greater percentage experimental error in their measurement. The  $\text{del}$  term is added so that these points are weighted slightly less. In PKQuest  $\text{del} = \text{Wt} \times (\text{Average experimental concentration})$  where “Wt” is input in the third panel of PKQuest, and the default is  $\text{del} = 0.1$ . If the input “Wt” is  $<0$  then the unweighted error function ( $= \text{Sum}(\text{Model} - \text{Exp})^2$ ) is used. These default error function parameters can be modified by changing the “Wt” and the “Err Funct” that is used.

It can be seen in Figure 2-4 that a 2-exponential transfer function (ie, 2-compartment) model provides a surprising good fit to the entire time course. When PKQuest is “Run”, a “PKQuest Output” panel opens which provides numerical data about the analysis. Much of the output in this example (eg, organ weights, blood flows, etc.) are irrelevant since there is no PBPK analysis. The relevant output is the following lines:

Writing plot output to Excel file ../pkquestOut.xls in pkquest home directory

Writing plot figure to file ../pkquestPlot.png in pkquest home directory

Classical non-compartment pharmacokinetics for model vein (Integral from  $t = 0$  to  $t = 34560.0$ ):

AUC = 3.563E3 AUMC = 4.83E7 Mean Inp. Time = 5E-1 Clearance = 2.806E-4 Volume of dist. = 3.804E0

Non-compartment Pharmacokinetics using exponential response function and integrating from  $t=0$  to infinity:

2 Exponential Response function =  $\text{Sum}(a[i] \exp(-t/b[i]) = a[1]=1.813\text{E-}1 \quad b[1]=1.046\text{E}3 \quad a[2]=1.588\text{E-}1$   
 $b[2]=3.243\text{E}4$

Average value of Error function = 5.711E-4

AUC = 5.339E3 AUMC = 1.672E8 MIT = 0.5

Clearance = 1.873E-4 Volume of distribution = 5.866E0

All the plots displayed in PKQuest are saved in the “PKQuest home directory”, the directory where PKQuest is stored and run from. Both a graphical (.png) and an Excel data file (.xls) are saved, allowing the user to analyze or replot the raw data. The file names may not be identical to that stated in the output. For example, in this example the Excel file is named “PBPK vein fit.xls”. A numerical measure of the quality of the model fit to the experimental data is given by

the “Average value of Error function” which is the Error (eq. (2.35) divided by the number of experimental points. In this example, it is equal to 5.711E-4 and, taking square root, indicates the average fractional difference between model and experiment is 0.02.

The parameters  $a[1]$ ,  $a[2]$ ,  $b[1]$ ,  $b[2]$  of the 2-exponential fit are listed in the output (see above). As discussed above (eq. (2.33)), at long times and if the inter-compartmental change is fast compared to the metabolic rate, then  $Cl_{ss}$  and  $V_{ss}$  can be determined from extrapolation of the 2-exponential  $C(t)$  to long times:

$$(2.36) \quad \begin{aligned} C(t) &= a[1]e^{-t/b[1]} + a[2]e^{-t/b[2]} \xrightarrow{t \rightarrow \infty} a[2]e^{-t/b[2]} \\ a[2] &= 0.1588 / \text{liter} = D / V_{ss}; \quad b[2] = 32430 \text{ min} = T = V_{ss} / Cl_{ss} \\ \Rightarrow V_{ss} &= 6.29 \text{ liters} \quad T = 22.5 \text{ days} \quad Cl_{ss} = 0.28 \text{ liters / day} \end{aligned}$$

(Note,  $D=1$ ). Also listed in the output are the estimates of the  $Cl_{ss}$  ( $=1.873 \times 10^{-4}$  liters/min = 0.27 liters/day) and  $V_{ss}$  (= 5.87 liters) using the, presumably, more accurate non-compartment approach:

Non-compartment Pharmacokinetics using exponential response function and integrating from  $t=0$  to infinity:  
Clearance = 1.873E-4    Volume of distribution = 5.866E0

(Note: above “Clearance” is in standard PKQuest units of liters/min, and  $1.873 \text{ E-4}$  liters/min = 0.27 liters/day). This will be discussed in detail in the next Section 3 (eq. (3.1)). At steady state, the endogenous rate of albumin synthesis ( $I_{ss}$ ) is equal to the metabolic rate ( $Q$ ) and is described by (eq. (2.19)):

$$(2.37) \quad I_{ss} = Q = Cl_{ss} C_1 = Cl_{ss} C_p^{ss} = (0.28 \text{ liters / day})(43 \text{ gm / liter}) = 12.04 \text{ gm / day}$$

where the normal human steady state plasma albumin concentration of  $C_p^{ss} = 43 \text{ gm/liter}$  has been used.

The plasma albumin volume of distribution ( $V_p$ ) can be determined from the first time point (15 min) when the albumin has equilibrated with the plasma but has not had time to leave the plasma:

$$(2.38) \quad V_p = D / C(t=0) \approx 1.0 / 0.347 \text{ liter}^{-1} = 2.88 \text{ liters}$$

Thus, the total body albumin volume of distribution ( $\approx 6.29$  liters) is about 2 times the plasma albumin volume. Finally, using the normal plasma albumin for this subject ( $C_p^{ss} = 43 \text{ gm/liter}$ ) and  $V_{ss}$ , the total body albumin amount ( $M_{ss}$ ) can be determined (eq. (2.23)):

$$(2.39) \quad M_{ss} = V_{ss} C_p^{ss} = (6.29 \text{ liter}) \times (43 \text{ gm / liter}) = 270 \text{ gms}$$

## 2.4 References.

1. Levitt DG, Levitt MD: **Human serum albumin homeostasis: a new look at the roles of synthesis, catabolism, renal and gastrointestinal excretion, and the clinical value of serum albumin measurements.** *Int J Gen Med* 2016, **9**:229-255.
2. Takeda Y, Reeve EB: **Studies of the metabolism and distribution of albumin with autologous I131-albumin in healthy men.** *J Lab Clin Med* 1963, **61**:183-202.

### 3. Non-compartmental PK: Steady state clearance ( $Cl_{ss}$ ), volume of distribution ( $V_{ss}$ ) and bioavailability.

The definition of  $V_{ss}$  in eq. (2.23) is unsatisfactory because it depends on the specific compartmental model that is assumed. Furthermore, it is a quite complicated calculation, requiring, first, finding the exponential fit, and then using these exponential parameters to determine the model rate constants. In addition, if the solute metabolism is not from the central compartment, e.g. Model 2 is correct, then the clearance is also time dependent (eq. (2.19)) and depends on the compartment model (eq. (2.27)). In this section we will review more general definitions of  $V_{ss}$  and  $Cl_{ss}$  that are simpler to calculate and that are not dependent on compartment modeling. These results, first discussed by Meier and Zierler [1] in 1954 represent the most important mathematical relations in PK and are one of the rare examples in biology where a subtle theoretical result has a practical physiological application.

The fundamental expressions for  $Cl_{ss}$  and  $V_{ss}$  will be first introduced here with a detailed derivation provided later in this section:

$$\begin{aligned}
 Cl_{ss} &= D / AUC \\
 (3.1) \quad V_{ss} &= D[AUMC / AUC^2 - MIT / AUC] \\
 AUC &= \int_0^{\infty} C(t) dt \quad AUMC = \int_0^{\infty} t C_A(t) dt \quad MIT = (1 / D) \int_0^{\infty} t I(t) dt
 \end{aligned}$$

where AUC is the classic “area under the curve integral”, AUMC is the “first moment” of this integral and MIT is the “mean input time” of  $I(t)$  (dose  $D$ ) that enters the systemic blood. Note the simplicity of these expressions, simply requiring time integration over the experimental concentration measurements. The following assumptions are required for the validity of eq. (3.1) : 1) The system is linear. This is the fundamental assumption required in the derivation. If the system is not linear, these classical PK relations for  $Cl_{ss}$  and  $V_{ss}$  breakdown. 2) For the  $Cl_{ss}$  expression, the only other requirement is that the  $C(t)$  in the AUC is sampled either from the artery or a vein draining a non-metabolizing organ. In particular, it is usually valid for antecubital vein sampling. 3) In contrast, the  $V_{ss}$  expression is strictly valid only if the arterial concentration is used in the AUMC integral, as emphasized by using the notation of  $C_A(t)$  in eq. (3.1) (see below). This assumption is usually ignored in the literature discussions of these equations. The error introduced by using, eg, the antecubital vein concentration in place of  $C_A(t)$  is relatively small (about 10%, see Section 3.3). 4) For the  $V_{ss}$  expression, the metabolism or excretion must be from the blood (central) compartment so that the clearance is time independent (eq. (2.19)). For example, if the metabolism occurs in the liver, this assumption is not valid. However, since the liver and blood are almost in equilibrium, this is also a small error.

The MIT characterizes the time course of the input. For a bolus input,  $MIT = 0$ . For a constant input from  $t=0$  to  $t=T$ :

$$(3.2) \quad \begin{aligned} I(t) &= D/T \text{ for } t \leq T \text{ and } I(t) = 0 \text{ for } t > T \\ MIT &= (1/D) \int_0^T t (D/T) dt = T/2 \end{aligned}$$

and MIT is equal to half the total input time T.

These expressions for AUC and AUMC take a simple form if the system response function ( $h(t)$ ) can be described by an N exponential function:

$$(3.3) \quad h(t) = \sum_{i=1}^N a_i e^{-t/b_i}$$

For a constant input of Dose = D of duration T, using the convolution relation (eq. (2.8)), the concentration C(t) is given by:

$$(3.4) \quad \begin{aligned} C(t) &= (D/T) \sum_{i=1}^N a_i b_i (1 - e^{-t/b_i}) \quad t \leq T \\ &= (D/T) \sum_{i=1}^N a_i b_i (e^{T/b_i} - 1) e^{-t/b_i} \quad t > T \end{aligned}$$

Substituting this expression for C(t) in the above definitions of AUC and AUMC (eq. (3.1)):

$$(3.5) \quad \begin{aligned} AUC &= D \sum_{i=1}^N a_i b_i \\ AUMC &= D \sum_i a_i b_i (b_i + T/2) \end{aligned}$$

The estimate of  $Cl_{ss}$  and  $V_{ss}$  requires determination of the integrals AUC and AUMC. One approach would be to use the discrete experimental data points  $C(t_i)$ ,  $i=1..n$  with some numerical integration technique. However, this has several problems. Firstly, experimental measurements at early times are inaccurate because of mixing delays between the input and sampling site. Since these early concentrations are large, these points contribute significantly to the integrals and one needs a method to extrapolate to  $t=0$ . Secondly, since the integrals need to be carried out to long times (infinity), one needs some way to extrapolate out beyond the last measurements. This long time extrapolation is especially important for the determination of AUMC because it is weighted by the time  $t$  and can dominate the integral (see PKQuest Example 3.2). Finally, one needs a numerical integration procedure that accurately interpolates between the  $C(t_i)$ . The solution to all these problems (and the approach that is used in PKQuest) is to assume that the system response function  $h(t)$  is a multi-exponential function, adjust the response function parameters to find the best fit to the experimental data  $C(t_i)$ , and then use this  $h(t)$  function in the integration from 0 to infinity (see eq. (3.5)). In doing this, one explicitly uses the known information about the input function  $I(t)$  (eg, eq. (2.10)) by using the convolution of  $I(t)$

with  $h(t)$  (eq. (2.8)) when finding the multi-exponential function. This approach should provide a good approximation for extrapolating the experimental data to both the early and long times.

Rigorous derivations of the  $Cl_{ss}$  and  $V_{ss}$  relations in eq. (3.1) are provided at the end of this section (Sections 3.5 and 3.6) that make use of more advanced mathematic relations (Laplace transform) and can be skipped if one is not interested in these details.

### 3.1 Bioavailability, first pass metabolism.

One of the most important applications of the clearance concept is in the determination of the “bioavailability” of a drug dose that is not administered by an IV injection directly into the systemic circulation. We will illustrate this concept for an orally administered drug, but it also applies to other routes such as nasal inhalation or dermal patches. Bioavailability is defined as the fraction of the drug dose that enters the systemic circulation. It is the single most important PK parameter for an oral drug and is an absolute requirement for determining oral dosage.

Figure 3-1 shows a schematic diagram of the factors involved in the intestinal absorption of an oral drug Dose ( $= D_{oral}$ ). The amount of the drug that reaches the systemic circulation ( $= D_{oral\_sys}$ ) is determined by: 1) the amount  $M$  absorbed from the intestine ( $M = F_A \text{ Dose}$ ), 2) the amount metabolized by the intestinal mucosa before entering the portal blood; 3) the amount metabolized by the liver before entering the systemic circulation. This is described by eq. (3.6):

$$(3.6) \quad \begin{aligned} D_{oral\_sys} &= D_{oral} F_A (1 - E_I)(1 - E_H) \\ \text{Bioavailability} &= D_{oral\_sys} / D_{oral} \end{aligned}$$

where  $F_A$  is the fraction of the oral dose that is absorbed out of the intestinal lumen,  $E_I$  is the fraction of the absorbed dose that is metabolized (“extracted”) by the intestinal mucosa, and  $E_H$  is the fraction of the dose that enters the portal vein that is extracted by the liver before entering the systemic circulation.  $E_I$  and  $E_H$  are also referred to as the “first pass intestinal metabolism” and “first pass hepatic metabolism”, respectively. The “bioavailability” is defined as the fraction of the oral dose that reaches the systemic circulation. The intestinal metabolism is usually neglected (i.e.  $E_I \approx 0$ ) because it cannot be directly measured and, for most drugs, is relatively small. The hepatic extraction can be very large (close to 1) and is an important factor in determining the bioavailability. As discussed below,  $E_H$  can be estimated from measurement of  $Cl_{ss}$  and an estimate of hepatic blood flow.



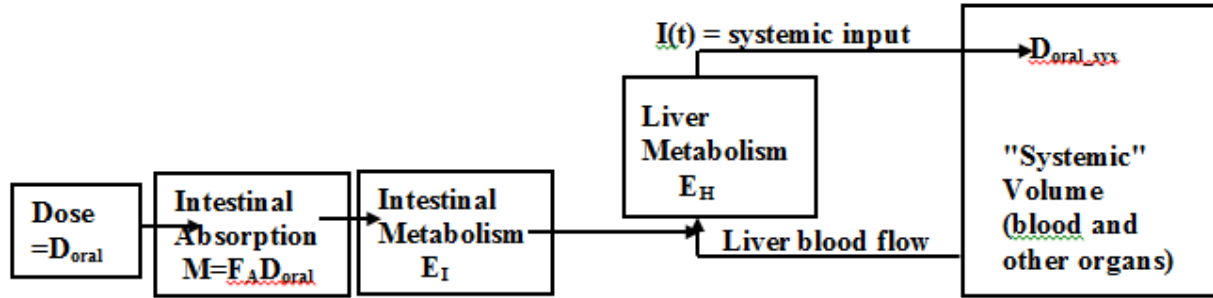


Figure 3-1 Schematic diagram of the PK of an orally administered drug.

The steady state clearance relationship (eq. (3.1)) for an IV dose is:

$$(3.7) \quad Cl_{ss} = D_{IV} / AUC_{IV}$$

Similarly, the  $Cl_{ss}$  relation for an oral dose is:

$$(3.8) \quad Cl_{ss} = D_{oral\_sys} / AUC_{oral}$$

where  $AUC_{IV}$  and  $AUC_{oral}$  are the integrals over the blood concentration following an IV or oral dose, respectively. Using eqs. (3.7), (3.8) and the definition of bioavailability:

$$(3.9) \quad \begin{aligned} \text{Bioavailability} &= D_{oral\_sys} / D_{oral} = Cl_{ss} AUC_{oral} / D_{oral} \\ &= (AUC_{oral} / D_{oral}) / (AUC_{IV} / D_{IV}) \end{aligned}$$

If the oral and IV doses are equal, then the bioavailability is simply the ratio of the (oral/IV) AUC. This is the fundamental relationship that is used to determine bioavailability. It is a very general result, with the only assumption required that the system is linear.

There are two different bioavailabilities: the “absolute” and the “relative” bioavailability. The “absolute” bioavailability is that defined in eq. (3.9) where one compares the AUC following an IV and oral dose. For some drugs, for regulatory reasons, one cannot administer a drug intravenously and  $AUC_{IV}$  cannot be measured. In this case, one can only determine a “relative” bioavailability which is based on a comparison of the  $AUC_{oral}$  for different drug formulations.

As shown in eq. (3.6), the bioavailability is determined by three parameters:  $F_A$ ,  $E_I$ , and  $E_H$ . One can estimate  $E_H$  as follows. The systemic clearance ( $Cl_{ss}$ ) is hepatic and/or renal. For most drugs, the systemic clearance is primarily hepatic and we will assume here for simplicity that  $Cl_{Hepatic} = Cl_{ss}$ . (For the general case, and one can estimate the renal clearance from measurement of the urinary clearance of unmetabolized drug). Then, the hepatic extraction ( $E_H$ ) of the systemic drug is equal to:

$$(3.10) \quad E_H = Cl_{ss} / F_L$$

where  $F_L$  is the liver blood flow. If one can neglect the intestinal metabolism ( $E_I = 0$ ), then:

$$(3.11) \quad \text{Bioavailability} = F_D (1 - E_H)$$

and one can determine the fraction of drug absorbed by the intestine ( $F_D$ ) from eqs. (3.10) and (3.9). This is not as general a result as eq. (3.9) because it depends on knowledge of the liver blood flow ( $F_L$ ) which has a large variability, changes with meals and is altered by some drugs. As the  $Cl_{ss}$  approaches the liver blood flow,  $(1 - E_H)$  approaches zero, and small errors in the estimate of  $F_L$  can lead to large changes in the estimated  $F_D$ . This is discussed in detail in the PKQuest Example 10.3 that presents a quantitative analysis of the intestinal absorption of propranolol.

### 3.2 PKQuest Example 1: Estimation of $Cl_{ss}$ and $V_{ss}$ for albumin.

In Section 2.3, the  $^{131}\text{I}$ -albumin data of Takeda and Reeve [2] was used to estimate the human albumin PK using the 2-compartment approach. This same data and PKQuest Example file will be used here to determine the non-compartmental  $Cl_{ss}$  and  $V_{ss}$ . Open PKQuest and click “Read”. The “Albumin I131PK.xls” file should be listed since it was used in the previous example. (It is also available in the downloaded “Example” files). Select this Excel file. Also, click the Semilog option. Clicking “Run” outputs the numerical output listed below. Two different estimates of  $Cl_{ss}$  and  $V_{ss}$  are output:

Classical non-compartment pharmacokinetics for model vein (Integral from  $t = 0$  to  $t = 34560.0$ ):

AUC = 3.563E3 AUMC = 4.83E7 Mean Inp. Time = 5E-1 Clearance = 2.806E-4 Volume of dist. = 3.804E0

Non-compartment Pharmacokinetics using exponential response function and integrating from  $t=0$  to infinity:

2 Exponential Response function =  $\text{Sum}(a[i] \exp(-t/b[i]) = a[1]=1.813E-1 \quad b[1]=1.046E3 \quad a[2]=1.588E-1$   
 $b[2]=3.243E4$

Average value of Error function = 5.711E-4

AUC = 5.339E3 AUMC = 1.672E8 MIT = 0.5

Clearance = 1.873E-4 Volume of distribution = 5.866E0

The first estimate uses the 2-exponential function and integrates from 0 to the “End” (last experimental time point = 34560 min) while the second is from  $t=0$  to infinity. The extrapolation to infinity increases AUC and AUMC by factors of 1.49 and 3.46, respectively. This dramatically illustrates that the extrapolation to infinity is essential and that AUC and, especially, AUMC (and, correspondingly,  $Cl_{ss}$  and  $V_{ss}$ ) may be dominated by the concentrations at times beyond those that are experimentally measured. This can lead to two types of errors. Firstly, if albumin distributes to a compartment with a very slow exchange constant (eg, 30 days) that was not sampled in the 24 day experimental measurement, it would be missed in the extrapolation to infinity, leading to large errors in the  $Cl_{ss}$  and  $V_{ss}$  estimates. For albumin this is unlikely and one would expect that the 24 day experimental measurement accurately sampled all the compartments. The second problem is that because the data points at long times are usually at the limit of experimental resolution, they may have significant random errors, producing large extrapolation errors.

Rerun PKQuest again, this time selecting the “N Exp” equal 3 option. This now uses a 3-exponential response function to fit the experimental data, with the following numerical output:

Non-compartment Pharmacokinetics using exponential response function and integrating from t=0 to infinity:

3 Exponential Response function =  $\text{Sum}(a[i] \exp(-t/b[i])$  a[1]=1.79E-1 b[1]=9.798E2 a[2]=7.717E-2  
b[2]=2.019E4 a[3]=8.55E-2 b[3]=4.767E4

Average value of Error function = 5.122E-4

AUC = 5.809E3 AUMC = 2.259E8 MIT =0.5

Clearance = 1.721E-4 Volume of distribution = 6.695E0

The 3-exponential  $Cl_{ss}$  is 6% smaller and  $V_{ss}$  is 14% larger than the 2-exponential result (see above). Even though the 3-exponential fit is slightly better (Error function of 5.122E-4 vs 5.711E-4), this does not necessarily mean that the  $Cl_{ss}$  and  $V_{ss}$  estimates are more accurate. The fit will always improve when one increases the number of adjustable parameters, in this case, from 4 to 6. However, if there are experimental errors in the concentration measurements at long times they will be heavily weighted by the third exponential, possibly leading to erroneous estimates when extrapolating to infinity. The choice of the number of exponentials is somewhat subjective and there are statistical approaches to making this decision which are not included in PKQuest.[3] This is discussed more in the Exercise (Section 3.4) discussed below.

### 3.3 PKQuest Example 2. Amoxicillin: comparison of non-compartmental and PBPK estimates of $V_{ss}$ and $Cl_{ss}$ .

Start PKQuest and Read the file “Amoxicillin NonCompart Example.xls”. The non-compartmental PK option requires that: 1) In the “Non-compartment PK” section **both the “NonPK” and “Fit Vein” boxes need to be checked**; 2) The experimental data is entered in the “Vein Conc1” table; and 3) Only the vein box is checked in the “Plot/Organs” Table. The serum antecubital PK data of Arancibia et. al. [4] following 500 mg IV amoxicillin as a bolus (10 second constant infusion) is input in “Vein Conc1”. The details of this bolus input are input in the “Regimen” table: : “Type = 1” (constant infusion); “Amount = 500” (total dose), “Start = 0”, “End = 0.25” (15 sec infusion), “Site = 0” (IV input). Running PKQuest with a “Plot” “End” time of 360 minutes shows that the 2-exponential response provides an excellent fit to the data (run first as “Plot/Absolute, then again as “Semilog”). “Run” PKQuest, getting the numerical output:

Non-compartment Pharmacokinetics using exponential response function and integrating from t=0 to infinity:

2 Exponential Response function =  $\text{Sum}(a[i] \exp(-t/b[i])$  a[1]=6.104E-2 b[1]=1.255E1 a[2]=4.388E-2  
b[2]=8.411E1

Average value of Error function = 1.184E-3

Constant Input of Dose = 5E2 Duration = 2E-1

AUC = 2.228E3 AUMC = 1.602E5 MIT =0.1

Clearance = 2.244E-1 Volume of distribution = 1.611E1

The non-compartmental  $Cl_{ss}$  and  $V_{ss}$  are 0.2244 liter/min and 16.1 liters, respectively. Close PKQuest.

The tissue/blood solute partition coefficient is a crucial PBPK parameter and, for the typical drug that has poorly characterized intracellular binding, this partition cannot be accurately predicted from just the drug structure. This represents the major weakness and limitation in the PBPK approach and is discussed in more detail in Section 4. However, for extracellular solutes such as Amoxicillin, which distribute only in the blood and interstitial space, the tissue/blood partition is determined primarily by the plasma and interstitial albumin binding and, since the normal interstitial albumin concentration of the different tissues is known, one can accurately predict this partition. This is illustrated in the following example and will be discussed in detail in Section 5.

Start PKQuest again and “Read” the file “Amoxicillin Example PBPK IV.xls”. This uses the same Arancibia et. al. [4] amoxicillin data for an IV input as was used above in the non-compartmental calculation. This is an example of an “Extracellular” solute which has predictable PBPK parameters. It is discussed in more detail in Example 5.1 where the PBPK parameters that characterize this extracellular solute are explained. Note that now the “NonPK” and “Fit Vein” boxes are **unchecked** – this turns off the non-compartment and turns on the PBPK option. The “Regimen” table has input the Arancibia IV dose: “Type = 1” (constant infusion); “Amount = 500” (total dose), “Start = 0”, “End = 0.2” (10 sec infusion), “Site = 0” (IV input). In the “Plot Organs Table”, the “antecubital” organ has been checked and “Conc Unit” = 4 (indicating plasma concentration). The experimental data has now been moved to the “Exp Data 1” table in the “Plot” panel. In the “Model Parameters” panel of PKQuest, the average weight (66.4 kg) for the Arancibia et. al. subjects has been entered. The tissue interstitial volumes and albumin concentrations for the “Standard” human are preprogrammed in PKQuest. Clicking the “Extracellular” check box in the top panel activates these parameters and specifies that the solute distributes only in the extracellular space. Amoxicillin has weak albumin binding, with about 83% free in plasma, and this parameter is input in the “Plasma fr. free” box in the top panel. Note that, so far, all the parameters are directly measured experimental values and no adjustable parameters have been used. This ability to model extracellular solutes with just a few adjustable parameters is a novel feature of PKQuest and is described in detail in reference [5].

The only adjustable PBPK parameter is the clearance. The amoxicillin clearance is entirely renal and the renal clearance can be adjusted to fit the serum data using the following procedure. First enter some approximate estimate of renal clearance in units of “Fraction of whole blood cleared in one pass through kidney” and enter this in the “Renal Clr” box in the top panel. For example, be sure the “Renal Clr” box is checked and input a value of 0.2. Clicking “Run”, one sees that the model antecubital vein concentration falls more slowly than the experimental, presumably because of too small a value of clearance. One approach to finding the actual clearance is simply by trial and error entering different values for the clearance. PKQuest also provides an automatic optimization procedure that uses a Powell minimization routine to find the optimal fit. This is turned on by clicking the “Parameters” button in the bottom “Minimize” panel. Clicking the “Clearance” check box for the “Kidney” turns on

this optimization. Run PKQuest again. It can be seen that, after minimization, the PBPK model finds a nearly perfect fit (average mean square error =  $1.518\text{E-}3$ ), using a renal clearance described in the following output:

kidney Clearance:: Fraction whole blood clearance =  $3.531\text{E-}1$  Total clearance (l/min) =  $4.327\text{E-}1$  Total Blood Flow (kg/min)  $1.225\text{E}0$

(You may get a slightly different result because the Powell minimization uses a random number generator). The optimal “Fractional whole blood renal clearance” is 0.353. Enter this value in the “Renal Clr” box and save this “Amoxicillin Example PBPK IV.xls” file, overwriting the old file, so that in future runs you do not need to use the Minimize routine. Now Run again (“Reading” the Amoxicillin Example.xls file) with this value of clearance and look at the last entry in the numerical output:

Classical non-compartment pharmacokinetics for model antecubital (Integral from  $t = 0$  to  $t = 360.0$ ):  
AUC =  $2.222\text{E}3$  AUMC =  $1.487\text{E}5$  Mean Inp. Time =  $1.25\text{E-}1$  Clearance =  $2.25\text{E-}1$  Volume of dist. =  $1.503\text{E}1$

This is the result of determining the AUC and AUMC integrals using the PBPK numerical estimate of  $C(t)$  (eq.(3.1)) and integrating from  $t=0$  to the  $t = 360$  min (=“End time” set in plot panel). In order to integrate to long times, set the “End” time to some large value (eg, 3,600 minutes) and run again, getting the following output:

Classical non-compartment pharmacokinetics for model antecubital (Integral from  $t = 0$  to  $t = 3600.0$ ):  
AUC =  $2.29\text{E}3$  AUMC =  $1.788\text{E}5$  Mean Inp. Time =  $1.25\text{E-}1$  Clearance =  $2.184\text{E-}1$  Volume of dist. =  $1.702\text{E}1$

These PBPK model estimates are close to the non-compartment result obtained above using a 2-exponential fit to the data: 0.224 (2-Exp) versus 0.218 liter/min (PBPK) for  $Cl_{ss}$  and 16.1 (2-Exp) versus 17.0 (PBPK) for  $V_{ss}$ .

Finally, it is of interest to compare these non-compartmental steady state estimates of  $Cl$  and  $V$  with the actual organ physiological values used to build the PBPK model. As discussed above, if excretion is from the central blood compartment, then the clearance should be independent of time (eq. (2.20)) and  $Cl_{ss}$  should equal the PBPK model clearance. The PKQuest output provides a conversion from the “Fraction whole blood clearance” by the kidney and the “Total clearance (l/min)” which depends on the renal blood flow:

kidney Clearance:: Fraction whole blood clearance =  $3.53\text{E-}1$  Total clearance (l/min) =  $4.325\text{E-}1$  Total Blood Flow (kg/min)  $1.225\text{E}0$

Note from the above output that for a renal “Fraction whole blood clearance” of 0.3531, the whole blood clearance (=fractional clearance x renal blood flow) is 0.432 liter/min, about twice the above estimate of  $Cl_{ss}$  (0.22). However, this PBPK clearance is for “whole blood” while the above non-compartmental  $Cl_{ss}$  was determined by integrating over the “plasma” concentration. As discussed previously (eq. (2.4)), plasma clearance should be equal to the whole blood

clearance time the blood/plasma concentration ratio. From the output of the PKQuest model run, the blood/plasma ratio for the PBPK model is:

Blood/plasma ratio = 0.518867924528302

This is the default PKQuest value assuming the extracellular solute is limited to the plasma. Multiplying this ratio times the whole blood renal PBPK clearance (0.432) yields an PBPK plasma clearance of 0.224 liter/min, identical to the non-compartmental value (0.224).

Also if the excretion is from the central compartment,  $V_{ss}$  should be equal to  $V_{eq}$ , the equilibrium volume of distribution (eq. (2.26)). From the output of the PKQuest run:

Equilibrium Volume of Distribution = 1.519E1 Water volume = 3.924E1

This PBPK model value (15.19 liters) is about 1 liter less than the  $V_{ss}$  determined from either the 2-exponential fit (16.1 liters) or the AUMC integral of the PBPK antecubital concentration curve (17.0 liters). However, it was emphasized in the derivation of the  $V_{ss}$  relation (eq. (3.21)) that this expression is valid only for the case when the integral is over the arterial concentration curve. One can directly test this by rerunning the PKQuest PBPK model, this time plotting the arterial curves (selecting “Artery” in the Plot Organs table, unclicking antecubital, and setting end time = 3600) :

Classical non-compartment pharmacokinetics for model artery (Integral from t = 0 to t = 3600.0):

AUC = 2.29E3 AUMC = 1.591E5 Mean Inp. Time = 1E-1 Clearance = 2.183E-1 Volume of dist. = 1.514E1

The non-compartmental  $V_{ss}$  using the arterial concentration (identical PBPK model as was used to fit the antecubital data) is 15.14 liters, nearly identical to the PBPK  $V_{eq}$  (15.19 liters). This calculation provides an estimate of the error introduced by using the antecubital vein experimental data to estimate  $V_{ss}$  (15.14 arterial vs 17 antecubital, about a 10% error).

### 3.4 Exercise 1: Morphine-6-Glucuronide pharmacokinetics.

This exercise will lead you through the steps in carrying out PBPK analysis of the extracellular solute morphine-6-glucuronide (M6G). M6G is a metabolite of morphine and is of interest because it is also an analgesic.[6] This example will use the experimental antecubital PK data of Pension et. al. [7]. Use the following steps, build a PBPK model for M6G:

I) Use the “Amoxicillin Example.xls” file as the prototype for an extracellular solute. Start PKQuest, read the Amoxicillin Example.xls and the “Save” it with a new file name (click Save, then the “Select or Create File”, browse to the directory you want to save it in, input the file name you want for M6G (eq, M6G PBPK Example.xls) **(be sure to add .xls to the end of the file name, this is NOT done automatically)**, and click Open. You may also want to change the “Comments” section so it refers to M6G. Save and close PKQuest

II) Start PKQuest again and open the M6G file.

Enter the PK data using the following steps:

1) Enter the experimental antecubital serum vein concentrations as a function of time for the IV input by clicking on the “Exp Data 1” button, and follow the directions for copying (Ctrl C) and pasting (Ctrl V) the following data into the table:

Time(min)	Conc (nanomoles/liter)
2	519.6204
5	387.4675
15	261.0157
30	196.8419
45	150.131
60	129.6418
90	90.34045
120	66.60846
150	49.66819
180	37.03629
210	31.98173
240	25.80861
300	15.70647
360	9.558552
479	5.949902
600	5.31484

2) The concentration is in nanomoles/liter (**Remember, the PKQuest volume unit is always in liters.**) Write “nanomole” in the “Amount unit” box. This is only a label in the plots and is not used in the actual concentration.

3) This data is for a 2 minute constant IV infusion of a total of 2 mg. Input this into the “Regimen” table. (Note: you need to convert mg to nanomoles).

4) The average weight of the subjects was 71 kg. Input this.

5) M6G does not have any significant plasma protein binding, i.e. the “fraction free” is 1.0. Input this.

6) The experimental data is carried out to 600 minutes. Use this for the “End Time”. For start time, just use a time less than the first experimental data point (2 min).

This completes the specification of the M6G PBPK model (except for the renal clearance, see next step). Save it and close PKQuest.

III) Open PKQuest and Run the M6G PBPK file. The fit between the experimental data and model curve is sort of OK, but the model data falls off faster than experimental, presumably because the renal clearance that was used for amoxicillin (0.353) is greater than the M6G

clearance. (If at this step, the experimental data is markedly different than the Model output, then you made some mistake at an earlier step. Go back and find your error).

To find the optimal Renal clearance, click the Parameter button, check the option “Clearance” in the “Kidney” row and Run again. If you did everything right, you should get the following output **using the Semilog option** (Figure 3-2):

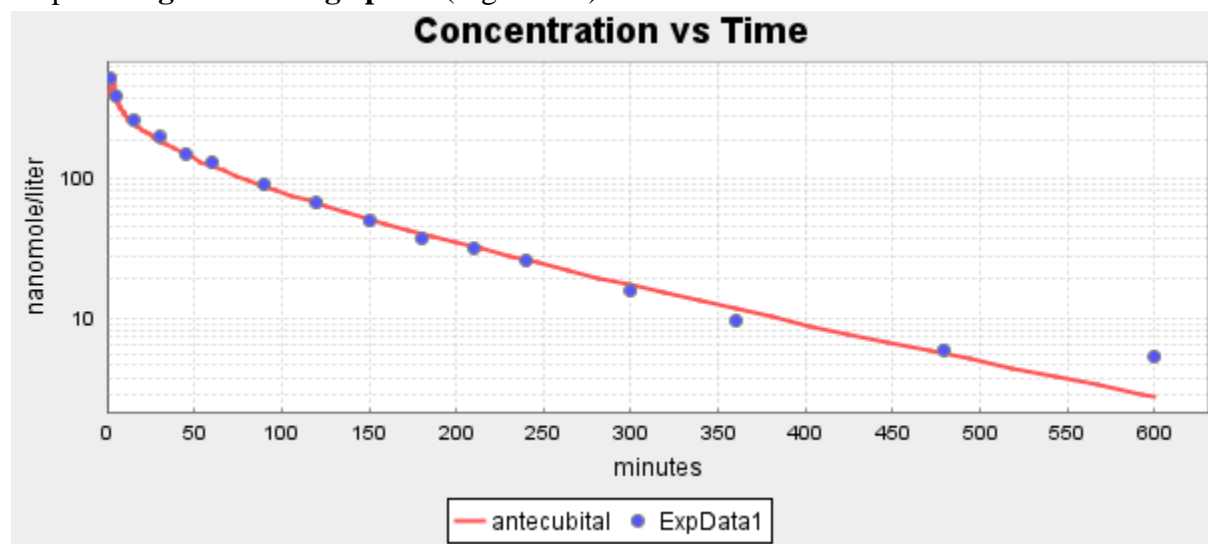


Figure 3-2 PKQuest PBPK model fit (red line) to the morphine-6-glucuronide experimental data (blue circles).

Note that the PBPK model fit is excellent, with the exception of the last point at 600 minutes which will be discussed in more detail below.

One should take a moment to reflect on this result. This ability to accurately predict the human PK of a drug using just one adjustable parameter (renal clearance) is remarkable and is one of the triumphs of the PBPK approach. However, it should be emphasized that this is an exception and is not possible for the great majority of drugs. It is only for the class of extracellular drugs (Section 5) and the class of highly lipid soluble drugs (Section 7) that it is possible. Most drugs are weak acids or bases that have variable intracellular binding that is not predictable.

IV. In this last section we will use non-compartmental PK to look at the implications of the poor fit to the last data point at 600 minutes. Open and Run the M6G file again. Copy the experimental data in the Exp Data 1 table to the “Vein Conc1” table. Then, to activate the non-compartmental option do the following:

1. Check the NonPk box.
2. Check the Fit Vein box
3. In the Plot/Organs table, uncheck the antecubital vein box.
4. Select N exp= 2 in the “N Exp” box in the Non-compartment PK panel.
5. Save this with a new file name (add .xls to name) (e.g. M6G NonComp.xls).



Now, Run, using the “Semilog” plot option. This is now simply fitting the data with a 2-exponential transfer function and is not doing any PBPK calculations. Note that this 2-exponential fit again underestimates the last data point, similar to the above PBPK fit.

Run again, setting N Exp = 3. Note that now the last data point is more closely fit. The third exponential, with a time constant =  $b[3] = 215$  minutes is heavily weighted by the last data point.

Compare the output for the non-compartmental  $Cl_{ss}$  and  $V_{ss}$  for the 2 and 3-exponential fits:

Non-compartment Pharmacokinetics using exponential response function and integrating from  $t=0$  to infinity

**2 Exponential Response function** =  $\text{Sum}(a[i] \exp(-t/b[i]) = a[1]=7.586E-2 \ b[1]=2.208E1 \ a[2]=3.335E-2 \ b[2]=1.419E2$

Average value of Error function =  $7.946E-3$

AUC =  $2.774E4$  AUMC =  $3.096E6$  MIT = 1.0

Clearance =  $1.561E-1$  Volume of distribution =  $1.726E1$

Non-compartment Pharmacokinetics using exponential response function and integrating from  $t=0$  to infinity:

**3 Exponential Response function** =  $\text{Sum}(a[i] \exp(-t/b[i]) = a[1]=6.622E-2 \ b[1]=5.143E0 \ a[2]=5.141E-2 \ b[2]=6.083E1 \ a[3]=1.413E-2 \ b[3]=2.115E2$

Average value of Error function =  $1.934E-3$

AUC =  $2.795E4$  AUMC =  $3.594E6$  MIT = 1.0

Clearance =  $1.549E-1$  Volume of distribution =  $1.977E1$

Note that, as expected, adding the two additional adjustable parameters specified by the third exponential significantly reduced the mean square error (0.0079 vs 0.0019), It also increased the volume of distribution ( $V_{ss}$ ) from 17.3 liter to 19.8 liter.

If one believes that the last data point is accurate then, of course, you would want to use the 3-exponential fit. This choice has important implications about the long time PK and, possibly, the clinical effect of the drug. The following Figure 3-3 shows the results of extrapolating the 2-exponential (green) and 3-exponential curves (red) out to two days (2880 minutes). (This plot is generated by using the raw data that PKQuest outputs to the Excel files in the PKQuest “home” directory). The PBPK fit to the data that you previously generated using the M6G PBPK file that you created above is also plotted (black line).

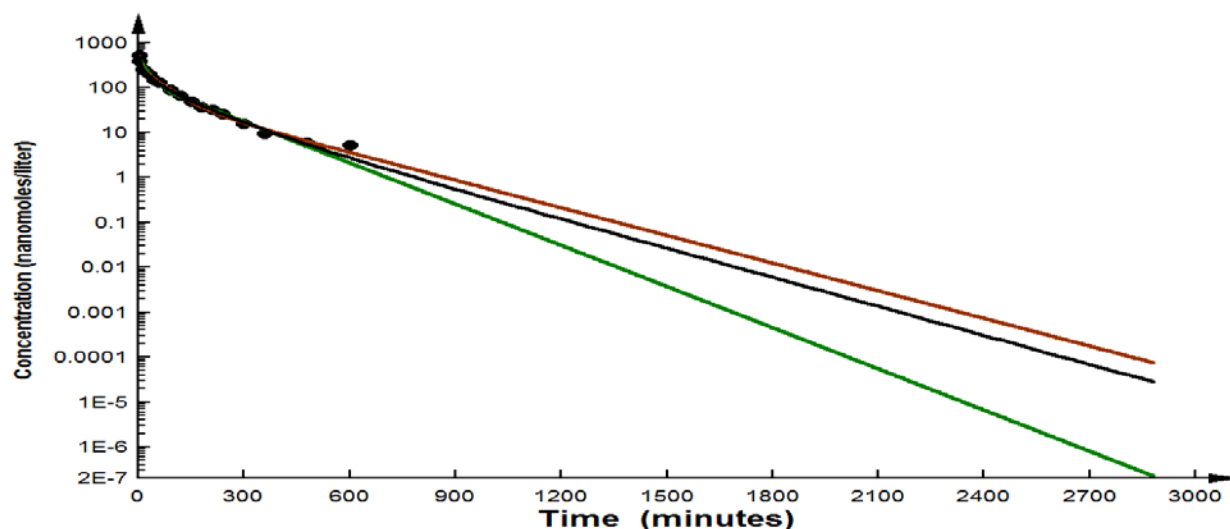


Figure 3-3 Morphine-6-G experimental data. The 2 exponential (green) and 3 exponential (red) response function optimal fits, and PBPK extracellular model best fit (black).

The three curves are nearly identical over the experimental range of the data (0 to 600 minutes) but they diverge at long times. At two days (2880 minutes), the concentration for the 3-exponential extrapolation is 335 times greater than that for the 2-exponential ( $7.48\text{E-}5 \text{ nm/l}$  vs  $2.23\text{E-}7 \text{ nm/l}$ ). Your interpretation of the results depends on your confidence in the experimental measurements at long times when the concentrations are low ( $5.3 \text{ nm/L}$ ) and may be inaccurate. The resolution limits are not normally reported in the publications, but the usual procedure is to carry out the measurements to the resolution limit of the analytical technique and the last points are usually at that limit. If one has confidence in the PBPK model, it can settle this question. Remember that in this case, for “Extracellular” M6G, the PBPK model has only one adjustable parameter (clearance) versus 4 and 6 parameters for the 2 and 3-exponential fits, respectively. In this case, the PBPK fit is closer to the 3-exponential fit.

### 3.5 Derivation of the $Cl_{ss}$ relation.

We will first derive the  $Cl_{ss}$  relationship starting with the general definition of the time dependent clearance:

$$(3.12) \quad Cl(t) = Q(t) / C_A(t)$$

where  $Q(t)$  is the total rate of solute removal from the system (metabolism, excretion, etc.) and  $C_A(t)$  is the arterial concentration. The removal may occur in a number of different organs (or the blood itself) all of which are supplied by the arterial blood. It will be assumed that the drug concentration  $C(t)$  is sampled from either the artery or, more generally, a vein draining an organ (or organs) that do not metabolize the drug, for example the antecubital vein. Writing the general convolution relation (eq. (2.8) for the case where there is a steady state constant input  $I_{ss}$ :

$$(3.13) \quad C(t) = I_{ss} \int_0^t h(\tau) d\tau$$

where  $h(t)$  is the general linear system transfer function. Since  $C$  is sampled from an organ that does not metabolize the solute, as  $t$  goes to infinity,  $C(t)$  will approach the steady state arterial concentration ( $C_{Ass}$ ):

$$(3.14) \quad C(t = \infty) = C_{Ass} = I_{ss} \int_0^{\infty} h(\tau) d\tau$$

Also, as  $t$  goes to infinity,  $Q(t) \rightarrow I_{ss}$  and, therefore, the steady state clearance (eq.(3.12)) is:

$$(3.15) \quad Cl_{ss} = I_{ss} / C_{Ass} = 1 / \int_0^{\infty} h(\tau) d\tau$$

The second part of this derivation uses the concept of the Laplace transform (LT) of a function  $F(t)$  which is defined by:

$$(3.16) \quad F_L(s) = \int_0^{\infty} F(t) e^{-st} dt$$

where the subscript  $L$  indicates the LT. The essential LT property is that the LT of a convolution of two functions is the product of their transforms. Thus, the LT of  $C(t)$  ( $=C_L(s)$ ) described by the convolution relation eq. (2.8) is equal to the product of the LT of the input function ( $I_L(s)$ ) and the LT of the response function ( $h_L(s)$ ):

$$(3.17) \quad C_L(s) = I_L(s) h_L(s)$$

Setting  $s=0$  and using eq. (3.15):

$$(3.18) \quad C_L(s=0) = \int_0^{\infty} C(t) dt = I_L(0) h_L(0) = \int_0^{\infty} I(t) dt \int_0^{\infty} h(t) dt = D / Cl_{ss}$$

using the fact that the integral over  $I(t)$  is the total dose  $D$  and the integral over  $h(t)$  is related to  $Cl_{ss}$  (eq. (3.15)). This completes the derivation for the steady state clearance ( $Cl_{ss}$ ):

$$(3.19) \quad Cl_{ss} = D / AUC \quad AUC = \int_0^{\infty} C(t) dt$$

where  $AUC$  ("area under the curve") is the integral of the  $C(t)$  curve out to very long times following an arbitrary input  $I(t)$ . Note that this expression for  $Cl_{ss}$  is valid for arbitrary site(s) of metabolism and excretion (not necessarily the central compartment) with the only assumption

that the system is linear and the site of sampling  $C(t)$  is from a vein draining a non-metabolizing organs.

### 3.6 Derivation of the $V_{ss}$ relation.

The derivation of the  $V_{ss}$  expression uses the same approach but is more complicated. It is also less general in that an essential assumption is that the clearance is from the central compartment, so that  $Cl$  is time independent and is equal to  $Cl_{ss}$  (see Model 1, eq. (2.19)):

$$(3.20) \quad Q(t) = Cl C_A(t) = Cl_{ss} C_A(t)$$

The general definition of  $V_{ss}$  is:

$$(3.21) \quad V_{ss} = M_{ss} / C_{Ass}$$

where  $M_{ss}$  is the total amount in the system and  $C_{Ass}$  is the arterial concentration after a steady state is established at long times after a constant input  $I_{ss}$ . The total amount of solute in the system as a function of time ( $M(t)$ ) for a steady state input  $I_{ss}$  is given by:

$$(3.22) \quad M(t) = In - Out = \int_0^t [I_{ss} - Cl_{ss} C_A(\lambda)] d\lambda = I_{ss} \int_0^t [1 - Cl_{ss} \int_0^\lambda h(\tau) d\tau] d\lambda$$

In the last equality, the convolution expression eq. (2.8) for  $C_A(\lambda)$  has been used. As  $t$  goes to infinity:

$$(3.23) \quad \begin{aligned} t \rightarrow \infty: \quad C_A(t) &\rightarrow C_{Ass} & Q(t) &\rightarrow I_{ss} = Cl_{ss} C_{Ass} \\ M(t) &\rightarrow M_{ss} = C_{Ass} V_{ss} = I_{ss} V_{ss} / Cl_{ss} \end{aligned}$$

Thus, letting  $t \rightarrow \infty$  in eq. (3.22):

$$(3.24) \quad V_{ss} / Cl_{ss} = M(\infty) / I_{ss} = \int_0^\infty [1 - Cl_{ss} \int_0^\lambda h(\tau) d\tau] d\lambda$$

Integrating eq. (3.24) by parts:

$$(3.25) \quad V_{ss} / Cl_{ss} = \lim_{\lambda \rightarrow \infty} \left\{ [1 - Cl_{ss} \int_0^\lambda h(\tau) d\tau] \lambda \right\} + Cl_{ss} \int_0^\infty t h(t) dt$$

From eq. (3.15), as  $\lambda$  goes to infinity, the term in brackets  $[ ]$  goes to 0 and, because  $h(\tau)$  is exponential (eq. (2.8)), it goes to 0 faster than  $\lambda$  goes to infinity, so that the first term in eq. (3.25) is zero and:

$$(3.26) \quad V_{ss} = (Cl_{ss})^2 \int_0^\infty t h(t) dt$$

The next step is to take the LT of  $t^*C_A(t)$  for an arbitrary input  $I(t)$  using the following property of the LT:

$$(3.27) \quad LT \{t f(t)\} = -\frac{df_L(s)}{ds}$$

Using eq. (3.17) for the LT of  $C_A(t)$ :

$$(3.28) \quad LT\{t C_A(t)\} = -\frac{d[I_L(s)h_L(s)]}{ds} = -I_L(s)\frac{dh_L(s)}{ds} - h_L(s)\frac{dI_L(s)}{ds}$$

Note that from the definition of LT (eq. (3.16)) the derivative is equal to:

$$(3.29) \quad \frac{dF_L(s)}{ds} = -\int_0^{\infty} t F(t) e^{-st} dt$$

Substituting this expression for  $dh_L/dt$  and  $dI_L/dt$  in eq. (3.28) and set  $s=0$  in all the LTs:

$$(3.30) \quad \int_0^{\infty} t C_A(t) dt = \int_0^{\infty} I(t) dt \int_0^{\infty} t h(t) dt + \int_0^{\infty} h(t) dt \int_0^{\infty} t I(t) dt$$

Substituting the definitions of AUMC (eq. (3.1), MIT (eq. (3.1)) and  $Cl_{ss}$  (eq. (3.15) and  $D$  equal the integral over  $I(t)$ :

$$(3.31) \quad AUMC = DV_{ss} / Cl_{ss}^2 + DMIT / Cl_{ss}$$

Solving eq. (3.31) for  $V_{ss}$ , we get the final result and complete the derivation.

$$(3.32) \quad V_{ss} = (Cl_{ss}^2 / D) AUMC - Cl_{ss} MIT \\ = D \left[ \frac{AUMC}{AUC^2} - \frac{MIT}{AUC} \right]$$

where, in the second line, the  $Cl_{ss}$  relation (eq.(3.19) has been used.

This  $V_{ss}$  has two assumptions that are not required for the  $Cl_{ss}$  derivation. The first is that the system's metabolism is from the central compartment. This is essential because it allows the expression of the time dependent metabolism  $Q(t)$  in terms of  $Cl_{ss}$  times  $C_A(t)$  (eq. (3.20). The second assumption, and one that is not usually recognized, is that the arterial blood concentration ( $C_A(t)$ ) must be sampled in AUMC because that is the concentration supplying the site of excretion (eg renal) or metabolism (eg liver). For example, since the antecubital blood concentration ( $C_{ac}$ ) at early times is significantly less than the arterial (see Figure 1-5), using it would underestimate  $Q(t)$  at early times. However, since  $C_{ac}$  differs from  $C_A$  only for a short

time (about 5 minutes) and AUMC is dominated by the integral at long times, this difference is minor.

### 3.7 References

1. Meier P, Zierler KL: **On the theory of the indicator-dilution method for measurement of blood flow and volume.** *J Appl Physiol* 1954, **6**(12):731-744.
2. Takeda Y, Reeve EB: **Studies of the metabolism and distribution of albumin with autologous I131-albumin in healthy men.** *J Lab Clin Med* 1963, **61**:183-202.
3. Ludden TM, Beal SL, Sheiner LB: **Comparison of the Akaike Information Criterion, the Schwarz criterion and the F test as guides to model selection.** *J Pharmacokinet Biopharm* 1994, **22**(5):431-445.
4. Arancibia A, Guttmann J, Gonzalez G, Gonzalez C: **Absorption and disposition kinetics of amoxicillin in normal human subjects.** *Antimicrob Agents Chemother* 1980, **17**(2):199-202.
5. Levitt DG: **The pharmacokinetics of the interstitial space in humans.** *BMC Clin Pharmacol* 2003, **3**:3.
6. van Dorp EL, Morariu A, Dahan A: **Morphine-6-glucuronide: potency and safety compared with morphine.** *Expert Opin Pharmacother* 2008, **9**(11):1955-1961.
7. Penson RT, Joel SP, Roberts M, Gloyne A, Beckwith S, Slevin ML: **The bioavailability and pharmacokinetics of subcutaneous, nebulized and oral morphine-6-glucuronide.** *Br J Clin Pharmacol* 2002, **53**(4):347-354.

#### 4. Physiologically based pharmacokinetics (PBPK): Tissue/blood partition coefficient; toxicological and other applications.

One of the main goals of current PK analysis is to be able to predict a drug's PK just based on its structure and physical chemical properties. This is especially important in the field of drug development where one needs to predict the clinical dosing regimens required to raise the target tissue drug concentration to the required therapeutic levels. If one could accurately predict the levels just based on the drug's structures it would remove the necessity for the large number of animal and human test subjects currently used. The standard approach to this problem is the use of PBPK modeling already used in the examples in the first 3 sections. This section will provide a brief general introduction to the PBPK modeling approach and its strengths and weaknesses. The PBPK parameters that are the most difficult to measure and most uncertain are the tissue/blood partition coefficients and they will be a focus of this section.

As discussed previously, the basic idea of PBPK is to describe the PK in terms of the drug kinetics in each or the major organs of the body using the following organ model (Figure 4-1).

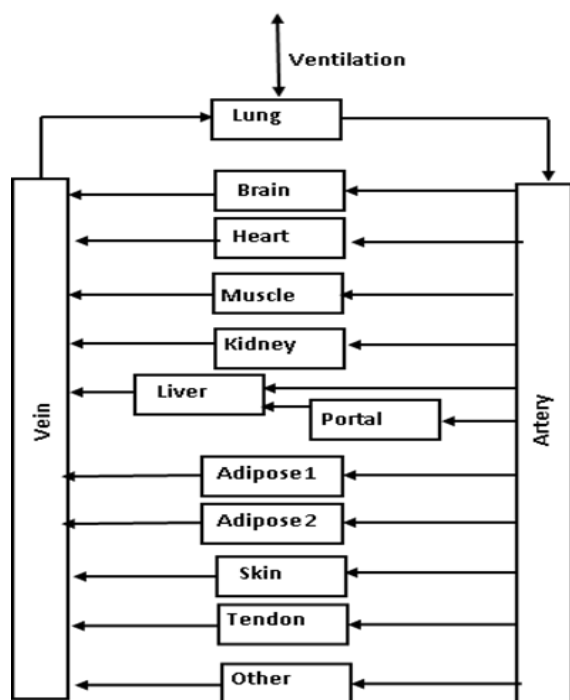


Figure 4-1 PBPK organ model.

Each organ is characterized by a set of parameters that includes, at a minimum, the organ blood flow and the volume of distribution, and possibly, some additional parameters such as metabolism, capillary permeability, protein binding, etc. With 14 organs and, at least, two

parameters/organ, there are a minimum of 28 parameters required to characterize the model. Obviously, the PBPK approach would be useless if all of these parameters were regarded as adjustable for each new solute that was investigated. The crucial step in PBPK analysis is to find a “Standard” parameter set (eg, organ blood flow, weight, etc.) that can be assumed and applied to any solute, minimizing the number of parameters needed to specify each specific solute.

The following diagram ( Figure 4-2) shows the model for organ i that is used to relate the organ parameters (flow, volume, etc.) to the solute PK:

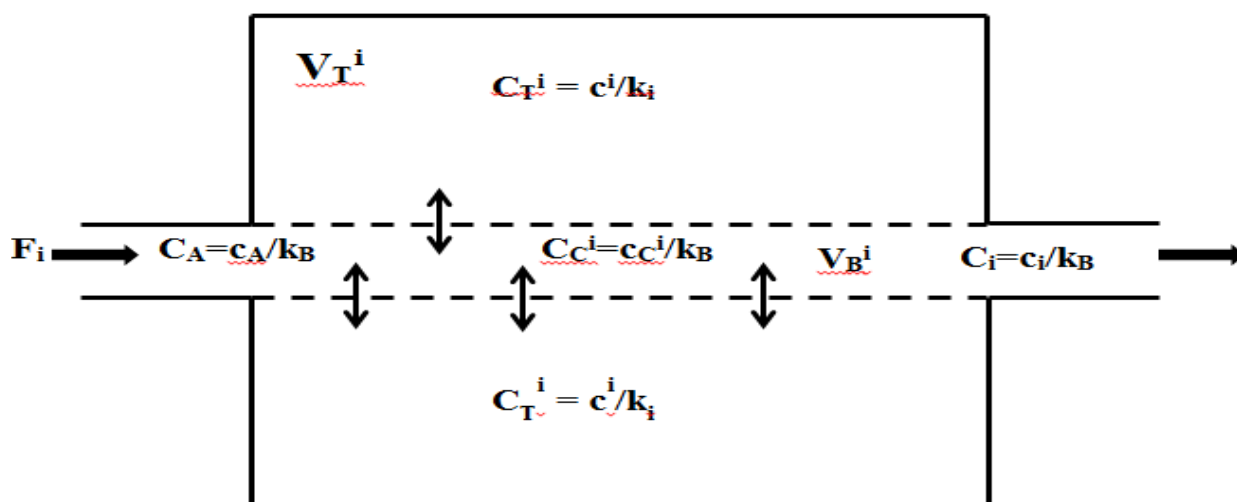


Figure 4-2 Diagram of blood tissue exchange for well-mixed, flow limited case.

$F_i$  is the organ blood flow,  $V_T^i$  and  $V_B^i$  are the anatomical tissue and blood volume and  $C_T^i$ ,  $C_A$ ,  $C_C^i$  and  $C_i$  are the tissue (extravascular), arterial, capillary and venous concentration, respectively. Since the solute may be protein bound, two different concentrations are shown: the total concentration indicated by capital C and the free unbound concentration indicated by the small case c. They are related by k, the fraction of total solute that is free (unbound):

$$(4.1) \quad \begin{aligned} k &= \text{Free Concentration} / \text{Total Concentration} = c / C \\ c &= k C \end{aligned}$$

In the diagram,  $k_B$  and  $k_i$  are the fraction unbound for the blood and organ tissue i, respectively. In Figure 4-2 the complicated and heterogeneous organ arrangement (flow, geometry, etc.) of the individual capillaries is neglected and it is assumed that the entire organ can be represented by one “typical” capillary/tissue region.

As the solute moves down the capillary it equilibrates with the tissue by diffusion across the capillary wall. Although both  $C_C$  and  $C_T$  should vary with the position (linear distance from artery, radial distance from capillary, etc.), it would be extremely complicated and impractical to



try to take account of this. For the case where the capillary permeability is large and not rate limiting, which is valid for the great majority of solutes, the usual PBPK approach is to assume that the organ is “well-mixed and flow limited”. The “well-mixed” assumption means that the tissue region is stirred and the “flow-limited” assumption means the solute in the capillary equilibrates rapidly with the tissue so that the venous concentration leaving the organ has completely equilibrated with the tissue. It should be emphasized that the **concentration that equilibrates is the “free, unbound” concentration c, not the total concentration**. Thus, the “well-mixed and flow-limited assumption implies that (**note that  $C_i(t)$  is the venous concentration leaving organ i**):

$$(4.2) \quad \begin{aligned} c_T^i(t) &= c_C^i(t) = c_i(t) \\ C_C^i(t) &= C_i(t) = c_i(t) / k_B & C_T^i(t) &= c_i(t) / k_i \\ \left( \frac{\text{Tissue Conc}}{\text{Blood Conc}} \right)_i &= C_T^i(t) / C_i(t) = k_B / k_i = K_B^i \end{aligned}$$

where  $K_B^i$  is the “tissue/blood” partition coefficient. Analogous to the definition of the whole body volume of distribution (eq. (2.1)), one can define the volume of distribution for organ i ( $V_i$ ) in terms of the venous concentration leaving organ i ( $= C_i$ ):

$$(4.3) \quad \begin{aligned} V_i C_i &\equiv \text{Total amount of solute in organ } i \\ &= V_B^i C_C^i + V_T^i C_T^i = C_i [V_B^i + K_B^i V_T^i] \\ &\Rightarrow V_i = V_B^i + K_B^i V_T^i \end{aligned}$$

Using this definition of  $V_i$ , the total amount of solute in organ i as a function of time ( $= V_i(t)C_i(t)$ ) is described by the following differential equation describing the balance between organ inflow ( $= F_i C_A(t)$ ) and outflow ( $= F_i C_i(t)$ ):

$$(4.4) \quad V_i \frac{dC_i(t)}{dt} = F_i [C_A(t) - C_i(t)] = F_i [C_A(t) - C_i(t)]$$

The sum of the  $V_i$  over the  $N=14$  compartments is equal to the total human equilibrium volume of distribution ( $V_{eq}$ ) which, as discussed above (eq. (2.27)), if the solute is metabolized in the central compartment, is equal to  $V_{ss}$ :

$$(4.5) \quad V_{ss} \approx V_{eq} = \sum_{i=1}^N V_i$$

Combing all the  $N (=14)$  organs in Figure 4-1 in the PBPK model, although numerically complicated, is conceptually simple. For example, the concentration in the “Vein” compartment is the result of the balance between the venous outflow from each of the  $N-3$  organs (not including the “Vein”, “Artery” and “Lung”) and the output to the “Lung”:

$$(4.6) \quad V_{\text{vein}} \frac{dC_{\text{vein}}(t)}{dt} = \sum_{i=1}^{N-3} F_i C_i(t) - F_{\text{CO}} C_{\text{vein}}(t) + I(t)$$

where  $F_{\text{CO}}$  is the cardiac output and  $I(t)$  is the experimental input to the Vein compartment, if there is any. There would be a similar equation for the “Artery” and “Lung”. In addition, one needs to add the metabolism or excretion term to whatever organ is involved. Numerically integrating the  $N$  coupled differential equations from time 0 to  $t_{\text{end}}$  provides the complete solution for each  $C_i(t)$  as a function of time. As implemented in PKQuest, clicking the “Plot”/“Organs” button lists all the  $N$  organs, and the user can select which of the  $C_i(t)$  are plotted.

Although this “well-mixed, flow-limited” assumption is obviously a great oversimplification, it works surprisingly well. A direct test of this approximation is provided by the PBPK model of the  $\text{D}_2\text{O}$  pharmacokinetics discussed in Section 1.2 (the  $\text{D}_2\text{O}$  PBPK case is the default in PKQuest and is selected by clicking “Run” without selecting any files).  $\text{D}_2\text{O}$  is the ideal solute for testing this assumption since it freely distributes in the blood and tissue water so that binding can be neglected (ie, is not an experimental parameter). In addition,  $\text{D}_2\text{O}$  is not metabolized and its excretion rate (eg, renal) is slow compared to the time course of the experiment and can be neglected. The PBPK model is completely characterized by just the organ water volumes and blood flows, both of which can, theoretically, be directly measured. Since the PBPK model provides a nearly perfect fit to the experimental data (see Figure 1-3), one might infer that the “well-mixed and flow limited” assumption is valid. However, this is not quite correct. The individual organ water volumes used in the PKQuest  $\text{D}_2\text{O}$  calculation are the independently determined, well established anatomical values. However the organ blood flows cannot be directly measured during the PK measurements and the reported normal ranges are quite large. Although the organ flows used in PKQuest are in the reported normal range, they have been tweaked to provide the optimal fit to the data [1]. (The PBPK organ volumes and flows can be seen by clicking the “Organ Par” button.) One can regard the PBPK model organ blood flow as an adjustable parameter that corrects for any errors in the “well-mixed and flow limited” assumption. The fact that the PBPK organ flows are in the ranges that have been directly measured indicates that this assumption is quite good and whatever “adjustment” that is needed is small.

#### 4.1 Tissue/blood ( $K_B^i$ ) or tissue/plasma ( $K_P^i$ ) solute partition coefficient.

The PBPK organ description in eq. (4.6) is deceptively simple. Each organ is characterized by only two parameters: the organ blood flow  $F_i$  and the organ volume of distribution  $V_i$ . Since  $F_i$  can be directly measured and should be relatively constant in, eg, the resting subjects used for PK determinations, and  $V_i$  should be related to the anatomic organ volumes, one might expect that it would be a trivial problem to use PBPK analysis to predict the PK for a given solute. The problem, of course, is the  $K_B$  term in  $V_i$  (eq. (4.3)). Since the value of  $K_B$  can vary from less than 1 to greater than 200, it dominates the PBPK kinetics. A major

focus of modern PK analysis is to predict the PK just from the structure and physical chemical drug properties and there have been intense efforts toward developing algorithms that can do this. As will be discussed in Sections 5 and 7, there are two special classes of solutes for which this prediction is quite accurate (errors of about 10%): 1) the extracellular solutes (eg, amoxicillin and morphine-6-G discussed previously), and 2) the highly lipid soluble solutes. However, for the great majority of drugs that are weak bases or acids it is surprisingly difficult to accurately predict  $K_B$ , which can vary markedly from drug to drug and from tissue to tissue, even for drugs with similar physical chemical properties. Most experimental measurements are of the tissue/plasma partition ( $K_P$ ) which is related to  $K_B$  by:

$$(4.7) \quad \begin{aligned} \text{Tissue / Plasma} = K_P &= (\text{Blood / Plasma})(\text{Tissue / Blood}) \\ &= (\text{Blood / Plasma}) K_B \end{aligned}$$

As an example of the difficulty of predicting  $K_B$ , consider the following Table 4-1 listing the Tissue/Plasma ( $K_P$ ) partition for the 3 weak bases quinidine, propranolol and imipramine.[2] The  $K_P$  of imipramine for two similar tissues such as heart and muscle differ by a factor of 2.5 and imipramine's  $K_P$  is 2 to 5 times higher than the other two drugs. None of these differences can be explained by the small differences in the acid dissociation constant ( $pK_a = 8.56$  (quinidine), 9.4 (imipramine), 9.42 (propranolol)) or lipid solubility ( $\log P = \log \text{octanol/water partition} = 3.44$  (quinidine), 4.8 (imipramine), 3.48 (propranolol)). There is suggestive evidence that these variations in tissue binding might be the result of binding to tissue phospholipids. But, whatever the mechanism, it is difficult to predict  $K_B$  a priori.

**Table 4-1 Tissue/Plasma partition ( $K_P$ ) of quinidine, propranolol and imipramine**

	Quinidine	Propranolol	Imipramine
Lung	43.0	54.2	127.4
Spleen	24.0	14.2	57.4
Kidney	20.7	15.3	45.5
Liver	16.5	11.6	51.9
Intestine	10.1	6.6	23.5
Pancreas	8.7	11.2	43.7
Heart	5.8	7.1	21.9
Muscle	4.3	4.3	8.8
Testis	2.2	8.6	23.7
Brain	0.9	14.0	23.0

The current “state of the art” in predicting  $K_B^i$  is illustrated by the algorithm developed by Poulin and colleagues over many years of analysis. [3] About 50% of the predictions are accurate to within a factor of 2, with about 15% of the predictions off by a factor of greater than 3 fold. How one interprets these errors depends on what the  $K_B^i$  are used for. For the purpose discussed in the introduction to this section of estimating the clinical dosage of a trial drug, this uncertainty is relatively unimportant and this sort of prediction is quite valuable. In contrast, if

one is using PBPK modeling to elucidate some specific PK details, such as the muscle blood flow influence on the D<sub>2</sub>O kinetics discussed in the first example (Figure 1-4), uncertainties of a factor of 2 in the  $K_B^i$  invalidate the advantage of a PBPK model. An error of a factor of 2 in  $K_B$  produces 2 fold changes in the plasma PK concentrations and one could fit the data just as well with, eg, a simple 1-compartment approximation just based on the  $Cl_{ss}$  and  $V_{ss}$  (eq. (2.7)). Thus, in this book, PBPK modeling will be used primarily in the discussion of the extracellular (Section 5) and high lipid soluble solutes (Section 7), solutes for which there is confidence in the accuracy of the  $K_B^i$  values.

There is another complicating factor in how the free concentration ( $c$ ) is defined. As defined above, the free tissue and blood concentrations are equal at equilibrium. This definition must be modified for charged solutes because the equilibrium intracellular free concentration will differ markedly from the blood free concentration because of the cell membrane potential.[3] For example, for a 60 mv resting membrane potential (inside negative), a positively charged solute (weak base) will have an intracellular free concentration 10 times the plasma free concentration while negatively charged solutes (weak acids) will have intracellular free concentration 10 fold less than the plasma free concentration. If one considers the membrane potential effect as a form of intracellular “binding” then using the  $K_B$  defined in eq. (4.2) as the equilibrium total tissue/blood concentration is valid even in the presence of a membrane potential.

Because of the importance of the membrane potential, when experimentally measuring the  $K_B^i$ , it is essential to maintain the normal cellular physiology and integrity. The ideal approach is to establish a steady state in some animal (eg, rat) model by a constant IV infusion. For the non-metabolizing organs, at steady state the blood and tissue are at equilibrium. Then, the animal is sacrificed, the organ tissue is rapidly sampled and homogenized and the average concentration determined. This is the approach that was used to obtain the data in Table 4-1. Because the constant IV infusion is onerous, commonly, the tissue is sampled at long times (eg, 24 hours) after a large bolus dose when the PK are in the “terminal phase” and the drug is in a pseudo steady state. When the tissue is homogenized, the solute in the organ vascular (arterioles, venules, capillaries) compartments are mixed with the extravascular tissue. Usually, this is ignored because the vascular space in most tissues is less than 1% of the total organ water and makes a negligible contribution to the total organ solute. [4] Rarely, for solutes with very low extravascular concentrations (eg, inulin), additional calculations must be applied to estimate the true  $C_{Tissue}$ . [4] It needs to be emphasized that these animal measurements of  $K_B^i$  are only approximations. Firstly, there is the question of whether, eg, values in the rat can be extrapolated to humans. Secondly, the sometimes surprisingly large differences in the values of  $K_B^i$  reported by different laboratories for, supposedly, identical measurement indicates that these are difficult measurements with a number of unknown variables.

## 4.2 Toxicological and other PBPK applications.

By far the most important application of PBPK modeling is in the field of human toxicology and risk assessment.[5] The fundamental assumption is that the toxic effects of a compound in different organs as determined from experimental animal studies will occur at the same tissue concentration in humans. To relate these animal studies to human exposure limits, it is essential to predict the human organ concentrations that result from a variety of exposure regimens and this requires PBPK modeling. Because of the enormous health and economic implications of these exposure limits, this PBPK modeling is highly specialized and focused, with, for example, a detailed set of EPA guidelines that must be met. [6] The software that is used for these calculations must be well characterized, validated and approved for the specific application. A general purpose and educational program such as PKQuest is not acceptable.

A typical PBPK toxicology analysis for a specific agent involves the following steps: 1) determine the organ (eg, brain, liver, etc.) tissue concentrations that produce toxic effects in animal models. 2) Develop an accurate human PBPK model for that agent. This requires animal measurements of  $K_B^i$  and PK validation and model refinement in human subjects. 3) Use the PBPK model to determine the human tissue concentration for a range of daily exposure regimens. This last step can be quite involved. For example, for a respiratory absorbed toxin, it would be necessary to model the effects of different exercise and ventilation levels. Finally, given this data, a government agency would set the exposure limit.

This modeling can become very complicated. For example, the primary toxicity might be from a metabolite and this would require PBPK modeling of both the agent and the metabolite, and their interaction through, eg, liver metabolism. Because of the expense and importance of these calculations, each PBPK model becomes essentially a one-off, with a software routine and set of calculations focused on the properties of this specific agent. For these reasons, these models, as a rule, are not useful for the general purpose PBPK modeling that, eg, PKQuest is used for in this book.

In addition to the toxicological studies, there are a several related uses of PBPK modeling. Because, as a rule, infants and children cannot be used in clinical dosage studies, PBPK modeling has become the favored approach for scaling from adults to children. This requires: 1) An accurate and validated adult PBPK model for the drug; and 2) information about how the adult PBPK parameters (organ blood flow and volume of distribution) scale as a function of age. This is, again, a somewhat specialized application and, although PKQuest could, potentially, be adapted for this, it is not implemented in the current version. One should consult specific references for more details. [7]

Finally, another PBPK application is for the analysis of drugs with non-linear kinetics. If the PK is non-linear, the standard compartmental and non-compartment analysis discussed in Sections 2 and 3 and not valid and concepts such as clearance and volume of distribution become meaningless. The most common reason for non-linearity is that the concentrations become high

enough to saturate either the liver metabolic systems or plasma binding sites. For example, if the liver metabolism saturates one must incorporate information about the liver solute concentration into the model in order to accurately describe the rate of metabolism and this usually requires some sort of PBPK model. Fortunately, the great majority of drugs have linear PK. The reason for this is that drugs, in general, are active at very low concentrations (micromolar or less) that are far below the plasma protein binding or metabolic enzyme (eg, cytochrome P450) capacity. It is only for drugs that are present at high concentrations that non-linearity becomes apparent. The most familiar example of a non-linear solute is ethanol, where blood concentrations routinely reach millimolar levels. The PK and PBPK analysis of ethanol will be discussed in detail in Section 11.

### 4.3 PBPK Software.

Most of the software used for specific toxicological investigations is designed and written just for the specific toxin under investigation and, therefore, is not useful as a general tool. When PKQuest was published in 2002 [1], it was the first general purpose routine specifically designed for general PBPK analysis. That is, it had the human standard PBPK parameters pre-programmed, and specific design features such as inputs of the solute's lipid solubility and protein binding properties. Since then, a number of other commercial PBPK software platforms have been developed, including PBPKPlus (GastroPlus), Simcyp Simulator (Certara), PK-Sym (Bayer) and Cloe PK (Cyprotex). These new programs are designed primarily to meet the drug development and regulatory needs of the pharmaceutical industry.

PKQuest differs from these commercial programs in some fundamental ways. It is designed, not for the specific requirements of pharmaceutical companies, but rather as a tool for learning and understanding PK. Over the 15 years of its development, it has been modified and revised and applied to the investigation of many general PK questions, including the following 7 PK topics: 1) PK of volatile anesthetics and highly lipid soluble compounds [8-11]; 2) PK of extracellular solutes [12, 13]; 3) Antecubital vein PK sampling [14]; 4) Ethanol and non-linear PK [15]; 5) Deconvolution [16]; 6) Capillary permeability limitation [10, 12, 13]; and 7) Oral drug absorption and intestinal permeability [17]. These areas are all topics of general PK interest and, as such, will be covered in this book. None of the commercial routines incorporate all of these features. PKQuest is also extremely user friendly and simple to use. The key feature is the availability of "Example files" illustrating all of the above applications. For any of these applications the user can simply read the appropriate example file and use it as a template for his/her specific application. Finally, and most important, unlike all the other PBPK software routines, PKQuest is free, making it accessible to students and available for use as a supplement in a PK course. The following four examples illustrate a range of different PKQuest applications.

#### 4.4 PKQuest Example: PBPK model for thiopental, a weak acid requiring input of tissue/partition ( $K_B^i$ ) parameters.

As discussed above, for weak acids or bases, PBPK modeling loses most of its predictive advantage because of the requirement for another set of adjustable parameters – the tissue/blood partition ( $K_B^i$ ). Because of this, there will be little discussion of these types of solutes in the book. However, PKQuest can handle these solutes and this will be illustrated in this example.

**Run PKQuest, and Read the “Thiopental.xls” example file.** Thiopental (also known as sodium pentothal) is a rapid onset, short acting barbiturate general anesthetic. It is a weak acid with a pKa of 7.55. This example uses the experimental human antecubital thiopental PK data of Burch et. al. [18] following a 6 mg/kg (=420 mg for 70 kg subject) bolus IV injection in subjects undergoing minor surgery (look at the “Exp Data 1” and “Regimen” tables for the experimental input). Because this is a weak acid, one cannot predict the tissue/blood partition just from its physical chemical properties and it is necessary to input the specific  $K_B^i$  for each organ. Note that in the “Model Parameters” panel, the “Partition” box has been checked. This activates additional options, including the “Partition” button, which opens the following Table 4-2.

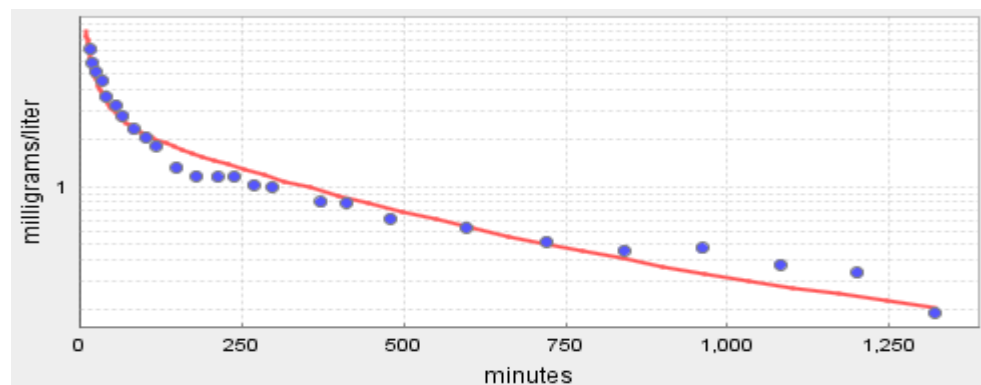
Table 4-2

Tissue/Plasma partition Table	
Organ	Tissue/plasma
liver	2.0
portal	0.7
kidney	3.0
brain	0.7
heart	0.7
muscle	0.4
skin	0.7
lung	0.7
tendon	0.7
other	0.7
adipose	7.0
For each organ set the value of the tissue/plasma partition ratio: The organ "intestine" refers to all organs drained by portal vein. The value of blood/plasma ratio is optional. If it is set = -1, then a default value will be used	

Use of this table requires that the  $K_B^i$  values are input for each organ. **Note that the values input are the “Tissue/Plasma” ( $K_P^i$ ) ratio (not Tissue/Blood)** because this is the value that is usually experimentally measured and reported. These are converted to Tissue/Blood by PKQuest using eq. (4.7) and the input value of “Bld/Plasma” which, in this case, is 1.0. The values of  $K_P^i$  in Table 4-2 are similar to those determined by Ebling et. al. [19] in the rat.

Because of the relatively large octanol/water partition ( $\log P = 2.85$ ) of thiopental, the adipose/plasma partition is quite large ( $\approx 7$ ). One also needs to set the value for the liver clearance. The optimal value for the whole blood “Liver Fr. Clear” is about 0.2. This can be found by picking an initial value of, eg, 0.4 and running the “Minimize” function by clicking the “Parameters” button and checking the box for “Liver”/ “Clearance”.

Running PKQuest with the “Semilog” option yields the follow PBPK model fit to the experimental data:



This is a reasonably good fit, but there clearly is a consistent deviation from experiment for the 100 to 250 and 800 to 1100 minute time periods. An important experimental limitation is that this data is for subjects undergoing minor surgery. This means that the physiological conditions (eg, muscle and intestinal blood flows) change as the subjects complete surgery, anesthesia wears off and the subjects became ambulatory at the later times. This is typical of the problems faced when modeling human data –one almost never has “perfect” experimental data. One might try modifying the model by using different sets of PK parameters for the early time when the subject is anesthetized versus the later ambulatory period. Although this can be done quite easily with PKQuest (see Section 7.1 for volatile anesthetics), there is a point where one is just adding more adjustable parameters and going beyond what the data justifies. The emphasis of this example is to illustrate how to input the partition  $K_B^i$  parameters, not to try and explain the fine points of thiopental PK.

#### 4.5 PKQuest Example: Rat PBPK model for antipyrine.

Although the main focus of this textbook and PKQuest is on application to the PK of humans, PKQuest is applicable to any animal model. This example illustrates the modifications required to apply it to the rat PK. It uses the PK data of Torres-Molin et. al. [20] for antipyrine following an IV input in chronically cannulated rats. Run PKQuest and Read the “Rat antipyrine Example.xls” file. Historically, antipyrine was used as a tracer of water because it is highly permeable and has little tissue binding, and the PBPK settings are similar to those used for the human  $D_2O$  PBPK model. What is modified for the rat is the “Model Organ Parameters” table (opened by clicking the “Organ Par” button). Table 4-3 compares the human versus rat organ weights and perfusion rates:



Organ	Weight (kg)		Perfusion (l/kg)	
	Human	Rat	Human	Rat
vein	4.29	2.83		
artery	1.21	1.415		
liver	1.8	2.184	0.25	0.4
portal	1.5	2.434	0.75	1.5
kidney	0.31	0.424	4	6.78
brain	1.4	0.34	0.56	0.45
heart	0.33	0.17	0.8	5.3
muscle	26	23.203	0.0225	0.1
skin	2.6	9.621	0.1	0.35
lung	0.536	0.243	-1	-1
tendon	3	1.132	0.01	0.075
other	-1	-1	0.02	0.02
adipose	-1	-1	0.07392	0.33
adipose 2	-1	-1	0.01408	0.17
bone	4	1.132	0	0

**Table 4-3 Comparison of PBPK human and rat organ weights and perfusion.**

**Note that these organ weights are for a standard 70 kg, 21% fat animal.** They are modified for the rat “Weight” (=0.335 kg) and “Fat fr” (=0.07) that are input on the top line of the PKQuest window. Running PKQuest, one sees that this PBPK model adequately fits the experimental rat data. Unlike the case for the human PBPK parameters that have been refined after applications to hundreds of different solutes, these rat parameters are just a first approximation that is used here to illustrate how to apply PKQuest to other animals. They will need to be modified for other rat applications.

#### **4.6 PKQuest Example: PBPK model for Amoxicillin oral input.**

There are two different approaches used in this book to estimate the rate and amount of intestinal absorption. The most direct, with the least ambiguity is the deconvolution method (see Sections 9 and 10). This method requires that one has plasma PK data for both a known IV dose, in addition to the oral dose. Ideally, this should be cross-over data in the same set of subjects. The alternative approach is to first develop a PBPK model and then, using this model, estimate the oral dose that would lead to the observed plasma concentration following the oral dose. This latter PBPK method will be illustrated here using the same Arancibia [21] amoxicillin data that is used for the deconvolution method in Section 9, Example 9.3.

Run PKQuest and Read the “Amoxicillin Example PBPK IV.xls” that was used previously in Example 3.3 (see that section for details about the PKQuest settings). Running PKQuest, one gets the following output (Figure 4-3):

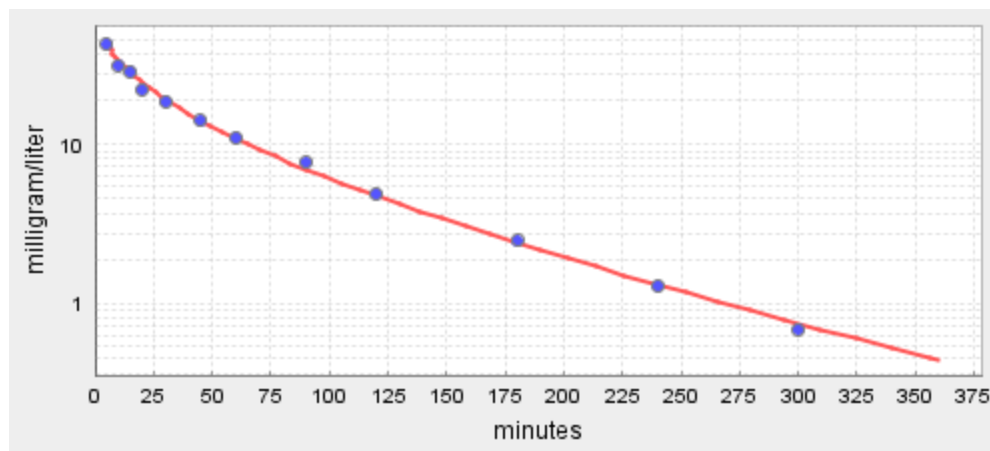


**Figure 4-3 PBPK model fit (red line) to experimental data following bolus IV amoxicillin input.**

It can be seen that the PBPK model provides a good fit to the experimental IV data. Because amoxicillin is an extracellular solute, its PBPK model has only one adjustable parameter (the clearance) and, therefore, one can have strong confidence in its validity.

Start PKQuest again and Read the “Amoxicillin Example PBPK Oral.xls” file. This uses the antecubital plasma PK data following a 500 mg oral capsule in the same set of patients used for the IV dose. [21] It uses same PBPK parameters as were determined using the IV fit, except for changing the site and type of input in the “Regimen” table. The instructions for filling out the Regimen table can be seen by hovering the pointer over the Regimen button. Opening the “Regimen” table:

Dose regimen table — □ ×

Input	Type (1=...	Amount	Start (min)	End or T	Site: 0=v...	N Hill or T	Duration
1	3	370	0	77	2	2.9	-1

There is 1 “Input” into “Site” =2, which specifies intestinal absorption into the box labeled “portal” in Figure 4-1. The input is of “Type=3” (Hill Function). The Hill Function describes the functional form of the intestinal input  $I_{int}(t)$  to the portal vein:

$$(4.8) \quad \text{Amount Absorbed}(t) = \frac{A t^h}{t^h + T^h}$$

$$\text{Absorption Rate} = I_{int}(t) = \frac{h A T^h t^{h-1}}{t^h + T^h}^2$$

where A is the total amount, T is a time constant and h is the Hill coefficient. In the Regimen table, T is input in the “End or T” box and h is input in the “N Hill or T” box. These 3 parameters can be adjusted by entering approximate values (eg, “Amount” = oral dose; “End or T” = 100; and “N Hill” =2) and checking the “Find In..” box. Clicking “Run” will then run a

Powell minimization to find the best parameter set. **Note: this can take up to 30 seconds and, occasionally, cannot find the best fit and needs to be manually stopped using “Task Manager”.** In this case we used the parameters (listed in above Regimen table) that were found by deconvolution in Example 9.3. (As discussed below, the deconvolution intestinal input may differ significantly from the PBPK intestinal input if there is significant first pass hepatic metabolism.) Running PKQuest, we get the output in Figure 4-4. It can be seen that for amoxicillin this deconvolution Hill function input to the PBPK model provides a good fit to the experimental oral data.

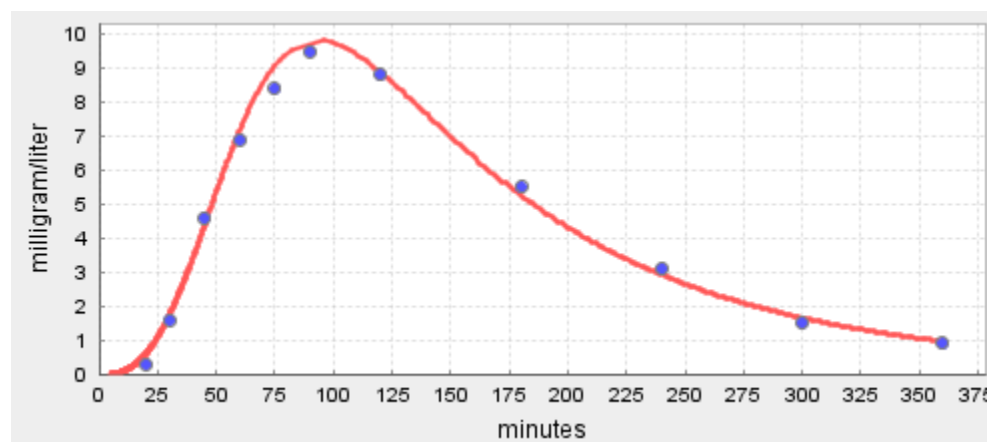


Figure 4-4 Amoxicillin PKQuest PBPK model plasma concentration (red line) for 500 mg oral dose.


As illustrated above, for amoxicillin the intestinal input determined by deconvolution provides a good fit to the PBPK oral input plasma data. There is an important difference between the input function ( $I_{int}(t)$ ) determined by this PBPK method versus that determined by deconvolution. **The PBPK method determines the total amount that is absorbed from the intestine and enters the portal vein while the deconvolution method determines the input into the systemic vascular system after leaving the liver.** They should have the same functional shape (ie, same  $T$  and  $h$ ) but the deconvolution amount ( $A$ ) will be less than the PBPK amount if there is significant “first pass metabolism” of the absorbed solute by the liver before entering the systemic circulation. For amoxicillin, since the clearance is primarily renal, hepatic metabolism is negligible and the PBPK and deconvolution absorption functions should be identical, which, as shown above, they are. Extracellular solutes such as amoxicillin, by definition, have very low cell membrane permeability, are highly polar, and, in general, would be expected to have negligible intestinal permeability. However, the  $\beta$ -lactam antibiotics are exceptions to this rule because they can be absorbed by the small intestinal mucosal peptide transporter. For amoxicillin, 370 mg was absorbed, 74% of the 500 mg oral dose.

#### 4.7 PKQuest Example: Amoxicillin PBPK model for 6 times/day oral dose.

Once the PBPK model has been developed and verified with a known IV dose, it can be used to predict the plasma and tissue levels for arbitrary doses and inputs. In this example we will find the plasma and connective tissue concentration for a standard oral amoxicillin regimen

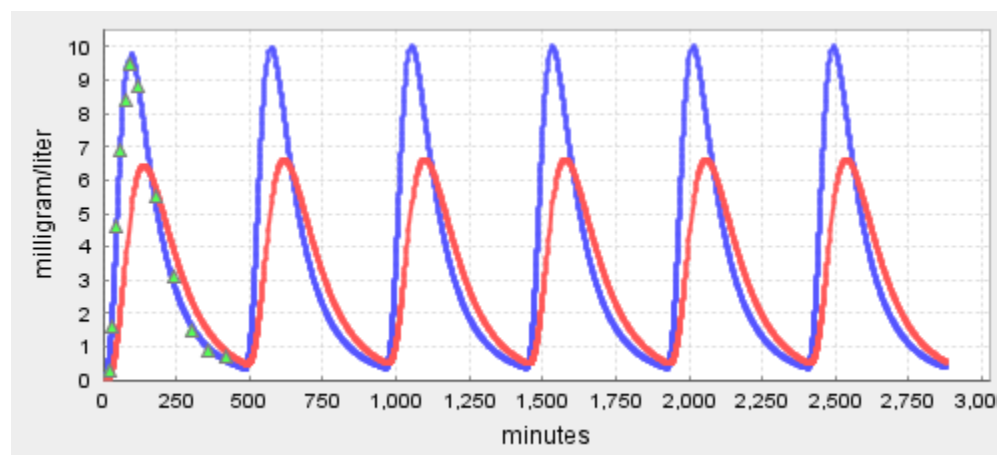
of one 500 mg capsule, 3 times/day. We will use the PBPK model developed above for the IV input along with the Hill function intestinal absorption input function determined above for a single 500 mg capsule.

Start PKQuest and Read the “Amoxicillin Example PBPK oral TID.xls” file. This has the same PBPK model as used previously. Click on the “Regimen” button to view the input:

 Dose regimen table — □ ×

Input	Type (1=c...	Amount	Start (min)	End or T	Site: 0=ve...	N Hill or T	Duration
1	3	370	0	77	2	2.9	-1
2	3	370	480	77	2	2.9	-1
3	3	370	960	77	2	2.9	-1
4	3	370	1,440	77	2	2.9	-1
5	3	370	1,920	77	2	2.9	-1
6	3	370	2,400	77	2	2.9	-1

There are now 6 inputs (set by inputting “6” in the “N input” box). Each one is identical to the Hill Input function determined previously for a single 500 mg capsule input. The 6 inputs are 8 hours apart (determined by the “Start” time). Note that in the “Plot” “Organs” table both the “antecubital” and “other” (connective tissue) boxes are checked. For the antecubital the “Conc Unit” =4 (plasma concentration) and for “other”, the Conc Unit =5 which is the free water tissue connective tissue concentration, which is probably the clinically important value. Run PKQuest, getting the following output:



It shows that the both the plasma and connective tissue concentration fall nearly to zero before the next dose.

#### 4.8 References:

1. Levitt DG: **PKQuest: a general physiologically based pharmacokinetic model. Introduction and application to propranolol.** *BMC Clin Pharmacol* 2002, **2**:5.

2. Yata N, Toyoda T, Murakami T, Nishiura A, Higashi Y: **Phosphatidylserine as a determinant for the tissue distribution of weakly basic drugs in rats.** *Pharm Res* 1990, **7**(10):1019-1025.
3. Poulin P: **A paradigm shift in pharmacokinetic-pharmacodynamic (PKPD) modeling: rule of thumb for estimating free drug level in tissue compared with plasma to guide drug design.** *J Pharm Sci* 2015, **104**(7):2359-2368.
4. Wiig H, DeCarlo M, Sibley L, Renkin EM: **Interstitial exclusion of albumin in rat tissues measured by a continuous infusion method.** *Am J Physiol* 1992, **263**(4 Pt 2):H1222-1233.
5. Campbell JL, Jr., Clewell RA, Gentry PR, Andersen ME, Clewell HJ, 3rd: **Physiologically based pharmacokinetic/toxicokinetic modeling.** *Methods Mol Biol* 2012, **929**:439-499.
6. **Approaches for the Application of Physiologically Based Pharmacokinetic (PBPK) Models and Supporting Data in Risk Assessment.** In. Edited by Agency USEP. Springfield, VA: National Technical Information Service; 2006.
7. Zhou W, Johnson TN, Xu H, Cheung S, Bui KH, Li J, Al-Huniti N, Zhou D: **Predictive Performance of Physiologically Based Pharmacokinetic and Population Pharmacokinetic Modeling of Renally Cleared Drugs in Children.** *CPT Pharmacometrics Syst Pharmacol* 2016, **5**(9):475-483.
8. Levitt DG: **PKQuest: volatile solutes - application to enflurane, nitrous oxide, halothane, methoxyflurane and toluene pharmacokinetics.** *BMC Anesthesiol* 2002, **2**(1):5.
9. Levitt DG: **Heterogeneity of human adipose blood flow.** *BMC Clin Pharmacol* 2007, **7**:1.
10. Levitt DG: **Quantitative relationship between the octanol/water partition coefficient and the diffusion limitation of the exchange between adipose and blood.** *BMC Clin Pharmacol* 2010, **10**:1.
11. Levitt DG, Schnider TW: **Human physiologically based pharmacokinetic model for propofol.** *BMC Anesthesiol* 2005, **5**(1):4.
12. Levitt DG: **PKQuest: capillary permeability limitation and plasma protein binding - application to human inulin, dicloxacillin and ceftriaxone pharmacokinetics.** *BMC Clin Pharmacol* 2002, **2**:7.
13. Levitt DG: **The pharmacokinetics of the interstitial space in humans.** *BMC Clin Pharmacol* 2003, **3**:3.
14. Levitt DG: **Physiologically based pharmacokinetic modeling of arterial - antecubital vein concentration difference.** *BMC Clin Pharmacol* 2004, **4**:2.
15. Levitt DG: **PKQuest: measurement of intestinal absorption and first pass metabolism - application to human ethanol pharmacokinetics.** *BMC Clin Pharmacol* 2002, **2**:4.
16. Levitt DG: **The use of a physiologically based pharmacokinetic model to evaluate deconvolution measurements of systemic absorption.** *BMC Clin Pharmacol* 2003, **3**:1.
17. Levitt DG: **Quantitation of small intestinal permeability during normal human drug absorption.** *BMC Pharmacol Toxicol* 2013, **14**:34.
18. Burch PG, Stanski DR: **The role of metabolism and protein binding in thiopental anesthesia.** *Anesthesiology* 1983, **58**(2):146-152.

19. Ebling WF, Wada DR, Stanski DR: **From piecewise to full physiologic pharmacokinetic modeling: applied to thiopental disposition in the rat.** *J Pharmacokinet Biopharm* 1994, **22**(4):259-292.
20. Torres-Molina F, Aristorena JC, Garcia-Carbonell C, Granero L, Chesa-Jimenez J, Pla-Delfina J, Peris-Ribera JE: **Influence of permanent cannulation of the jugular vein on pharmacokinetics of amoxycillin and antipyrine in the rat.** *Pharm Res* 1992, **9**(12):1587-1591.
21. Arancibia A, Guttman J, Gonzalez G, Gonzalez C: **Absorption and disposition kinetics of amoxicillin in normal human subjects.** *Antimicrob Agents Chemother* 1980, **17**(2):199-202.

## 5. Extracellular Solutes: The pharmacokinetics of the interstitial space.

Solutes that are highly polar or charged are impermeable to cell membranes and, therefore, are limited to the extracellular body space. Since they are not subject to the variable and irregular intracellular binding discussed in the last section, their PK become simpler and more predictable. This was illustrated for the two previously discussed PKQuest PBPK examples of Amoxicillin (Section 3.3 and 4.6) and Morphine-6-glucuronide (Section 3.4) where their complete PK could be accurately predicted with just one adjustable PK parameter (the clearance). It needs to be emphasized that this implies that, not only can one accurately predict the serum drug concentration versus time, but it also means that one has confidence in the PBPK model that is used to predict the tissue concentration and time course in the different body organs, and this has clinical implications.

Unfortunately, only a small minority of drugs are in this extracellular class. Obviously, because they cannot enter cells, their site of action must be extracellular. By far the largest extracellular drug class are the bacterial antibiotics. Since most bacteria remain extracellular, these drugs do not need to enter cells. In fact, this is advantageous because it means there is less likelihood of an adverse drug action. In addition, nearly all hepatic metabolites are extracellular solutes because the main purpose of the liver catabolic machinery is to convert the solutes to a highly water soluble, cell membrane impermeable, form that can be excreted by the kidney. Although these metabolites represents a huge number of solutes, they are usually not of pharmacological interest, with some few exceptions such as morphine-6-G. Another extracellular drug class are the peptide hormones (insulin, TSH, etc.) whose site of action is on cell surface receptors.

PBPK modeling of extracellular solutes requires accurate information about the volume and binding characteristics for each organ  $i$  of the interstitial space ( $V_{Int}^i$ ) which is defined as the extracellular water volume ( $V_{Ecf}^i$ ) minus the plasma water volume ( $V_P^i$ ). The interstitial space is a relatively poorly studied and characterized subject. Following a comprehensive review of the literature by Levitt [1], the following tabulation of  $V_{Ecf}^i$  was developed and is now used in PKQuest.

**Table 5-1 Human extracellular ( $V_{Ecf}$ ) and total water volume and interstitial albumin/plasma concentration ratio ( $K_a$ )**

Organ	Weight (Kg)	Lipid Fraction	Solid Fraction	Solid (Kg)	ecf Fraction	water (L)	water/Kg	$V_{Ecf}$ water(L)	$K_a$
Blood	5.5	0	0.18	0.99	0.595	4.51	0.82	2.68345	
liver	1.8	0	0.3	0.54	0.23	1.26	0.7	0.2898	0.5
portal	1.5	0	0.22	0.33	0.3	1.17	0.78	0.351	0.2
muscle	26	0	0.22	5.72	0.15	20.28	0.78	3.042	0.3
kidney	0.31	0	0.2	0.062	0.165	0.248	0.8	0.04092	0.2

brain	1.4	0	0.2	0.28	0	1.12	0.8	0	0.1
heart	0.33	0	0.2	0.066	0.25	0.264	0.8	0.066	0.3
lung	0.536	0	0.2	0.107	0.2	0.428	0.8	0.08576	0.2
skin	2.6	0	0.3	0.78	0.6	1.82	0.7	1.092	0.2
tendon	3	0	0.15	0.45	1	2.55	0.85	2.55	0.2
other	5.524	0	0.15	0.828	0.8	4.695	0.85	3.75632	0.2
bone	4	0	1	4	0.5	0	0	0	0
adipose	17.5	0.8	0	0	1	3.5	0.2	3.5	0.2
<b>Total</b>	<b>70</b>	<b>0.2</b>		<b>14.15</b>		<b>41.84</b>		<b>17.4572</b>	

It can be seen that  $V_{\text{Ecf}}$  is surprisingly large, with a total water volume of 17.46 liters, or 42% of the total body water. The major organs that contribute to this volume are blood (2.68 l), muscle (3.04 l), skin (1.09 l), adipose (3.5 l), tendon (2.55 l) and “other” (3.76 l).

The inclusion of “other” and “tendon” as main contributors to ecf volumes in this table is an indication of the poorly characterized nature of the  $V_{\text{Ecf}}^i$ . The starting point for the development of this table are the non-compartmental PK measurements of the total steady state volume of distribution ( $V_{\text{ss}}$ ) of extracellular solutes such as amoxicillin or morphine-6-G. This provides a value for the total  $V_{\text{Ecf}}$  (= 17.46 l) that the individual organ  $V_{\text{Ecf}}^i$  must sum to. The  $V_{\text{Ecf}}^i$  for the well-defined organs such as blood, muscle, etc have been directly measured. However, these organs can only account for about 65% of the total  $V_{\text{Ecf}}$ . To account for the rest of the volume, it is necessary to assign it to poorly characterized connective tissue, which has been arbitrarily divided between the two low blood flow organs “tendon” and “other”, with blood flows of 0.01 and 0.02 l/min/kg, respectively. These connective tissue assignments, although based loosely on direct measurements, have been adjusted to provide an optimum fit to the PK of extracellular solutes. The best measure of their validity is that this single PBPK parameter set accurately predicted the PK pharmacokinetics of a diverse set of 11 different extracellular solutes.[1]

Extracellular solutes are protein bound, primarily by albumin, and this binding contributes to the organ volume of distribution. From the general definition of volume of distribution for organ i ( $=V_i$ , eq. (4.3)):

$$(5.1) \quad V_i = V_p^i + K_p^i V_{\text{Int}}^i$$

where  $V_p^i$  is the plasma volume and  $K_p^i$  is the interstitial/plasma partition coefficient. Also, from a consideration of albumin binding kinetics [1], it can be shown that:

$$(5.2) \quad K_p^i = C_{\text{Int}}^i / C_p^i = (1 - K_A^i) k_p + K_A^i$$



where  $k_p$  is the fraction of solute that is free (unbound) in plasma and  $K_A^i$  is the interstitial/plasma concentration ratio of albumin. If the albumin binding is very weak, then  $k_p \approx 1$ , and  $K_P^i \approx 1$ . If the solute is highly bound by albumin, then  $k_p \approx 0$  and  $K_P^i \approx K_A^i$ . Thus, for extracellular solutes,  $K_P^i$  can be predicted from the in vitro measurement of  $k_p$  and the previously tabulated values of  $K_A^i$  (Table 5-1).

Another complicating factor is that the interstitial space is filled with collagen and hyaluronic fibers that can exclude large solutes. This can be directly measured by comparing, eg, the albumin concentration in lymph, which samples the concentration in the “non-excluded” volume, versus the total albumin concentration in the interstitial volume determined with a small solute, eg, EDTA, that distributes in all the interstitial space. This provides a measure of  $V_{Int}^A/V_{Int}^{EDTA}$ , the ratio of the interstitial albumin/EDTA volume, which varies from 0.44 to 0.7 for various tissue measurements. [1].

### 5.1 PKQuest Example: amoxicillin.

This example will illustrate how these concepts are used to model extracellular solutes in PKQuest. Start PKQuest, and Read the “Amoxicillin Example PBPK IV.xls” for the  $\beta$ -lactam antibiotic used previously (Section 3.3). Note that the “Extracellular” box is checked, which turns on the extracellular solute option and activates 3 other parameters: 1) “Plasma fr. free”, which is the value of  $k_p$  in eq. (5.2); 2) “ECF”, which is a scaling factor for  $V_{Int}$ , allowing the possibility of a reduced value of  $V_{Int}$  because of excluded volume effects; and 3) “Cap perm” which is discussed in detail in Section 6. Note that  $k_p$  has been set to 0.83 which is the experimentally determined value of the fraction free in plasma. Also,  $ECF = 1.0$ , so the default PKQuest  $V_{Int}^i$  values are used, and  $Cap\ perm = 1.0$ , which is the flow limited, high capillary permeability condition. Arbitrarily set the Renal Clr = 0.5 and find the optimal renal clearance by clicking the “Parameters” button in the “Minimize” panel and checking the “kidney”/“clearance” box in the table and then “Run”. You should find a good fit to the experimental plasma data for a Renal Clr of 0.35. Save the file (as “Amoxicillin Example.xls”) and exit. **Note: the “Renal Clr” that is entered is the “fraction of whole blood renal flow cleared” in one pass through kidney.** You need to multiply this by the renal blood flow (listed in the “PKquest Output”) to convert to total clearance. Both the fractional and total clearance are listed in the output:

```
kidney Clearance:: Fraction whole blood clearance = 3.53E-1  Total clearance (l/min) = 4.325E-1 Total Blood
Flow (kg/min) 1.225E0
```

As mentioned above, clicking the “Extracellular” box also activates the “Cap perm” option. This allows for a capillary permeability limitation, no longer using the standard “flow limited” tissue assumption. Although this is a special case for extracellular solutes, the experimental documentation of a permeability limitation is such a unique feature of PKQuest that it is the focus of the next section.

## 5.2 References.

1. Levitt DG: **The pharmacokinetics of the interstitial space in humans.** *BMC Clin Pharmacol* 2003, **3**:3.

## 6. Capillary Permeability Limitation.

As discussed in Section 4, it is usually taken as a basic assumption in PBPK modeling that the tissue region is “Well-stirred and flow-limited”. The “flow-limited” assumption means that the capillary permeability is high enough that the venous blood leaving the organ has equilibrated with the tissue. The vast majority of solutes satisfy this assumption. Actually, since one usually cannot experimentally evaluate this assumption, it is more accurate to say that the PK of most solutes can be reasonably well described using this assumption. This flow-limited assumption is so pervasive that most modeling routines are not easily modified to allow for a permeability limitation. In this section, the general formalism for a permeability limitation, along with its implementation in PKQuest will be described. It will be shown that, not only are there are some clear examples of solutes that are definitely permeability limited, but that these examples have may have clinical implications. Capillary permeability limitation is a topic that is rarely discussed in the PK literature and certainly not in PK textbooks. However, since these PKQuest results provide the only available experimental evidence that some drugs are permeability limited, this section was added to make this information and approach more widely available.

In the following figure, the tissue-blood exchange diagram used for the flow limited case ( Figure 4-2) has been redrawn in order to emphasize that the free concentration in the capillary ( $c_c^i(x)$ ) varies with the distance  $x$  from the artery ( $L$  is the capillary length):

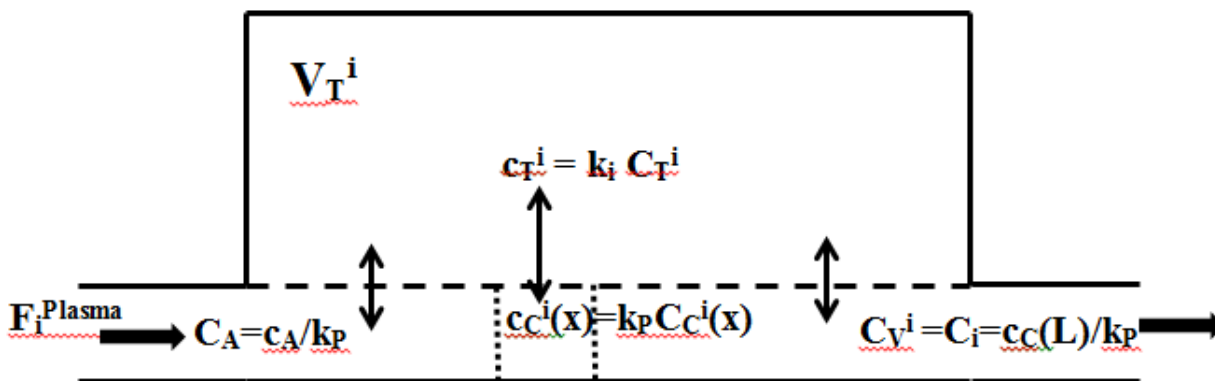


Figure 6-1 Diagram of blood-tissue exchange for diffusion limited, well-mixed organ  $i$ .

where  $F_i^{\text{Plasma}}$  is the organ plasma flow,  $C_A$ ,  $C_T^i$ ,  $C_C^i$  and  $C_V^i = C_i$  are the arterial, capillary and venous plasma concentration, respectively,  $C_T^i$  is the interstitial concentration,  $V_T^i$  is the interstitial volume,  $k_p$  and  $k_i$  are the fraction free in plasma and tissue, respectively, and the small case  $c$  are the effective free concentrations. Note that it is still assumed that the tissue compartment is “well-mixed” so that the tissue concentration ( $c_T^i$ ) does not vary with position.

The exchange rate ( $J$ ) across the narrow segment of the capillary (of length  $dx$ ) indicated by the dotted lines is equal to:

$$(6.1) \quad J = 2\pi a dx P_i (c_c^i(x) - c_t^i)$$

where  $a$  is the capillary radius and  $P_i$  is the capillary permeability and  $2\pi a dx$  is the capillary surface area of the differential region. We will first assume a steady state, so that all concentrations are independent of time. In this steady state, the differential equation describing the balance between capillary solute flow (at rate  $F_i$ ) into and out of the segment is balanced by the diffusive flux across the capillary wall:

$$(6.2) \quad -F_i \frac{dc_c^i(x)}{dx} = -(F_i / k_p) \frac{dc_c^i(x)}{dx} = 2\pi a P_i [c_c^i(x) - c_t^i]$$

Integrating eq. (6.1) over the length of the capillary, from  $x=0$  (artery) to  $x=L$  (vein):

$$(6.3) \quad c_v^i = c_c^i(L) = c_t^i + [c_A - c_t^i] \exp\left(-\frac{k_p P_i S_i}{F_i}\right)$$

Note that for this equation, it has again been assumed that the complicated and heterogeneous organ arrangement (flow, geometry, etc.) of the individual capillaries can be neglected and that the entire organ can be represented by  $N$  “typical” capillary/tissue region illustrated in Figure 6-1. For example, the  $S$  in eq. (6.3) corresponds to the total organ capillary surface area ( $S=2\pi aLN$ ).

The fraction of the solute that “equilibrates” with the tissue ( $f_{Eq}$ ) is defined by:

$$(6.4) \quad f_{Eq}^i = (c_A - c_v^i) / (c_A - c_t^i) = 1 - \exp\left(-\frac{k_p P_i S_i}{F_i}\right)$$

In the limit where the permeability is very large ( $P_i S_i \gg F_i$ ),  $c_v^i = c_t^i$  and  $f_{Eq}^i = 1$ , which is the standard, flow-limited case assumed in Section 4. In the limit where the permeability is small ( $P_i S_i \ll F_i$ ),  $f_{Eq}^i$  approaches 0,  $c_v^i \rightarrow c_A$ , and the capillary is impermeable. Although eq. (6.4) is strictly valid only for a steady state, it is assumed that the change in the total tissue concentration is slow compared to the capillary flow and that eq. (6.4) describes the time dependent relationship between the venous concentration ( $C_v^i = C_i = c_v^i / k_p$ ) leaving organ  $i$  and the tissue concentration ( $C_t^i = c_t^i / k_i$ ) for the general permeability limited case. This relationship is then used to derive a generalization of the flow limited differential equation (eq. (4.4)) for the amount of solute in organ  $i$  as a function of time [1] (details not shown) and this is used in PKQuest.

A theme that is emphasized in this book is that, as the number of PBPK parameters increases, the confidence one has that the PBPK model is valid decreases. The introduction of capillary permeability parameters  $f_{Eq}^i$ , by necessity, introduces more parameters. An attempt has

been made in PKQuest to limit the parameter number by using the following procedure to set the capillary permeability of the different organs. The user inputs just one value, the  $f_{Eq}$  for skeletal muscle, and this, by default, sets the  $f_{Eq}$  for all the other organs: 1) It is assumed that organs with fenestrated capillaries (intestine, kidney) or sinusoids (liver) are flow limited; 2) Muscle, skin, adipose, etc. are assumed to have the same PS as skeletal muscle and their value of  $f_{Eq}^i$  is determined using the known  $F_i$  for these organs; 3) Because of the blood brain barrier, it is assumed that brain capillaries are impermeable for all extracellular solutes. There is also an option in PKQuest that allows the user to arbitrarily input values of  $f_{Eq}$  for each organ.

As shown in eq. (6.4), the degree of deviation from the flow limited case is characterized by the parameter  $\kappa_i$ :

$$(6.5) \quad \kappa_i = \frac{k_p P_i S_i}{F_i}$$

It depends on three different organ properties: 1) the organ blood flow  $F_i$ , 2) the “intrinsic” capillary permeability surface area product  $P_i S_i$ ; and 3) the fraction of solute that is free in the plasma ( $k_p$ ). Although  $k_p$  is of crucial importance, there is almost no recognition of its influence on capillary permeability in the PK literature. The only example that I am aware of is in the use of carbon monoxide (CO) to measure the lung diffusion capacity.[2] Because the exchange of most respiratory gases are flow limited in resting subjects, they cannot be used to determine pulmonary blood-gas permeability. However, because CO has a very small  $k_p$  due to its very tight hemoglobin binding (affinity 220 times that of  $O_2$ ), it is diffusion limited and measurements of its pulmonary exchange rates provide direct measurements of the lung intrinsic permeability (PS).

The extracellular solutes are the most likely to be permeability limited because their low lipid partition coefficient means that they can only leave the capillary via the water filled intercellular clefts and, thus, have a low intrinsic PS. [3] The fact that, as discussed in Section 3.3, the amoxicillin PK can be described using the flow limited model is only suggestive evidence that it is flow limited because of the uncertainties and adjustable parameters in the PBPK models. In fact, there are reasons to suspect that amoxicillin might be permeability limited since EDTA, which is smaller than amoxicillin (292 kD vs 365 kD) does have a measurable capillary permeability in muscle [3]. The diffusion limitation should increase as protein binding increases (ie.  $k_p$  decreases, eq. (6.4)). Dicloxacillin is another  $\beta$ -lactam antibiotic that has much higher plasma protein binding (97% bound, fraction free  $=k_p = 0.03$ ) [4] than amoxicillin ( $k_p = 0.83$ ) and might be expected to have increased capillary permeability limitation. This is discussed in detail in the following PKQuest example.

## 6.1 PKQuest Example: Dicloxacillin, a highly protein bound, diffusion limited $\beta$ -lactam antibiotic.

First, determine the non-compartment  $Cl_{ss}$  and  $V_{ss}$ . Start PKQuest and Read “Dicloxacillin NonComp Example.xls”. This uses the antecubital vein PK data from Lofgren et. al. [5] following a 2 gm constant 30 min IV infusion. Run, using the Semilog plot option. From the output:

AUC = 2.359E4   AUMC = 2.228E6   MIT =15.0  
Clearance = 8.477E-2   Volume of distribution = 6.734E0

The non-compartmental  $V_{ss}$  of 6.73 liters, is less than half that of the 16.1 liters we obtained previously for amoxicillin. Dicloxacillin and amoxicillin are both  $\beta$ -lactam antibiotics. The major difference is that dicloxacillin is highly protein (albumin) bound, with a free plasma fraction of 0.03 versus 0.85 for amoxicillin. Because of this high albumin protein binding, the interstitial volume of distribution is restricted to the interstitial albumin concentration which is less than half the plasma albumin ( $K_A$ , Table 5-1). The volume of distribution of the highly protein bound extracellular solutes provides a direct experimental measurement of the total interstitial albumin [6], a fact that does not seem to be widely recognized.

Start PKQuest again and Read “Dicloxacillin PBPK Example.xls”. This uses the same PK data and tries to fit it with the extracellular, protein binding PBPK model described above. The “Plasma fr. free”. has been set to 0.03 ( $=k_p$ ), the experimental value.[4] Because of this small value of  $k_p$ , one would expect that there might be a significant capillary permeability limitation (see eq. (6.4)). The best fit is obtained with a “Cap Perm”, which is the fractional equilibration ( $=fr_{Eq}$ ) that occurs in skeletal muscle, of about 0.3. That is, there is only 30% equilibration during passage through the muscle. (The flow limited case would be  $fr_{Eq}=1$ , 100% equilibration). The  $fr_{Eq}^i$  for the other organs are then set using eq. (6.4) and the default values of  $(PS)_i/(PS)_{muscle}$ . The PBPK values of  $fr_{Eq}^i$  are displayed in the “Capillary Perm” column of the table opened by clicking the “Organ Par”. (Because of the blood brain barrier, the brain capillary permeability is zero for all extravascular solutes.) Run PKQuest, outputting a good PKPK fit to the experimental data. It should be emphasized that this fit was obtained with just 2 adjustable parameters (“Cap perm” and “Renal Clr”).

To directly see the effect of the capillary permeability limitation, set “Cap perm” =1 (flow limited) and run again. The short and long time comparison of the permeability limited (black line) versus the flow limited predictions are shown in Figure 6-2.

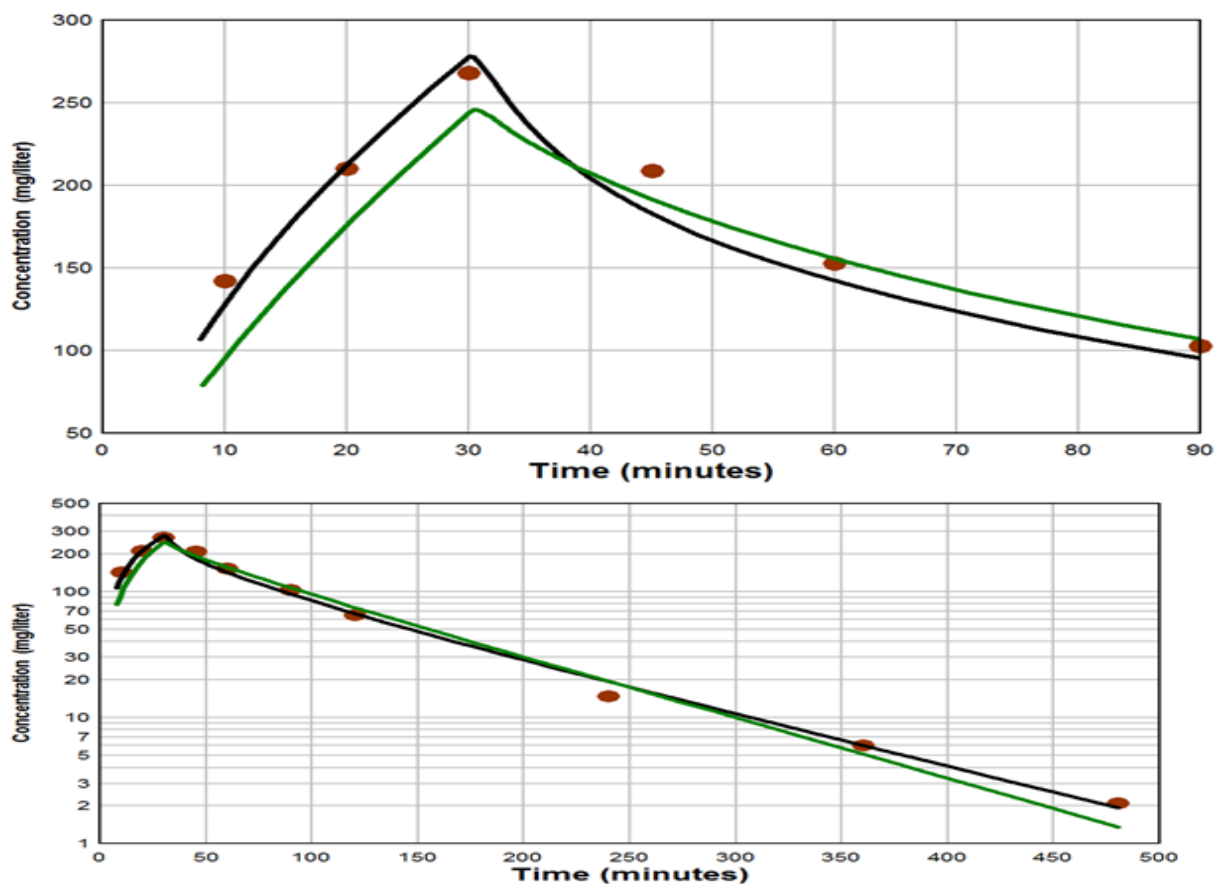


**Figure 6-2** Comparison of permeability limited (Cap Perm = 0.3; black) versus flow limited (Cap Perm=1; green) PBPK model at early (top panel) and long times (bottom panel).

As predicted, the main effect of the permeability limitation is to increase the early time plasma concentration (by about 14%) because the initial rate of loss of dicloxacillin from the vascular system is decreased.

To get an estimate of the clinical significance of this permeability limitation, Run “Dicloxacillin PBPK Example.xls” again. For treatment of, eg, a connective tissue infection, the pharmacologically important parameter would be the “free” concentration in the tissue “other” (= connective tissue). To visualize this, click on the “Plot/Organs” button and unclick “antecubital” and click “other”. Leave the “Conc. Unit” at the default value (=5), which corresponds to free interstitial concentration. Also, set the “Plot/Exp S...” to 0, so that the experimental data is not plotted. Figure 6-3 compares this “Other” interstitial concentration for the permeability limited versus flow limited settings.

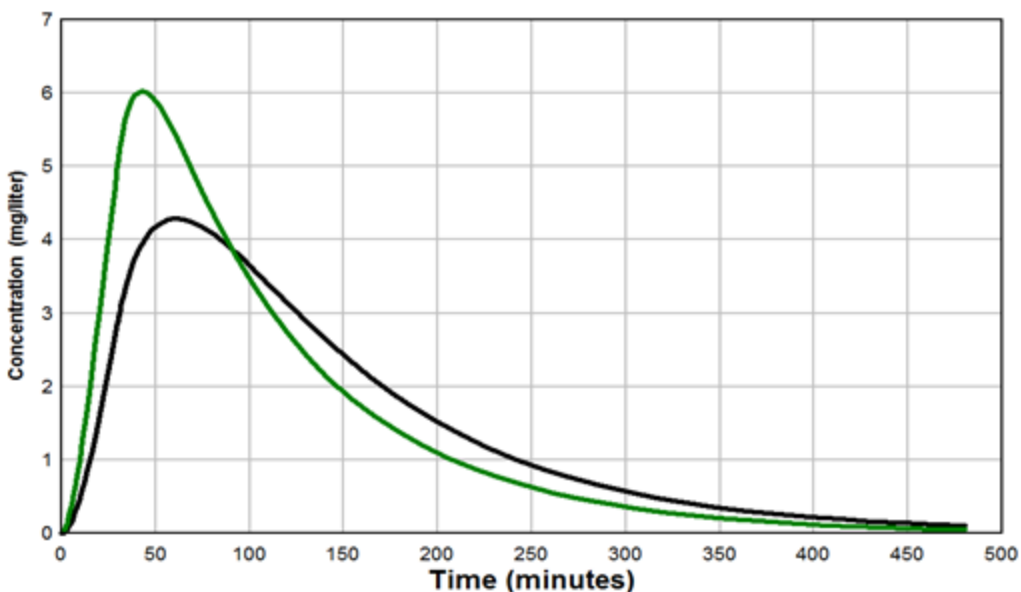


Figure 6-3 Free interstitial dicloxacillin concentration in connective tissue for permeability limited (black) versus flow limited (green) PBPK model.

The peak concentration is about 30% higher for the flow limited case, but the average concentrations are similar, suggesting that the permeability limitation would not have significant clinical effects.

## 6.2 References.

1. Levitt DG: **PKQuest: a general physiologically based pharmacokinetic model. Introduction and application to propranolol.** *BMC Clin Pharmacol* 2002, **2**:5.
2. Bates DV, Boucot NG, Dormer AE: **The pulmonary diffusing capacity in normal subjects.** *J Physiol* 1955, **129**(2):237-252.
3. Crone C, Levitt DG (eds.): **Capillary permeability to small solutes.** Bethesda, Md.: American Physiological Society; 1984.
4. Roder BL, Frimodt-Moller N, Espersen F, Rasmussen SN: **Dicloxacillin and flucloxacillin: pharmacokinetics, protein binding and serum bactericidal titers in healthy subjects after oral administration.** *Infection* 1995, **23**(2):107-112.
5. Lofgren S, Bucht G, Hermansson B, Holm SE, Winblad B, Norrby SR: **Single-dose pharmacokinetics of dicloxacillin in healthy subjects of young and old age.** *Scand J Infect Dis* 1986, **18**(4):365-369.
6. Levitt DG: **The pharmacokinetics of the interstitial space in humans.** *BMC Clin Pharmacol* 2003, **3**:3.



## 7. Highly lipid soluble solutes (HLS): Pharmacokinetics of volatile anesthetics, persistent organic pollutants, cannabinoids, etc.

The PK of the HLS is dominated by their partition into the blood and tissue lipids. Since the “standard” human lipid composition of blood and the different organs can be independently measured, this allows one to predict the PK using a PBPK approach with a minimum of adjustable parameters. The major variable is the body fat content, and this can be roughly estimated from the Body Mass Index (BMI). [1, 2]. This section will review the factors that determine the PK of the HLS, including the distribution of fat in the different organs, with a focus on the adipose tissue and the crucial parameter of adipose blood flow.

The basic assumption that distinguishes the PK of HLS is that the tissue/blood partition coefficient ( $K_B^i$ , eq. (4.2)) is determined solely by the lipid/water partition coefficient ( $P_{L/W}$ ), a parameter that can be measured in a test tube. Figure 7-1 is a diagram of the equilibrium blood and tissue concentrations of a typical organ using this assumption, with  $C_W$  the “free” water concentration,  $C_L^B$  and  $C_L^T$  the blood “lipid” and tissue “lipid” concentration, respectively, and  $f_L^B$  and  $f_L^T$  the lipid fractions of blood and tissue respectively.

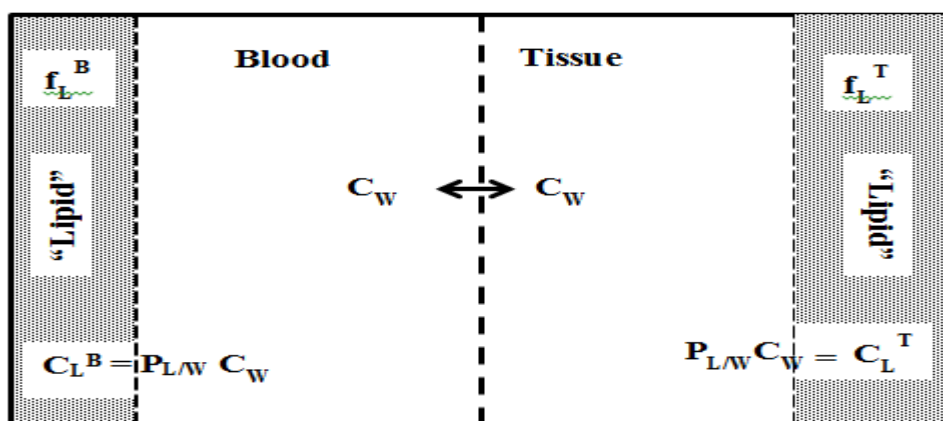


Figure 7-1 Partition of highly lipid soluble solutes between tissue and blood.

Since the blood and tissue  $C_W$  are equal at equilibrium and the lipid concentration is equal to  $P_{L/W} C_W$  where  $P_{L/W}$  is the lipid water partition coefficient, the tissue lipid ( $C_L^T$ ) and blood lipid ( $C_L^B$ ) are also equal ( $C_L^T = C_L^B$ ). With this assumption, the expression for the equilibrium tissue/blood ( $K_B$ ) partition is:

$$\begin{aligned}
 K_B &= \frac{C_T}{C_B} = \frac{(1-f_L^T)C_W + f_L^T C_L^T}{(1-f_L^B)C_W + f_L^B C_L^B} = \frac{C_W[(1-f_L^T) + P_{L/W} f_L^T]}{C_W[(1-f_L^B) + P_{L/W} f_L^B]} \\
 (7.1) \quad &\Rightarrow K_B = \frac{(1-f_L^T) + P_{L/W} f_L^T}{(1-f_L^B) + P_{L/W} f_L^B}
 \end{aligned}$$

Thus,  $K_B$  is determined simply by the fraction of lipid ( $f_L$ ) in the tissue and blood and the lipid/water partition coefficient ( $P_{L/W}$ ).

When  $P_{L/W}$  becomes large ( $>1000$ ), the above expression for  $K_B$  has the following limit:

$$(7.2) \quad K_B = \frac{(1-f_L^T) + P_{L/W} f_L^T}{(1-f_L^B) + P_{L/W} f_L^B} \xrightarrow{P_{L/W} > 1000} f_L^T / f_L^B$$

In this limit,  $K_B$  simply becomes equal to the ratio of the tissue lipid fraction ( $f_L^T$ ) divided by the blood lipid fraction ( $f_L^B$ ). Since most HLS have  $P_{L/W}$  greater than 1000, this is the applicable equation. As discussed below, the appropriate value for  $P_{L/W}$  is ambiguous (within a factor of about 10), but, for this limit, this becomes irrelevant since  $P_{L/W}$  cancels out. In this limit, the adipose blood partition is about 115 ( $f_L^{\text{Adipose}}=0.8$ ,  $f_L^B=0.007$ ). This limit is an important result that is not widely recognized. One of the most important application of PBPK is for the modeling of the “persistent organic pollutants” (POPs) such as polychlorinated biphenyls (PCPs), DDT, dioxins, etc. which have  $P_{L/W}$  of 1 million or more and have lifetimes in humans measured in years. There is a good correlation between the  $P_{L/W}$  and the persistence lifetimes and it is often assumed that this is the result of increased partition into adipose tissue. For example, in an authoritative review, it is stated that “It is now appreciated that physical chemical partitioning of contaminant ... is the primary cause of bioconcentration.” [3] However, as shown in eq. (7.2), the adipose/blood partition reaches a maximum of about 100 for a  $P_{L/W}$  of 1000, and does not increase beyond this limiting value, even for solutes with a  $P_{L/W}$  of 1 million or more. Thus, adipose/blood partitioning, seemingly, cannot explain the increasing biological persistence with increasing  $P_{L/W}$  that is observed for the organic pollutants. This is discussed in detail in Section 8 which focuses on the PK of POPs.

The “Lipid” fraction in Figure 7-1 is in parenthesis to emphasize that the tissue and blood “Lipid” represents all the blood and tissue hydrophobic components, including the membrane lipids and hydrophobic protein regions, in addition to the tissue triglyceride. Albumin is a classic example of a protein that has hydrophobic regions that bind lipid soluble solutes with a high affinity, contributing to the  $P_{L/W}$ . [4] What is the appropriate  $P_{L/W}$  that characterizes this “lipid” partition? A large number of different solutes have been suggested for the “L” component of  $P_{L/W}$ , including olive oil, octanol, decane, hexadecane, and retention on a variety of reverse phase hydrophobic chromatography columns. Unquestionably, a triglyceride such as olive oil ( $P_{oil/W}$ ) should provide the most accurate predictor of  $P_{L/W}$ , for adipose tissue lipid, which is

mostly triglyceride,. There is less certainty about what to use for the non-triglyceride lipids (eg, phospholipids, hydrophobic proteins). Primarily because of its experimental convenience, the octanol/water partition coefficient ( $P_{\text{oct/W}}$ ) is the standard PK parameter that is commonly used to characterize the “lipid”/water partition. Figure 7-2 shows a plot of the ( $\log P_{\text{oct/W}} - \log P_{\text{oil/W}}$ ) versus  $\log P_{\text{oct/W}}$  for nonpolar and polar solutes. [5] It can be seen that for non-polar solutes (left panel),  $P_{\text{oil/W}}$  and  $P_{\text{oct/W}}$  are nearly identical, differing by about 0.1 log unit ( $\approx 25\%$ ). However for polar solutes (right panel) with just one aliphatic hydroxyl,  $P_{\text{oct/W}}$  is about 1 log unit (i.e. 10 fold greater than  $P_{\text{oil/W}}$ , presumably because the octanol hydroxyl increases the affinity for these solutes. The difference becomes greater as the solute polarity increases. Thus, using  $P_{\text{oct/W}}$  for polar solutes will overestimate the true  $K_B$  for adipose tissue by a factor of 10 or more. Although there is suggestive evidence that  $P_{\text{oct/W}}$  is superior to  $P_{\text{oil/W}}$  for predicting partitioning into the non-triglyceride “lipids” (eg, phospholipids, etc.), the evidence is quite limited.[6] Poulin and Haddad [7] have developed a partition model in which the tissue “lipid” is proportioned into “triglyceride” (with  $P_{\text{oil/W}}$ ) and “non-triglyceride” (with  $P_{\text{oct/W}}$ ). Although this addition of another adjustable parameter improves the partition predictions, it increases the PBPK model complexity and ambiguity. The following, simpler, approach has been developed in PKQuest and it has been very successful in predicting the PK of HLS. [5]

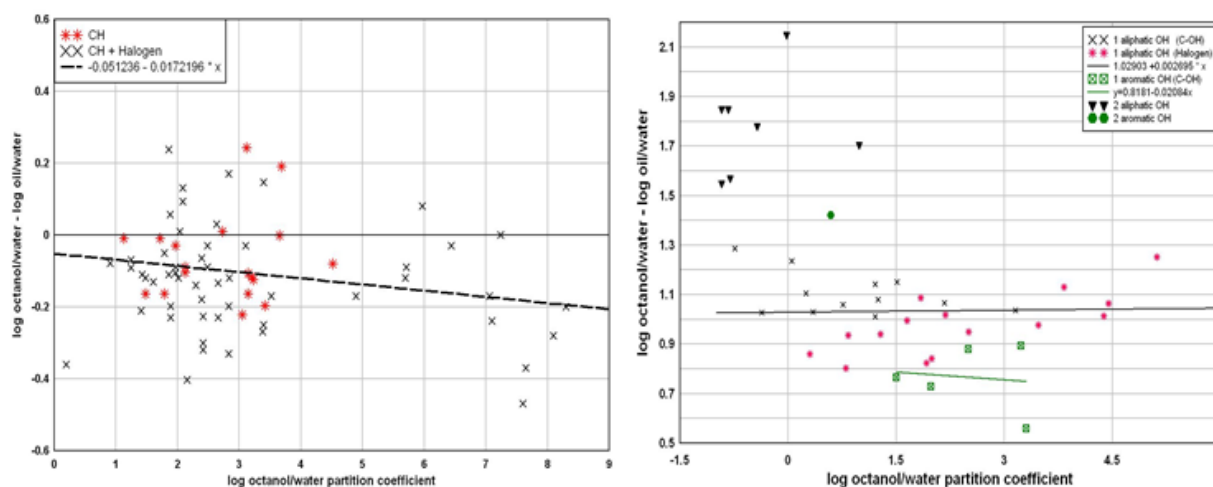


Figure 7-2 Plot of  $\log \text{octanol/water} - \log \text{oil/water}$  versus  $\log \text{octanol/water}$  for nonpolar (left) and polar (right) solutes.

The approach used in PKQuest to avoid the uncertainty in the definition of  $P_{L/W}$  is to arbitrarily use  $P_{\text{oil/W}}$  for  $P_{L/W}$  and then find the equivalent “oil” fractions ( $f_L^i$ ) for blood and the other PBPK tissues. There have been extensive measurements of the four in vitro partition coefficient that completely characterize PK of the volatile anesthetics: the water/air ( $P_{W/\text{air}}$ ), olive oil/air ( $P_{\text{oil}/\text{air}}$ ), blood/air ( $P_{\text{bld}/\text{air}}$ ) and homogenated tissue/air ( $P_{T/\text{air}}^i$ ). The tissue/water ( $C_T^i/C_W$ ) and blood/water ( $C_B/C_W$ ) partition are then described by (see eq. (7.1)):

$$\begin{aligned}
 (7.3) \quad C_T^i / C_W &= P_{T/air}^i / P_{W/air} = (1 - f_L^{T_i}) + P_{oil/W} f_L^{T_i} \\
 C_B / C_W &= P_{bld/air} / P_{W/air} = (1 - f_L^B) + P_{oil/W} f_L^B \\
 P_{oil/W} &= P_{oil/air} / P_{W/air}
 \end{aligned}$$

Equations (7.3) can then be solved for the blood ( $f_L^B$ ) and tissue ( $f_L^T$ ) lipid fractions which determine  $K_B$  (eq. (7.1)).[5] Because of the use of the olive/oil partition, these should be interpreted as the “triglyceride equivalent” lipid fractions. Table 7-1 summarizes the results of this analysis for the Standard 70 kg, 21% fat human. These are the parameters that are used in PKQuest.

**Table 7-1 Triglyceride equivalent “Lipid” fractions of blood and organs for Standard 70 kg, 21% fat human**

Organ	Weight (kg)	Perfusion l/min/kg	Lipid Fraction	Total Lipid
vein	4.29		0.05 -1.5	0.0429
artery	1.21		0.05 -1.5	0.0121
lung	0.536		0.0136	0.00729
liver	1.8	0.25	0.02	0.036
portal	1.5	0.75	0.016	0.024
kidney	0.31	4	0.0136	0.004216
brain	1.4	0.56	0.0176	0.02464
heart	0.33	0.8	0.0136	0.004488
muscle	26	0.0225	0.0136	0.3536
skin	2.6	0.1	0.0136	0.03536
tendon	3	0.01	0.0136	0.0408
other	5.6	0.02	0.0136	0.07616
adipose	8.67	0.07392	0.8	6.936
adipose 2	8.67	0.01408	0.8	6.936
Bone	4	0		0
<b>Total</b>	<b>70</b>			<b>14.53</b>

Of the total 14.6 kg of “lipid”, 13.92 or 95% is in the adipose tissue. Since, the adipose tissue dominates the PK of the highly lipid soluble solutes (HLS), accurate estimates of the adipose perfusion rates are essential for the PBPK predictions of the PK for HLS. Note that in Table 7-1 the adipose tissue has been divided into two equal weight compartments (“adipose” and “adipose 2”), with perfusion rates differing by a factor of about 5. The well-mixed flow limited time constant ( $T_{FL}$ ) for adipose tissue equilibrium is:

$$(7.4) \quad T_{FL} = (\text{Adipose} / \text{Blood Partition}) / (\text{Perfusion Rate}) = K_B^{Ad} / F_{Ad}$$

Since the adipose/blood partition coefficient is about 50 for the volatile anesthetics, T varies from about 11 hours for “adipose” to 2.5 days for “adipose 2”. Recognition of these extremely long equilibration times is essential for understanding the PK of the HLS, and it is not appropriately emphasized in most PK textbooks. In order to accurately characterize this adipose perfusion heterogeneity, it is essential to have PK measurements that are at least 3 days long, which are extremely rare. Probably the best measurements of this type are those of Eger and colleagues that determined the 6 day washout of the volatile anesthetics desflurane, isoflurane, halothane, and sevoflurane. [8, 9] These were the measurements that were modeled with PKQuest in order to determine the perfusion rates for “adipose” and “adipose 2” in Table 7-1. This is discussed in more detail in the next three sections.

## 7.1 Volatile anesthetics

Volatile anesthetics provide the ideal solute to use to calibrate the PBPK parameters for a highly lipid soluble solute (HLS) because they are not metabolized and their excretion rate is determined only by respiratory exchange. The PKQuest PBPK modeling of the three anesthetics isoflurane, sevoflurane and desflurane will be described in this section. Their PK are completely characterized by the three in vitro partition coefficients: water/air ( $P_{W/air}$ ), olive oil/air ( $P_{oil/air}$ ) and blood/air ( $P_{bld/air}$ ) listed in Table 7-2

Table 7-2 Partition coefficients for volatile anesthetics

	Blood/air	Water/air	Oil/air
Isoflurane	1.33	0.544	88.2
Sevoflurane	0.62	0.37	47
Desflurane	0.52	0.225	17.9

PBPK modeling of the volatile anesthetics requires two modifications of the standard PBPK approach discussed in Section 4. First, one must modify eq. (4.3) for the volume of distribution of the lung ( $V_{Lung}$ ) (defined in terms of the concentration in the blood leaving the lung =  $C_{Lung}$ ) to take account of the alveolar gas space:

$$\begin{aligned}
 V_{Lung} C_{Lung} &\equiv \text{Total amount of solute in Lung} \\
 (7.5) \quad &= V_B^{Lung} C_{Lung} + V_T^{Lung} C_T^{Lung} + V_{Alv} C_{Alv} = C_{Lung} [V_B^{Lung} + K_B^{Lung} V_T^{Lung} + V_{Alv} / P_{bld/air}] \\
 &\Rightarrow V_{Lung} = V_B^{Lung} + K_B^{Lung} V_T^{Lung} + V_{Alv} / P_{bld/air}
 \end{aligned}$$

where  $V_B^{Lung}$  is the blood lung volume,  $V_T^{Lung}$  is the solid tissue volume,  $V_{Alv}$  is the alveolar volume and  $C_{Alv}$  is the alveolar gas concentration. The tissue/blood partition ( $K_B^{Lung}$ ) is given by the standard relation for highly lipid soluble solutes (eq.(7.1)). Equation (7.5) assumes that the alveolar gas is in equilibrium with the blood concentration leaving the lung ( $C_{Lung}$ ) so that  $C_{Alv} = C_{Lung}/P_{bld/air}$ . Second, one also needs to modify the mass balance relation (eq. (4.4)) to take account of the alveolar ventilation  $\dot{V}_{Alv}$ :

$$(7.6) \quad V_{Lung} \frac{dC_{Lung}(t)}{dt} = F_{CO} [C_V(t) - C_{Lung}(t)] + \dot{V}_{Alv} [C_{Inhaled}(t) - C_{Lung}(t) / P_{Bld/air}]$$

where  $F_{CO}$  is cardiac output (= lung blood flow),  $C_V(t)$  is the mixed venous blood concentration that enters the lung and  $C_{Inhaled}(t)$  is the inhaled gas concentration, which is one form of inputting volatile solutes. Equation (7.6) is the ideal lung relation. In the actual lung, there is some degree of “perfusion/ventilation mismatch” which increases during anesthesia or lung disease and PKQuest has an option for including this (see [10] for details). The following two examples will provide detailed illustrations of using PKQuest for the PBPK modeling of the volatile anesthetics.

## 7.2 PKQuest Example: Short term PK of volatile anesthetics.

In this section, PKQuest will be used to model the short term (3 hours) PK of the isoflurane, sevoflurane and desflurane using the data from Yasuda et. al. [8, 9] for anesthetized humans. Start PKQuest and read the file “Isoflurane Example.xls”. The following lists the PKQuest input parameters that characterize this experimental data:

- 1) For a respiratory gas input, everything scales for ventilation which scales with weight, so the weight = 70 kg is arbitrary. The “Fat fr” = 0.154 is based on the experimental subjects weight and height.
- 2) The “Volatile” check box is checked, turning on this option and activating the inputs  $K_{air}$  ( $=P_{Bld/air}$ ),  $K_{wair}$  ( $=P_{W/air}$ ),  $K_{fwat}$  ( $=P_{oil/air}/P_{W/air}$ ) which have the values listed in Table 7-2. The “Blood fat fr” is optional, and can be used to estimate  $P_{Bld/air}$  if it is not available. The “Perf/vent stdf” and the “stdV” are both set = 2, which are the standard values of ventilation/perfusion mismatch for humans while anesthetized. The rate of alveolar ventilation(= “Vent”) is set = 3.9 l/min/70 kg, which was experimentally determined during the first 180 minutes of the anesthesia. This is an important parameter since it determines the rate of uptake of isoflurane during the first 30 minutes and the excretion rate for the following time. The alveolar volume (= “Vol” = 3 liters) is the normal standard value.
- 3) The experimental input in these subjects was the inhalation of a fixed isoflurane gas concentration for 30 minutes. Corresponding to this, the “Input/Regimen” table has a constant input (“Input” = 1) for  $t=0$  to 30 minutes, that is inhaled (“Site” = 9). The “Inspired Conc” is arbitrarily set = 1, because the experimental data (see below) is relative to this inspired concentration.
- 4) The “Exp Data 1” table are the experimental “end expiration” gas concentration ( $= C_{Alv}$ ). They are in units of expired/(inspired input).

5) The “Input/Amount Unit” = centiliter, so the concentration = centiliter/liter which equals percent of the input concentration.

6) The “Plot/Organs” table has the “Lung” box checked with the “Conc Unit” = 6, which is the alveolar gas concentration which equals the experimentally measured end expiratory gas concentration.

Running PKQuest, yields the following output Figure 7-3 for the Absolute (left panel) and Semi-log plots (right panel). It should be emphasized that this excellent agreement with experiment was obtained with a model that had **zero** adjustable parameters. The only inputs are the three in-vitro partition coefficients listed in Table 7-2. The excretion rate is determined by the experimentally measured alveolar ventilation and is not an adjustable parameter.

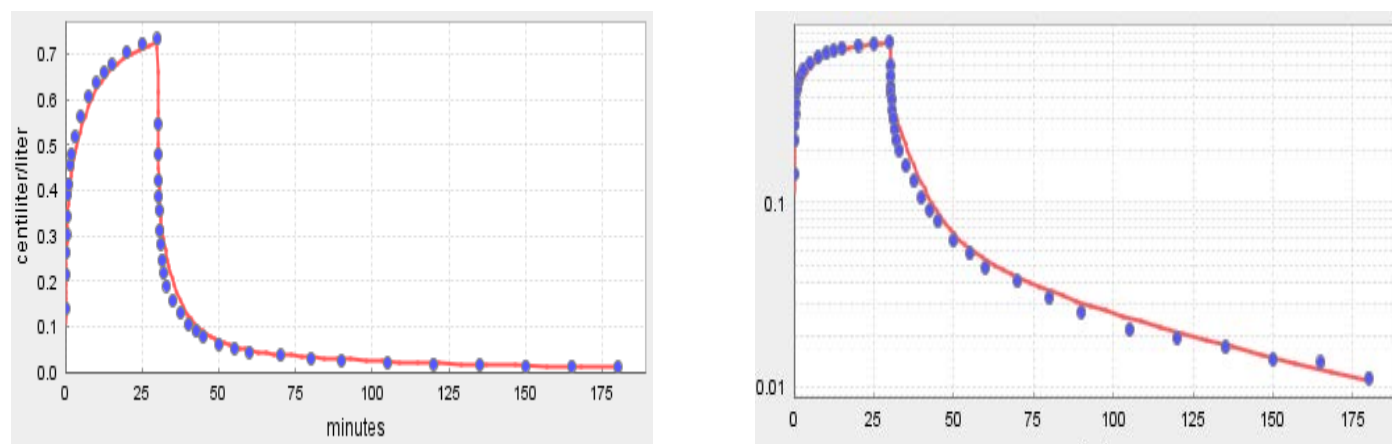


Figure 7-3 PKQuest PBPK output for Isoflurane. Absolute (right panel) and Semi-log (left panel).

The “Example” folder also includes the PKQuest files for the sevoflurane and desflurane experiments using the partition parameter sets in Table 7-2. You should “Read” and “Run” these yourselves. Figure 7-4 shows the semi-log plot for the 3 gases. The fit for desflurane (purple) at times greater than 100 minutes is considerable worse than that for isoflurane (black) or sevoflurane (green).

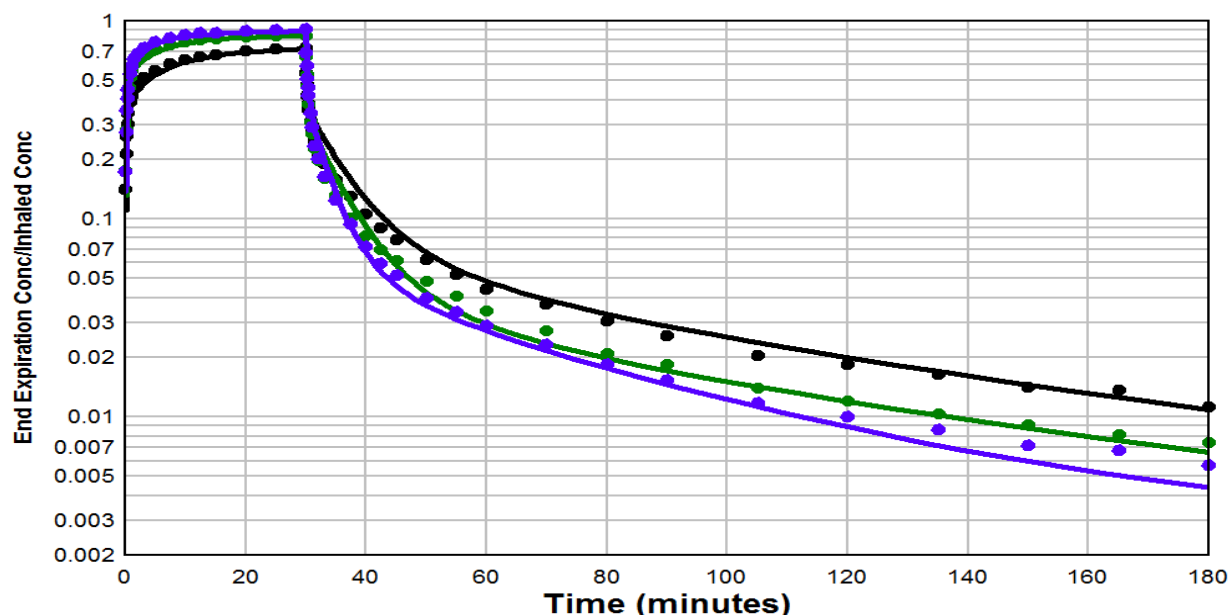


Figure 7-4 PKQuest PBPK model (solid lines) for isoflurane (black), sevoflurane (green) and desflurane (purple).

### 7.3 PKQuest Example: Adipose tissue perfusion heterogeneity and time dependent PBPK calculations.

The above PBPK plots used a PBPK model with two adipose compartments, one with a perfusion rate about 5 times the other. This example describes the experimental basis for this. Start PKQuest and “Read” “Isoflurane Example.xls” again. Open the “Organ Par” Table and modify the “Perfusion” rates for the two adipose organs so they have identical rates, equal to the average perfusion for the two organs ( $=0.044$  l/kg/min). That is, there is now, effectively, just one adipose organ with the same total adipose perfusion as in the original case. Run PKQuest again, and note that the agreement of the model with the experimental values is nearly as good as in the original, heterogeneous case. This is just what one predict from the above discussion of the time constant  $T$  (eq. (7.4)) for the adipose tissue. The adipose/blood partition for isoflurane is 56, so that  $T$  for the two adipose compartments with perfusion rates of 0.074 and 0.014 l/min/kg is 756 and 4000 minutes, respectively. During the 180 minute time course of the above PBPK runs, the adipose tissue is far from saturation and behaves like an infinite sink and the only parameter that affects the PK is the total adipose blood flow, which is identical for the two cases that you just tried. In order to see clear indications of the heterogeneity of the adipose blood flow, the experiments must be carried out to times greater than 4000 minutes (2.8 days). In this section, PBPK analysis of the PK data of Yasuda et. al. [8, 9] out to 5 days will be modeled.

There is an additional complication with this data in that the PBPK parameters change during the course of the experiment. During the first 180 minutes, the patients were anesthetized and ventilated at a rate of about 3.9 l/min (the value input in the above PBPK calculations).



However, after about 500 minutes, the patients wake up, become ambulatory and increase their average alveolar ventilation ( $\dot{V}_{Alv}$ ). Since  $\dot{V}_{Alv}$  determines the excretion rate of the anesthetic, it is a crucial parameter in the determination of the PK. In order to model this data it is necessary to use a time dependent PBPK model. This is illustrated in the this example, where  $\dot{V}_{Alv}$  is 3.9 l/min for the first 500 minutes, and then increases by a factor of 1.3 to 5.1 l/min after 500 minutes out to 5 days. This is, of course, only a rough approximation since the  $\dot{V}_{Alv}$  obviously varies markedly during the day, depending on the level of activity. Although it was not directly measured and was adjusted to provide an optimal fit to the data, 5.1 l/min is a reasonable estimate for the average 24 hour alveolar ventilation. [11]

Start PKQuest and Run the “Isoflurane Long Example.xls” file. Note that “Vent” ( $=\dot{V}_{Alv}$ ) has been set to 5.1 l/min, the desired rate during the ambulatory time. Everything else is identical to “Isoflurane Example.xls” except that there is no input (N input = 0) and the “Exp Data 1” table now has data out to 7,200 minutes (5 days). The goal is to run “Isoflurane Example.xls” ( $\dot{V}_{Alv}$ = 3.9 l/min) for the first 500 minutes and then switch to “Isoflurane Long Example.xls” ( $\dot{V}_{Alv}$ = 5.1 l/min) for the rest of the time. Use Excel to view the file “Isoflurane time dependent Example.xls”. This is the PKQuest format required to determine the sequence of PKQuest files that are run. The first line is a comment and is arbitrary. The second line is of the form: “Number of files” | N (where N is the input number of files). The third line is “File Name” | “End Time”. Line 4 through 4+N-1 are the complete File Path to PKQuest file | End time. Note that in “Isoflurane time dependent Example.xls” there are N = 2 files, with “Isoflurane Example.xls” the first, followed by “Isoflurane Long Example.xls” (**Note: need complete file path**), and the time of the switch between the two files is at 500 minutes.

Restart PKQuest and check the “Time Dependent” check box and then “Read” the “Isoflurane time dependent Example.xls” file. (**Note: it is essential that the check box is checked before this file is read**). Click the “Data Files” button to view the sequence of files that are used. Select the “Semilog” option and Run, getting the following excellent agreement between the experimental results and PBPK prediction (Figure 7-5):

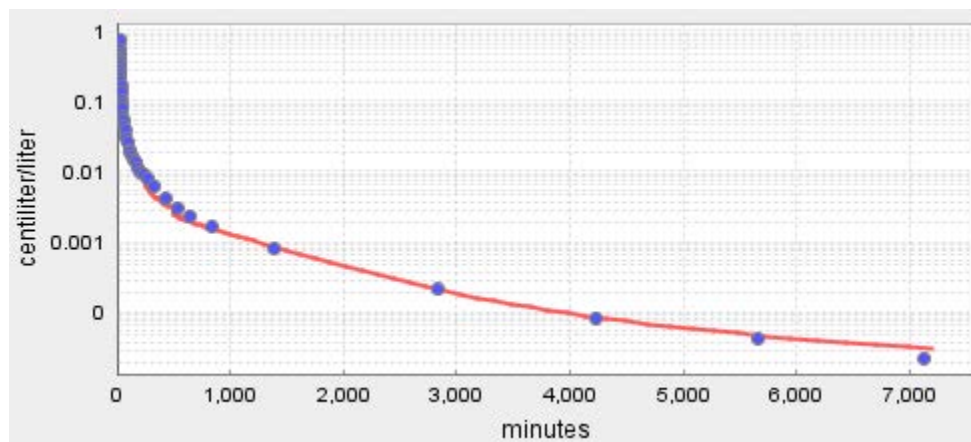


Figure 7-5 Semi-log plot of PKQuest output for time-dependent PKQuest model. Alveolar ventilation is 3.9 l/min for the first 500 minutes, and 5.1 l/min after 500 minutes.

There is one adjustable parameter in this PBPK model, the value of the ambulatory  $\dot{V}_{Alv}$  after 500 minutes.

Also included in the Example folder are the PKQuest files “Isoflurane 1 adipose Example.xls”, “Isoflurane long 1 adipose Example” and “Isoflurane time dependent 1 adipose Example.xls”, that are the corresponding time dependent files for the case where the two adipose tissues have identical perfusion rates equal to the average (effectively one adipose compartment). Figure 7-6 shows the comparison of the two models:

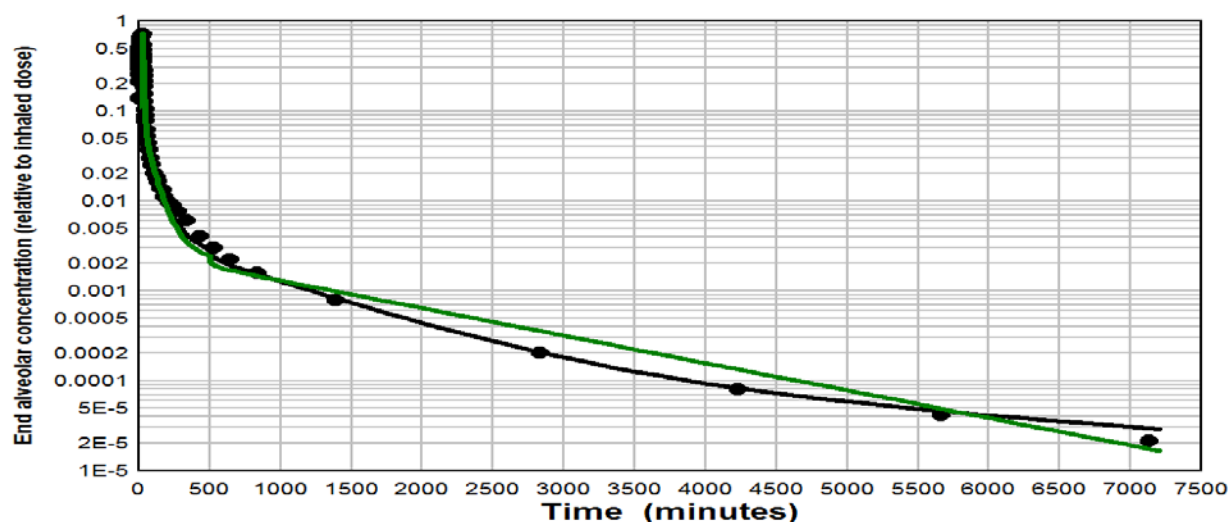


Figure 7-6 Isoflurane PK. Comparison of the heterogeneous 2 adipose compartment model (black) versus the 1 compartment model (green).

It can be seen that, although the one adipose compartment model (green line) fit to the data is significantly worse than two compartment model (black), it is still satisfactory for most prediction purposes.

## 7.4 PKQuest Example: Cannabinol – Non-volatile highly lipid soluble solute.

It may be expected that the PBPK model using the “lipid” fractions ( $f_L$ ) determined for the volatile anesthetics (eq. (7.1)) provide a good fit to the PK of the volatile anesthetics. A better test is whether this model also predicts the PK of other classes of highly lipid soluble solutes (HLS). Cannabinol is an HLS with an estimated  $P_{oil/W}$  of 257,000, extrapolated from  $P_{oct/W}$ . [5] For solutes with this very high  $P_{oil/W}$ , the expression for  $K_B$  (eq. (7.1)) has the limiting form of eq. (7.2) with  $K_B$  equal to the tissue/blood lipid fraction.

This PKQuest example use the PK data of Johnsson et. al. [12] for the antecubital plasma cannabinol concentration following a 2 min IV infusion of 20 mg (=20,000 micrograms, the plasma concentration unit). Start PKQuest and Read the “Cannabinol Example.xls” file. The HLS option is selected for this non-volatile solute by checking the “Fat/water partition” check box which then activates the three parameters “Kfwat”, “free plasma fr” and “Blood fat fr”. Kfwat is equal to  $P_{L/W}$  which, as discussed above, if it is large enough (ie, >10,00) just leads to the limit in eq.(7.2). That is, any large value will produce the same PK. Unlike the case for the volatile solutes where the experimental measurement of  $P_{bld/air}$  determined the blood fat fraction, for cannabinol the blood fat fraction has been set to 0.0075, the normal blood fat fraction. (For other HLS solutes that might have some specific albumin binding, this blood fat fraction might be larger and could be regarded as an adjustable parameter). As shown in Figure 7-7, the agreement between the PBPK model prediction and experimental data is excellent.

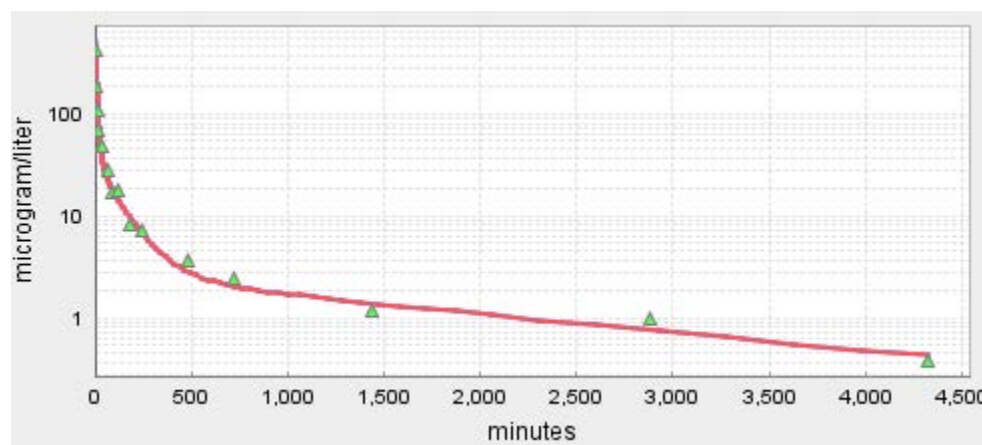


Figure 7-7 Cannabinol antecubital vein concentration following 20 mg, 1 min IV infusion.

This example illustrates that this HLS PBPK model is applicable to a wide range of solutes, from the volatile anesthetics with a  $P_{L/W}$  of about 100 (Table 7-2) to cannabinol with  $P_{L/W}$  of 250,000.

## 7.5 References.

1. Levitt DG, Heymsfield SB, Pierson RN, Jr., Shapses SA, Kral JG: **Physiological models of body composition and human obesity.** *Nutr Metab (Lond)* 2007, **4**:19.
2. Levitt DG, Heymsfield SB, Pierson RN, Jr., Shapses SA, Kral JG: **Physiological models of body composition and human obesity.** *Nutr Metab (Lond)* 2009, **6**:7.
3. Mackay D, Fraser A: **Kenneth Mellanby Review Award. Bioaccumulation of persistent organic chemicals: mechanisms and models.** *Environ Pollut* 2000, **110**(3):375-391.
4. Valko K, Nunhuck S, Bevan C, Abraham MH, Reynolds DP: **Fast gradient HPLC method to determine compounds binding to human serum albumin. Relationships with octanol/water and immobilized artificial membrane lipophilicity.** *J Pharm Sci* 2003, **92**(11):2236-2248.
5. Levitt DG: **Heterogeneity of human adipose blood flow.** *BMC Clin Pharmacol* 2007, **7**:1.
6. Seydel JJ, Wiese M: **Octanol-Water Partitioning versus Partitioning into Membranes.** In: *Drug-Membrane Interactions: Analysis, Drug Distribution, Modeling. Volume 15*, edn. Edited by Seydel JJ, Wiese M: Wiley; 2002.
7. Poulin P, Haddad S: **Advancing prediction of tissue distribution and volume of distribution of highly lipophilic compounds from a simplified tissue-composition-based model as a mechanistic animal alternative method.** *J Pharm Sci* 2012, **101**(6):2250-2261.
8. Yasuda N, Lockhart SH, Eger EI, 2nd, Weiskopf RB, Johnson BH, Freire BA, Fassoulaki A: **Kinetics of desflurane, isoflurane, and halothane in humans.** *Anesthesiology* 1991, **74**(3):489-498.
9. Yasuda N, Lockhart SH, Eger EI, 2nd, Weiskopf RB, Liu J, Laster M, Taheri S, Peterson NA: **Comparison of kinetics of sevoflurane and isoflurane in humans.** *Anesth Analg* 1991, **72**(3):316-324.
10. Levitt DG: **PKQuest: volatile solutes - application to enflurane, nitrous oxide, halothane, methoxyflurane and toluene pharmacokinetics.** *BMC Anesthesiol* 2002, **2**(1):5.
11. Brochu P, Brodeur J, Krishnan K: **Derivation of cardiac output and alveolar ventilation rate based on energy expenditure measurements in healthy males and females.** *J Appl Toxicol* 2012, **32**(8):564-580.
12. Johansson E, Ohlsson A, Lindgren JE, Agurell S, Gillespie H, Hollister LE: **Single-dose kinetics of deuterium-labelled cannabinal in man after intravenous administration and smoking.** *Biomed Environ Mass Spectrom* 1987, **14**(9):495-499.

## 8. Persistent organic pollutants (POP): why are they “persistent”?

POPs are extremely lipid soluble, with  $P_{L/W}$  ranging from  $10^5$  to greater than  $10^7$ , characterized by persistent human life times of several years.[1] Because of these long lifetimes and the near impossibility of obtaining accurate experimental PK data, POP modeling and prediction has become one of the most common PBPK applications. As discussed above, since the lifetimes in animals of POPs are roughly proportional to their  $P_{L/W}$ , it is tempting to assume that these long lifetimes are the result of their high adipose partition and the resulting slow washout. [2] What is not commonly recognized is that, as described in eq. (7.2), for  $P_{L/W}$  greater than about 1000,  $K_B^{Ad}$  reaches a maximum value equal to  $f_L^{Ad}/f_L^B$ , and further increases in  $P_{L/W}$  do not increase it above this maximum value. Thus, the maximum possible flow limited time constant ( $T_{FL}$ ) for adipose/blood exchange is described by:

$$(8.1) \quad \begin{aligned} K_B^{Ad} &\xrightarrow{P_{L/W} > 1000} f_L^{Ad} / f_L^B = 0.8 / 0.005 = 160 \\ T_{FL} = K_B^{Ad} / F_{Ad} &\xrightarrow{P_{L/W} > 1000} 160 / 0.014 \text{ min}^{-1} = 11,428 \text{ min} \end{aligned}$$

where  $F_{Ad}$  is the perfusion rate for the slow adipose compartment = 0.014 l/min/kg,  $f_L^{Ad} \approx 0.8$  (Table 7-1), and  $f_L^B \approx 0.005$  for the POPs [3]. Thus, the maximum  $T_{FL}$  for adipose exchange is 11,428 minutes or about 8 days, far short of the experimental  $T$  of several years.

One possible explanation is that eq. (8.1) is incorrect because it assumes that the adipose/blood exchange is flow limited, while, as clearly shown by Levitt [3], it becomes diffusion limited for some POPs. This diffusion limitation arises because the high  $P_{L/W}$  of the POP result in such a low free water concentration that diffusion through the capillary wall becomes rate limiting. However, even taking account of this diffusion limitation, the adipose exchange time constant is at least 10 fold shorter than the POP lifetimes and cannot be responsible for the observed human POP persistence. Section 8.2 provides a detailed discussion of this POP diffusion limitation and can be skipped if one is not interested in these details.

### 8.1 POP metabolism limited kinetics.

The explanation of the discrepancy between the adipose POP time constant and the whole body human time constant is simply that the POPs are limited by their extremely low rate of metabolism and excretion, not by the adipose/blood exchange. If the time constant for excretion is long compared to the time constant for adipose and other tissue exchange, then at long times, one can ignore the PBPK model details and the plasma concentration can be described by a simple 1-compartment model characterized by its excretion rate (=clearance) and volume of distribution ( $V$ ) (eq. (2.5):

$$(8.2) \quad C(t) = (D/V)e^{-(Cl/V)t} = (D/V)e^{-t/T_c} \quad T_c = V / Cl$$

where  $T_c$  is the 1-compartment excretion time constant. This is illustrated quantitatively in the following example.

For the above cannabino PKQuest example (Figure 7-7, “Cannabino Example.xls”) the volume of distribution for the entire body is about 1,800 liters and the hepatic clearance is 1 liter/min, corresponding to a  $T_c = V/Cl = 1,800 \text{ min} = 1.25 \text{ days}$  (eq. (8.2)). Since this is much less than the flow limited adipose time constant  $T_{FL} = 11,428 \text{ min} \approx 8 \text{ days}$  (eq. (8.1)), the adipose exchange is rate limiting and, not surprisingly, as shown in the top panel of Figure 8-1, the one compartment model is a very poor approximation to the cannabino PBPK model. The lower two panels in Figure 8-1 compare the one compartment versus the PBPK as the hepatic clearance is reduced to 0.1 liter/min ( $T_c = 12.5 \text{ days}$ ) (middle panel) and 0.01 liter/min ( $T_c = 125 \text{ days}$ ) (bottom panel). It can be seen (bottom panel) that when the metabolic excretion rate becomes rate limiting ( $T_c = 125 \text{ days} \gg T_{FL} = 8 \text{ days}$ ), the one compartment model provides a good prediction of the PK, after the initial  $\approx 8 \text{ day}$  transient period when the adipose tissue is filling.

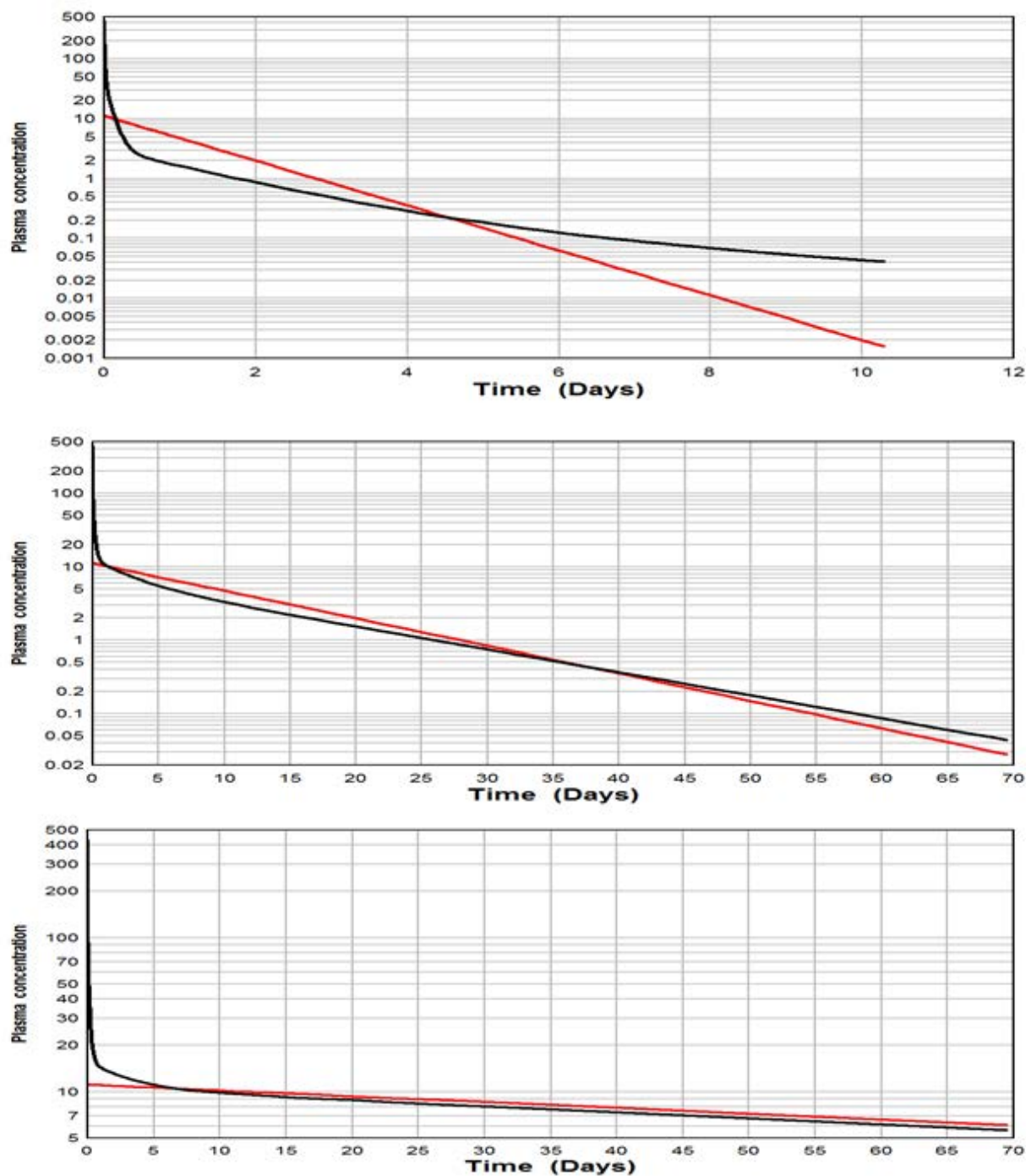


**Figure 8-1** Comparison of one compartment (red) vs PBPK (black) model for highly lipid soluble solute (ie, cannabinol) with a adipose time constant  $T$  of 8 days. Metabolic time constant = 1.25 (top), 12.5 (middle), 125 days (bottom panel)

As discussed above, PK modeling of POPs is of crucial importance because their long life times and toxicity make them impossible to investigate experimentally in any detail. It is a bit disappointing that PBPK modeling is superfluous for the POPs. All that is needed to characterize the PK of a POP is its metabolic clearance ( $Cl_{ss}$ ) and its steady volume of distribution ( $V_{ss}$ ). Because the metabolic clearance is rate limiting, POPs have time to

equilibrate with body fat and are in a pseudo steady state with  $V_{ss} \approx V_{Eq}$ , the equilibrium volume of distribution. Although,  $V_{Eq}$  has been discussed previously (eq. (4.5)), it will be reviewed here in the specific context of POPs.  $V_{Eq}$  is defined as:

$$(8.3) \quad \begin{aligned} V_{Eq} C_B &= \text{total amount POP in body} \\ &= V_B C_B + \sum_{i=1}^N V_i C_T^i = C_B [V_B + \sum_{i=1}^N V_i C_T^i / C_B] = C_B [V_B + \sum_{i=1}^N V_i K_B^i] \end{aligned}$$

For the POPs,  $K_B^i$  is simply equal to the ratio  $f_L^i / f_L^B$  (eq. (7.2)):

$$(8.4) \quad V_{Eq} = V_B + (1 / f_L^B) \sum_{i=1}^N V_i f_L^i = V_B + V_L / f_L^B$$

where  $V_L$  is the total body lipid, roughly equal to the total body fat.

In theory,  $f_L^B$  (the blood lipid fraction) should be independent of the POP and known from in vitro measurements. However, as discussed above, there can be some specific hydrophobic albumin lipid binding that contributes to  $f_L^B$ , effectively, making it a variable that should be determined for each solute. For the series of POPs in which  $K_B^{Ad}$  was directly determined from the rat adipose PK [3],  $f_L^B$  varied by a factor of about 2, from 0.003 to 0.006. In humans,  $f_L^B$  varies from about 0.0075 for cannabiniol to about 0.01 for the volatile anesthetics. Human POP PK information is usually based on incidental or accidental exposure and is not well characterized. Given this limited quantitative accuracy, as a first approximation,  $V_{Eq}$  can be approximated by (assuming  $f_L^B \approx 0.005$ ):

$$(8.5) \quad V_{Eq} = V_B + V_L / f_L^B \approx 200 * (\text{Total Body Fat})$$

As discussed above, the good correlation between  $P_{L/W}$  and the persistence lifetimes of POPs in humans led to the erroneous assumption that the adipose/blood exchange was the rate limiting process [2], while, in fact, it is actually metabolic rate that is rate limiting. Although, increasing the log  $P_{oct/W}$  above about 1000 does not change the adipose/blood exchange rate (ignoring the diffusion limitation), it does decrease the free blood water concentration  $C_W$  (eq (8.10)):

$$(8.6) \quad C_W / C_B \approx (f_L^B P_{oct/w})^{-1}$$

Since  $C_W$  is the effective concentration at the liver enzymes active site, the metabolism would be expected to decrease as log  $P_{oct/W}$  increases. Although there are additional metabolic factors, such as difficulty of metabolizing chlorinated compounds, they are probably secondary to this concentration effect.



## 8.2 POP diffusion limited adipose tissue exchange.

This section presents a detailed discussion of recent analysis of Levitt [3] that shows that the adipose/blood exchange becomes diffusion limited for POPs that have extremely high  $P_{oil/W}$ . This analysis is nearly identical to that used previously (Section 6) to describe the capillary permeability limitation for the extracellular solutes and Figure 8-2 is a slightly modified version of Figure 6-1. The only difference is that the free water fractions  $k_p$  and  $k_i$  are replaced by the water/blood ( $P_{W/B}$ ) and water/adipose ( $P_{W/Ad}$ ) partition coefficients. The POPs are carried bound to albumin and lipid in the blood. The rate limiting step in adipose/blood exchange is the diffusion through the aqueous barrier presented by the capillary wall that separates them.

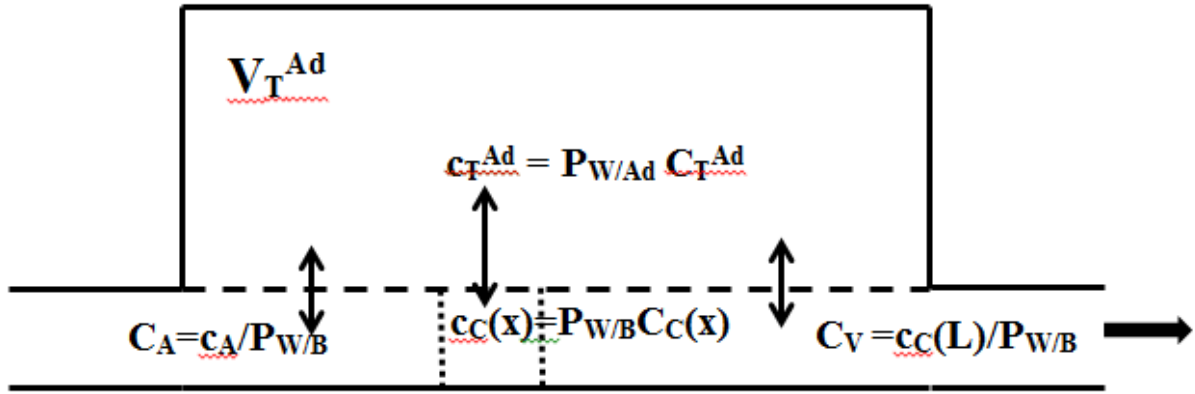


Figure 8-2 Diagram of the diffusion limited capillary/adipose tissue exchange ( $c$  and  $C$  are the total and free water concentration, respectively, and  $P_{W/B}$  and  $P_{W/Ad}$  are the water/blood and water/adipose partition coefficients, respectively)

The fractional equilibration ( $f_{Eq}^{Ad}$ ) in one pass through the adipose tissue is (see eqs. (6.1) to (6.5)).

$$(8.7) \quad f_{Eq}^{Ad} = (c_A - c_V^{Ad}) / (c_A - c_T^{Ad}) = 1 - \exp(-\kappa) \quad \kappa = \frac{P_{W/B} P_{Ad} S_{Ad}}{F_{Ad}}$$

$$\Rightarrow c_A - c_V^{Ad} = f_{Eq}^{Ad} (c_A - c_T^{Ad}) \Rightarrow C_A - C_V^{Ad} = f_{Eq}^{Ad} (C_A - C_T^{Ad} / K_B^{Ad})$$

where  $P_{Ad}$  and  $S_{Ad}$  are the adipose capillary permeability and surface area, respectively and the last equality use the relation  $K_B^{Ad} = P_{W/B} / P_{W/Ad}$ . The parameters  $f_{Eq}^{Ad}$  and  $\kappa$  characterizes the capillary permeability, with  $f_{Eq}^{Ad} = 1$  and  $\kappa = \infty$  for flow limited and  $f_{Eq}^{Ad} = 0$  and  $\kappa = 0$  for impermeable. Although the POPs have a very large intrinsic permeability ( $P_{Ad} S_{Ad}$ ), because of its very low  $P_{W/B}$  of about  $10^{-5}$  (see eq. (8.10)), its “effective” capillary permeability ( $= P_{W/B} P_{Ad} S_{Ad}$ ) is small enough to make it diffusion limited.

Using eq. (8.7), the differential equation describing the balance between adipose inflow and outflow is (see eq. (4.4)):

$$\begin{aligned}
 \frac{dC_T^{Ad}(t)}{dt} &= F_{Ad} [C_A(t) - C_V^{Ad}(t)] = f_{Eq}^{Ad} F_{Ad} [C_A(t) - C_T^{Ad}(t) / K_B^{Ad}] \\
 (8.8) \qquad \qquad \qquad &= F_{Ad}^{ap} [C_A(t) - C_T^{Ad}(t) / K_B^{Ad}] \qquad F_{Ad}^{ap} = f_{Eq}^{Ad} F_{Ad}
 \end{aligned}$$

where  $F_{Ad}$  is the anatomic adipose perfusion rate (=flow rate/volume) and  $F_{Ad}^{ap}$  is the “apparent” perfusion rate that is produced by the diffusion limitation. It can be seen from eq. (8.8) that the adipose concentration  $C_T^{Ad}(t)$  is determined by two parameters: the “apparent” perfusion rate ( $F_{Ad}^{ap} = f_{Eq}^{Ad} F_{Ad}$ ) and the adipose/blood partition ( $K_B^{Ad}$ ). There are extensive measurements in the rat of the plasma ( $C_A(t)$ ) and adipose ( $C_T^{Ad}(t)$ ) POPs concentration as a function of time following either IV or oral input. The procedure used by Levitt [3] to estimate the permeability (or diffusion) limitation ( $f_{Eq}^{Ad}$ ) was to numerically solve eq.(8.8) for the adipose concentration ( $C_T^{Ad}(t)$ ) using the experimental plasma concentration for  $C_A(t)$ , and then find the parameters  $F_{Ad}^{ap}$  and  $K_B^{Ad}$  that optimize the fit of this  $C_T^{Ad}(t)$  to the experimental value (see Section 8.3 for a detailed PKQuest example). The fraction equilibration ( $f_{Eq}^{Ad}$ ) is then equal to  $F_{Ad}^{ap}/F_{Ad}$  where  $F_{Ad}$  is the known anatomic adipose perfusion rate.

This approach was applied to the data of Oberg et. al. [4] who simultaneously measured the rat plasma and adipose tissue concentrations following an oral dose of a mixture of 13 different polychlorinated biphenyls (PCBs), varying from 3 to 7 substituted chlorines. The log octanol/water partition ( $\log P_{oct/W}$ ), which should be approximately equal to the  $\log P_{oil/W}$  (see Figure 7-2), varied from 5.67 to 7.36. The POP with the lowest lipid solubility ( $\log P_{oct/W} = 5.67$ ) had a fractional equilibration ( $f_{Eq}^{Ad} = F_{Ad}^{ap}/F_{Ad}$ ) of about 1, ie, was flow limited. As  $P_{oct/W}$  increased, the POPs became diffusion limited, with the POP with a  $\log P_{oct/W}$  of 7.36 having a  $f_{Eq}^{Ad}$  of about 0.03. [3]

There are a number of assumptions in this capillary permeability model. In particular, it is assumed that the adipose tissue is well mixed, the capillary is mixed the radial direction and diffusion through the aqueous capillary wall is the rate limiting step. The crucial test of the model is see if  $f_{Eq}^{Ad}$  ( $=F_{Ad}^{ap}/F_{Ad}$ ) varies with increasing  $P_{W/B}$  as predicted by eq. (8.7):

$$\begin{aligned}
 F_{Ad}^{ap} / F_{Ad} &= f_{Eq}^{Ad} = (c_A - c_V^{Ad}) / (c_A - c_T^{Ad}) = 1 - \exp(-\kappa) \\
 (8.9) \qquad \kappa &= \frac{P_{W/B} P_{Ad} S_{Ad}}{F_{Ad}} \qquad P_{W/B} \approx (P_{oct/W} f_L^B)^{-1} \\
 \Rightarrow \kappa &= B / P_{oct/W} \qquad B = \frac{P_{Ad} S_{Ad}}{f_L^B F_{Ad}}
 \end{aligned}$$

In eq. (8.9), the water/blood partition water partition ( $P_{W/B}$ ) has been expressed in terms of the blood lipid fraction ( $f_L^B \approx 0.005$ ) using eq. (7.2):

$$(8.10) \quad \begin{aligned} C_B / C_W &= (1 - f_L^B) + P_{L/W} f_L^B \xrightarrow{P_{L/W} > 1000} P_{L/W} f_L^B \\ P_{W/B} &= (C_B / C_W)^{-1} = (P_{L/W} f_L^B)^{-1} \approx (P_{oct/W} f_L^B)^{-1} \end{aligned}$$

For the POP,  $f_L^B \approx 0.005$ , and a POP with a  $P_{oct/W}$  of  $10^{-7}$  would have a  $P_{W/B} \approx 2 \times 10^{-5}$ . Since the adipose intrinsic capillary permeability ( $P_{Ad}$ ) should have only minor variations for the different POPs,  $B$  in eq. (8.9) can be assumed to be a constant. Figure 8-3 shows a plot  $F_{Ad}^{ap}/F_{Ad}$  for the 13 Oberg et. al. POPs as a function of their  $P_{oct/W}$ . There is an excellent fit between the model predictions of eq. (8.9) (red line) and the experimental data.

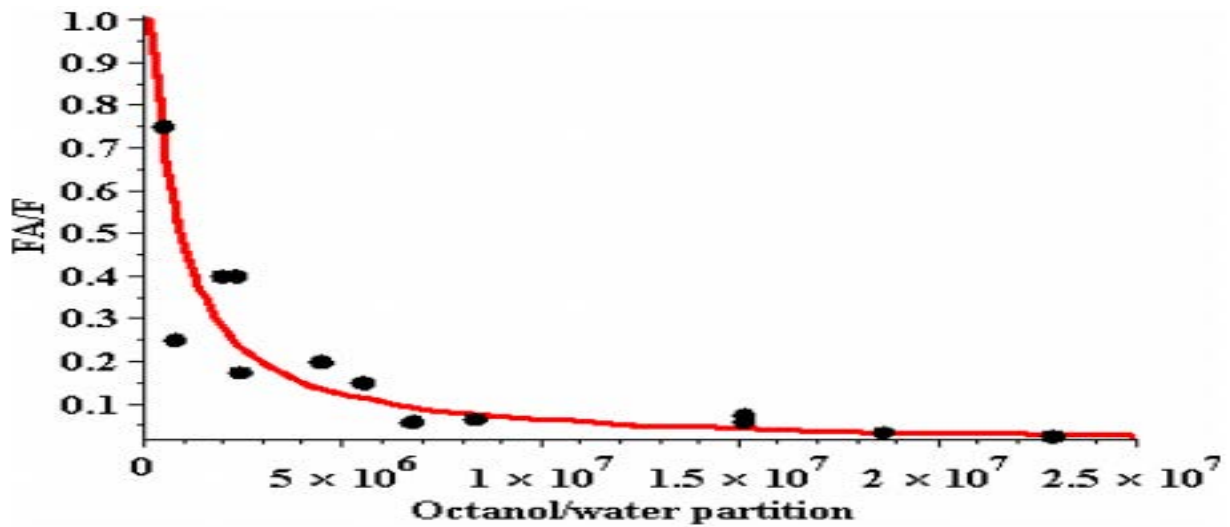


Figure 8-3 Plot of diffusion limitation (=fractional equilibration = FA/F) versus  $P_{oct/W}$  partition for the 13 PCBs studied by Oberg et. al.

The model line in Figure 8-3 is for a  $B$  of  $0.75 \times 10^6$ , which corresponds to  $P_{Ad}S_{Ad}$  of  $750 \text{ min}^{-1}$ , assuming an anatomic adipose perfusion rate of  $0.2 \text{ l/min/kg}$  and  $f_L^B$  of  $0.005$ . [3] To put this very large  $P_{Ad}S_{Ad}$  value in perspective, the highest capillary permeability that has been directly measured is a PS of about  $1/\text{min}$  for  $\text{Na}^+$  in heart capillaries. [5] The POPs become diffusion limited only because of the very small  $P_{W/B}$ . Since the rat adipose capillary surface area ( $S_{Ad}$ ) is about  $35 \text{ cm}^2/\text{cm}^3$  [6], the permeability ( $P_{Ad}$ ) is about  $0.36 \text{ cm/sec}$ . One can use this  $P_{Ad}$  to estimate the aqueous thickness ( $W$ ) of the permeability barrier that it would correspond to:

$$(8.11) \quad \begin{aligned} P_{Ad} &= (\text{Aqueous Diffusion Coeff}) / W = D / W \\ \Rightarrow W &= D / P_{Ad} = (5 \times 10^{-6} \text{ cm}^2 / \text{sec}) / (0.36 \text{ cm} / \text{sec}) = 14 \times 10^{-6} \text{ cm} = 0.14 \mu \end{aligned}$$

assuming a POPs aqueous diffusion coefficient of  $5 \times 10^{-6} \text{ cm}^2/\text{sec}$ . [7] This estimated thickness of  $0.14 \mu$  is close to that of the rat adipose capillary endothelium ( $0.25 \mu$ ), providing good support for the basic model assumptions.

Can this diffusion limitation explain the PK time constants of years that are observed for POPs in humans? For a diffusion limited POP, it is necessary to modify the expression for the flow limited time constant  $T_{FL}$  (eq. (7.4):

$$(8.12) \quad \begin{aligned} \text{Flow limited: } T_{FL} &= K_B^{Ad} / F_{Ad} \\ \text{Diffusion limited: } T_{DL} &= K_B^{Ad} / F_{Ad}^{ap} = T_{FL} F_{Ad} / F_{Ad}^{ap} = T_{FL} / f_{Eq}^{Ad} \end{aligned}$$

For example, consider the the Oberg et. al. POP with the highest  $\log P_{oct/W}$  ( $= 7.36$ ). It had a  $f_{Eq}^{Ad}$  of about 0.03 and this would increase the rat adipose time constant ( $T_{DL}$ ) by a factor of 33 greater than then the flow limited estimate. This rat result must be scaled to the human. The degree of diffusion limitation for a given  $K_{oct/W}$  is determined in eq. (8.9) by the parameter  $B = (P_{Ad} S_{Ad}) / (f_L^{Ad} F_{Ad})$ . Since rats and humans have similar adipose capillary anatomy,  $P_{Ad}$  should the same for rats and human. Also, since rats and humans have similar capillary density,  $S_{Ad}$  should also be the same, and the adipose lipid fraction  $f_L^{Ad}$  is also the same. However, the rat anatomic adipose perfusion rate ( $F_{Ad}$ ) of 0.2 l/min/kg is 2.7 and 14 times greater than the high flow (.074 l/min/kg) and low flow (0.014 l/min/kg) human adipose compartments, respectively. (see Table 7-1). Thus, the slowest adipose compartment will have a  $B$  and  $\kappa$  that is 14 times greater than the rat, corresponding to a  $f_{Eq}^{Ad}$  (eq. (8.9)) of 0.34. That is, the diffusion limitation will increase the flow limited time constant estimate in eq. (8.1) by a factor of about 3, to 34,300 minutes, or 23 days ( $= T_{DL}$ ), still much less than the years that are experimentally observed. And this is for the POP with an  $\log P_{oct/W}$  of 7.36. Most POPs of clinical importance have  $P_{oct/W}$  less than this, and will have correspondingly shorter  $T_{DL}$ . In conclusion, the human time constants for adipose POP exchange are at least 10 times faster than what is observed experimentally, even when diffusion limitation is taken into account,

### 8.3 PKQuest Example: Determine the apparent rat adipose perfusion rate ( $F_{Ad}^{ap}$ ) and adipose/blood partition ( $K_B^{Ad}$ ) for POPs.

As describe in the above diffusion limited Section 8.2, the differential eq. (8.8) was solved numerically to find the two parameters  $F_{Ad}^{ap}$  and  $K_B^{Ad}$  that optimized the fit to the experimental adipose tissue concentration as a function of time. This example describes how to use PKQuest to do this for two PCBs: 1) PCB 2 4 4 with a relatively low  $\log P_{oct/W}$  of 5.67; and 2) PCB 2 2 3 4 4 5 5 with a high  $\log P_{oct/W}$  7.36. These examples use the data of Oberg et. al. [4] and were analyzed by Levitt [3] in the determination of the POP diffusion limitation. This PKQuest routine is quite simple: it uses the experimental blood POP concentration (fit with an “N Exp” response function) for  $C_A(t)$  in eq. (8.8) and calculates the resulting adipose tissue concentration  $C_T^{Ad}(t)$ . The user adjusts  $F_{Ad}^{ap}$  and  $K_B^{Ad}$  manually to find the best values.

Start PKQuest and Read the file “PCB 2 4 4 (#28) Rat Fat Ober.xls”. This routine is selected by clicking the “Fit Vein” check box. (The “NonPK” check box should be unchecked).

Also, the “Fat/water partition” check box is checked and  $K_{fwat}$  is set to any very large value. The “Regimen” table is POP input function. The amount is arbitrary since  $C_A(t)$  will be adjusted to fit the experimental value. However, the input time should be similar to the experimental since it is used to determine the unit response function used to fit  $C_A(t)$ . In “Plot” table, “adipose” and “vein” are checked. There are two sets of experimental data: 1) the rat blood PCB concentration – input in the “Vein Conc 1” table; and 2) the adipose tissue PCB concentration – input in the “Exp Data 1” table. The two parameters are adjusted manually: 1) the “Blood fat fr” ( $=f_L^{Ad}$ ) which determines  $K_B^{Ad}$  ( $=0.8/f_L^{Ad}$ , eq. (8.1)); and 2)  $F_{Ad}^{ap}$  which is adjusted as the “adipose” Perfusion in the “Organ Par” table. Select the “Semilog” option and “Run” getting following output.

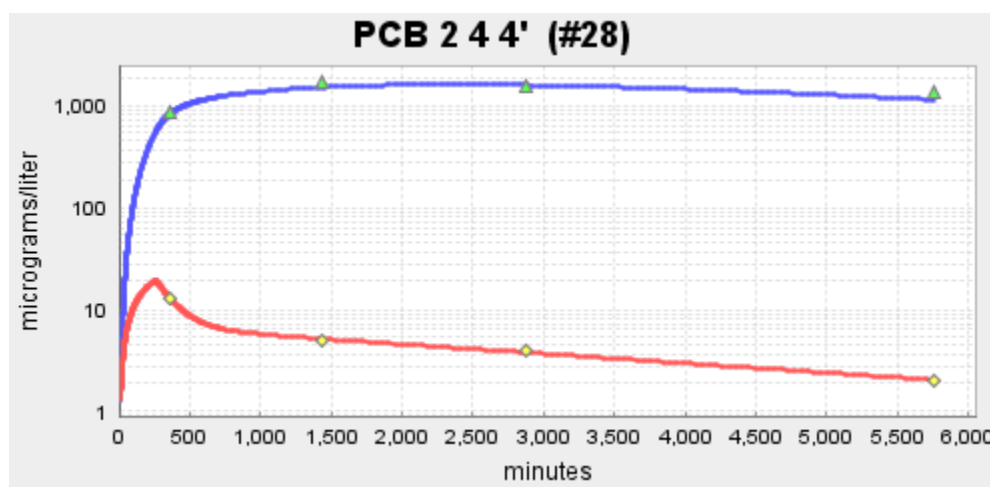


**Figure 8-4 PKQuest output.** The experimental rat blood concentration (red) has been fit with a 2-exponential function and used as input to determine the rat adipose tissue POP concentration (blue). POP  $\log P_{oct/W} = 5.67$ .

Note that this optimal fit was obtained for a Blood fat fr = 0.0025 ( $K_B^{Ad} = 0.8/0.0025 = 320$ ) and an  $F_{Ad}^{ap} = 0.15$  liter/min/kg, which is approximately equal to the rat anatomic adipose perfusion rate ( $\approx 0.2$ ) and therefore, this POP is probably flow limited.

Start PKQuest again, Read “PCB 2 2 3 4 4 5 5 (#180) Rat Fat Oberg.xls”, click Semilog option and Run, getting the following output in Figure 8-5. Note that for this POP with 7 chlorines and a very high fat solubility ( $\log P_{oct/W}$ ) has a  $F_{Ad}^{ap} = 0.005$  liter/min/kg, 30 fold less of then that of the less lipid soluble PCB 2 4 4. That is, this POP has a large diffusion limitation with the fraction that equilibrates in one pass ( $f_{Eq}^{Ad}$ , eq.(8.9)) of about 0.03.

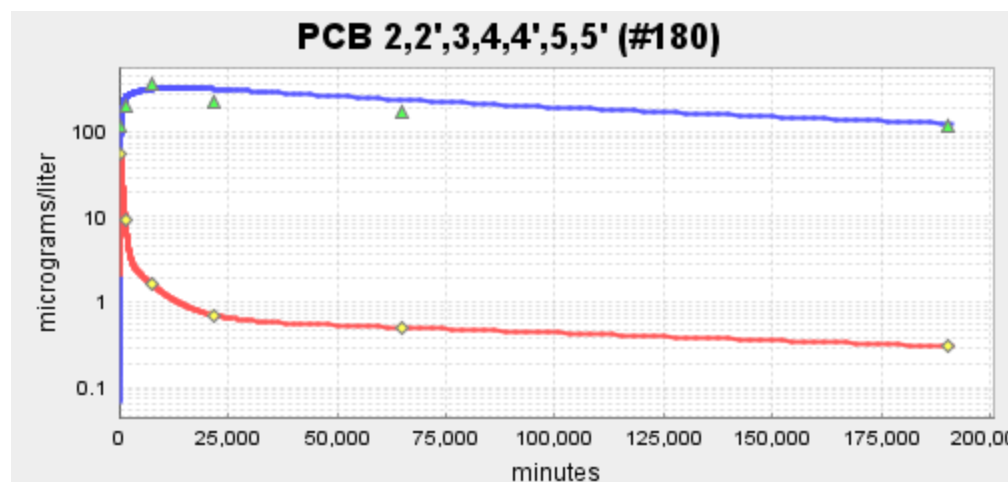


Figure 8-5 PKQuest output. The experimental rat blood concentration (red) has been fit with a 2-exponential function and used as input to determine the rat adipose tissue POP concentration (blue). POP log  $P_{oct/W} = 7.36$ .

## 8.4 References.

1. Michalek JE, Pirkle JL, Needham LL, Patterson DG, Jr., Caudill SP, Tripathi RC, Mocarelli P: **Pharmacokinetics of 2,3,7,8-tetrachlorodibenzo-p-dioxin in Seveso adults and veterans of operation Ranch Hand.** *J Expo Anal Environ Epidemiol* 2002, **12**(1):44-53.
2. Mackay D, Fraser A: **Kenneth Mellanby Review Award. Bioaccumulation of persistent organic chemicals: mechanisms and models.** *Environ Pollut* 2000, **110**(3):375-391.
3. Levitt DG: **Quantitative relationship between the octanol/water partition coefficient and the diffusion limitation of the exchange between adipose and blood.** *BMC Clin Pharmacol* 2010, **10**:1.
4. Oberg M, Sjodin A, Casabona H, Nordgren I, Klasson-Wehler E, Hakansson H: **Tissue distribution and half-lives of individual polychlorinated biphenyls and serum levels of 4-hydroxy-2,3,3',4',5-pentachlorobiphenyl in the rat.** *Toxicol Sci* 2002, **70**(2):171-182.
5. Crone C, Levitt DG (eds.): **Capillary permeability to small solutes.** Bethesda, Md.: American Physiological Society; 1984.
6. Paaske WP: **Absence of restricted diffusion in adipose tissue capillaries.** *Acta Physiol Scand* 1977, **100**(4):430-436.
7. Werner D, Ghosh U, Luthy RG: **Modeling polychlorinated biphenyl mass transfer after amendment of contaminated sediment with activated carbon.** *Environ Sci Technol* 2006, **40**(13):4211-4218.



## 9. Deconvolution: a powerful, underutilized tool.

In Section 2 we introduced the idea of the “convolution” describing, for example, the plasma  $C(t)$  that results from an arbitrary systemic input  $I(t)$  to a linear system with a known bolus response function  $h(t)$ :

$$(9.1) \quad C(t) = \int_0^t I(\tau) h(t-\tau) d\tau = \int_0^t I(t-\tau) h(\tau) d\tau$$

Deconvolution is the inverse, where we are given  $C(t)$  and  $h(t)$  and want to find the corresponding input  $I(t)$ . Although we will focus on the procedure required to determine the rate  $I(t)$  of intestinal absorption of an orally administered drug, it can be applied to any other type of unknown input (dermal patch, subcutaneous, nasal, etc.) There are two steps: Step 1) Using the experimental plasma concentration  $C_{IV}(t)$  that results from a known IV input  $I_{IV}(t)$ , determine  $h(t)$ . Step 2) From the plasma  $C_{Int}(t)$  following the oral input, determine the intestinal absorption rate  $I_{Int}(t)$  by deconvolution of eq. (9.1). PKQuest provides a simple interface for performing these two steps. One only needs to input the experimental  $C_{IV}(t)$  and  $C_{Int}(t)$  plasma data points and select one of six different deconvolution methods. The solution for  $I_{Int}(t)$  is output, along with additional plots that characterize the quality of the solution. Because the  $h(t)$  was determined following a known intravenous (IV) input, the  $I_{Int}(t)$  that is determined by deconvolution is also the input into the systemic circulation. This may differ from the intestinal absorption rate if there is significant “first pass metabolism” of the absorbed solute by the liver before it enters the systemic circulation. This is discussed in detail in the next Section 10 which focuses on the physiology and PK of intestinal absorption. Deconvolution is the most rigorous and accurate approach for determining an unknown input function. It is underutilized primarily because of the lack of a freely available simple software routine. It is hoped that PKQuest solves this problem.

Step 1 is straight forward and is identical to the procedure that was used in Section 3 to determine the non-compartmental  $V_{ss}$  and  $Cl_{ss}$ . It is assumed that  $h(t)$  can be approximated by a  $N$ -exponential function (eq. (3.3)) so that the integral in eq. (9.1) (using known  $I_{IV}(t)$ ) is then a function of the  $2N$  parameters that describe  $h(t)$ . A non-linear minimization routine is then used to find the  $2N$  parameter  $h(t)$  that provide the best fit to the experimental  $C_{IV}(t)$ . This is the procedure that has been implemented in PKQuest in the previous sections to generate the continuous plasma concentration curves. As discussed in detail in Section 3.4, in most cases, a two exponential response function can provide a surprisingly good fit to experimental plasma concentration curves. In rare cases, 3 exponentials are required, but, no more than 3. If, eg, 3 exponentials are used, then, obviously, one must have at least 6 experimental data points (hopefully, more) for  $C_{IV}(t)$  in order to determine the 6 parameters that characterize  $h(t)$ .



In order to have an accurate description of  $h(t)$ , it is desirable to sample  $C_{IV}(t)$  at times that overlap with  $I_{IV}(t)$ . Because of the inherent mixing and time delays in the venous system, one cannot accurately determine a true "mixed" venous concentration  $C_{IV}(t)$  at times earlier than about 2 minutes. For example, if one uses a nearly "bolus"  $I_{IV}(t)$  of, eg, 10 seconds, then  $h(t) \approx C_{IV}(t)$  and if one takes the first  $C_{IV}$  plasma sample at 5 minutes, then one completely misses the early ( $t < 10$  minutes) component of  $h(t)$ . In contrast, if one used a 30 minute constant  $I_{IV}$  input, one can accurately estimate the early times for  $h(t)$  even if the first plasma sample is at 5 minutes. Because the importance of using slow and extended  $I_{IV}(t)$  for deconvolution calculations is not widely recognized, it is often not satisfied in the experimental literature. For example, the amoxicillin example discussed below (Section 9.3) used a 10 second  $I_{IV}(t)$ . Fortunately, as discussed in more detail by Levitt [1], for most solutes this introduces only a small error in the estimate of  $I_{Int}(t)$ .

Step 2 (deconvolution) is more complicated and there is not a single procedure that can be used for all cases. Step 1 was simple because one could assume, in general, that an  $N$  exponential function would provide a good approximation to  $h(t)$ . In contrast, for deconvolution, we do not necessarily know the functional form of the unknown  $I_{Int}(t)$ . There are two different approaches that are used: 1) Assume a functional form for  $I_{Int}(t)$  characterized by  $N$  parameters and use a minimization routine to determine the  $N$  parameters that provide the best fit to the  $C_{Int}$  experimental data points. 2) Use a more general approach where no functional form is imposed, a priori, on  $C_{Int}(t)$ . The second approach is a more mathematically challenging problem that has elicited a number of sophisticated numerical approaches.[1] As currently implement in PKQuest, there are 6 different deconvolution options, four are of the first type using a variety of assumed functional forms, and two are of the second general type. They are illustrated in the following examples.

One of these two general types is the method of Veng-Pedersen in which the experimental time points of  $C_{Int}(t)$  are exactly fit by a spline function  $C_{Sp}(t)$ , and eq. (9.1) solved for the corresponding  $I_{Int}(t)$ . [2-4] Although this provides a perfect fit to the experimental oral data, it is highly influenced by errors and noise in the data and can produce  $I_{Int}(t)$  that have non-physiologic oscillations, and negative absorption rates. [1] In order to limit this problem, one can input a "smoothing" parameter  $S$  that remove the sharp discontinuities and, hopefully, more exactly reproduces the true, error free data. The other general method implemented in PKQuest is the spline function method of Verotta in which a set of spline "breakpoints" are assumed.[5, 6] This method restricts the absorption rate  $I_{Int}(t)$  to non-negative values. If the number of breakpoints is less than the number of experimental oral experimental data points, the method forces some smoothing of the "noise" in the data. There is also a smoothing parameter that can be input that penalizes the fits that have too sharp a curvature.

There is no standard, generally accepted, criteria for evaluating the validity of the deconvolution solution. An obvious criterion is the agreement of the deconvolution estimate of  $C_{Int}(t)$  with the experimental  $C_{Int}$  data points. However, if the number of adjustable parameters

in the input function  $I_{\text{Int}}(t)$  equals the number of experimental data points in  $C_{\text{Int}}$ , then one can always obtain a  $C_{\text{Int}}(t)$  that perfectly fits the experimental points. This is the case for the Pedersen spline function approach with no smoothing (see example below). Other things being equal, the fewer the parameters in the  $I_{\text{Int}}(t)$  function, the more confidence one can place in the result. Clearly, if one has confidence that you know the functional form of the  $I_{\text{Int}}(t)$ , then one should use a function of this form with a small number of parameters to force  $I_{\text{Int}}(t)$  to have this form. However, this approach will miss any unexpected behavior in  $I_{\text{Int}}(t)$ , such as a second delayed absorption peak as a result of enterohepatic recirculation. There is, unfortunately, an unavoidable degree of subjectivity in the use of the deconvolution approach. This is illustrated in the following PKQuest examples.

### 9.1 PKQuest Example: Determination of nitrendipine absorption rate by deconvolution.

Start PKQuest, “Read” and “Select” and the “nitrendipine Mikus.xls” example file. It uses the data of Mikus et. al. [7] in which nitrendipine was simultaneously administered as an oral 20 mg solution and as a 2 mg constant 30 min IV infusion of the  $^{13}\text{C}$  labeled nitrendipine (Subject 6). This use of a labeled form of the drug so that the oral and IV administration are simultaneous is the ideal for deconvolution since it guarantees that the response function  $h(t)$  is identical for the two inputs. This is rarely done and, in most cases, the next best alternative is used in which the two inputs are given to the same set of subjects, but a week or so apart. This is an example of experimental data that, for some reason, has an input oral input function that is not easily fit by deconvolution and illustrates the strengths and weaknesses of the different deconvolution methods. In the third panel (“Non-compartment PK, Deconvolution,...”) of PKQuest, the “Deconvolution”, “Fit vein” and “Non PK” boxes have been checked, turning on this option. The “Regimen” table describes the known IV input (2000 micrograms over 30 min). The experimental antecubital plasma concentrations ( $C_{\text{IV}}(t)$ ) following the IV input are entered into the “Vein Conc 1” table and the antecubital concentrations ( $C_{\text{Int}}(t)$ ) following the oral input are entered in the “Vein Conc 2” table. The “N Exp” is set = 3, indicating that a 3 exponential function is used to approximate the response function  $h(t)$ . The “Est Dose” provides a starting value for the numerical routines that find the oral absorption rate ( $I_{\text{Int}}(t)$ ). In most cases, it only needs to be accurate within an order of magnitude, and setting it equal to the oral dose should work well. In this case it was set equal to 1000 micrograms, 10% of the oral dose. Note that is assumed that the plasma concentration is the “vein”. This is arbitrary and the only requirement is that the plasma was sampled from the same site for both inputs.

The “Method” selection box has 6 different deconvolution options that will be discussed in detail below. Because of the delay while the drug is in the stomach, intestinal absorption rate ( $I_{\text{Int}}(t)$ ) is initially delayed. The default method selected in this Example file is the “Hill Function” which is a 3 parameter (A, T, h) S shaped function that is often a good approximation for this initial delay:

$$(9.2) \quad \text{Amount Absorbed}(t) = \frac{A t^h}{t^h + T^h}$$

$$\text{Absorption Rate} = I_{\text{Int}}(t) = \frac{h A T^h t^{h-1}}{[t^h + T^h]^2}$$

where A is the total amount absorbed, h is the Hill coefficient and T is a time delay parameter. The “Amount Absorbed” function is the integral of the “Absorption Rate”. “Run” PKQuest, which finds the 3 parameters (A, h, T) that provide the optimal fit to the experimental  $C_{\text{Int}}(t)$  data points and outputs the 4 plots shown in Figure 9-1. The upper left panel shows the agreement between the experimental plasma data following the known IV input  $I_{\text{IV}}(t)$  and the  $C_{\text{IV}}(t)$  (red line) determined using eq. (9.1) with a 3-exponential  $h(t)$ . The upper right panel is a comparison of the experimental plasma concentration following the oral input  $C_{\text{Int}}(t)$  determined from deconvolution using the deconvolution estimate of  $I_{\text{Int}}(t)$ . The two lower panels are the deconvolution estimates of the rate and amount of absorption as a function of time.

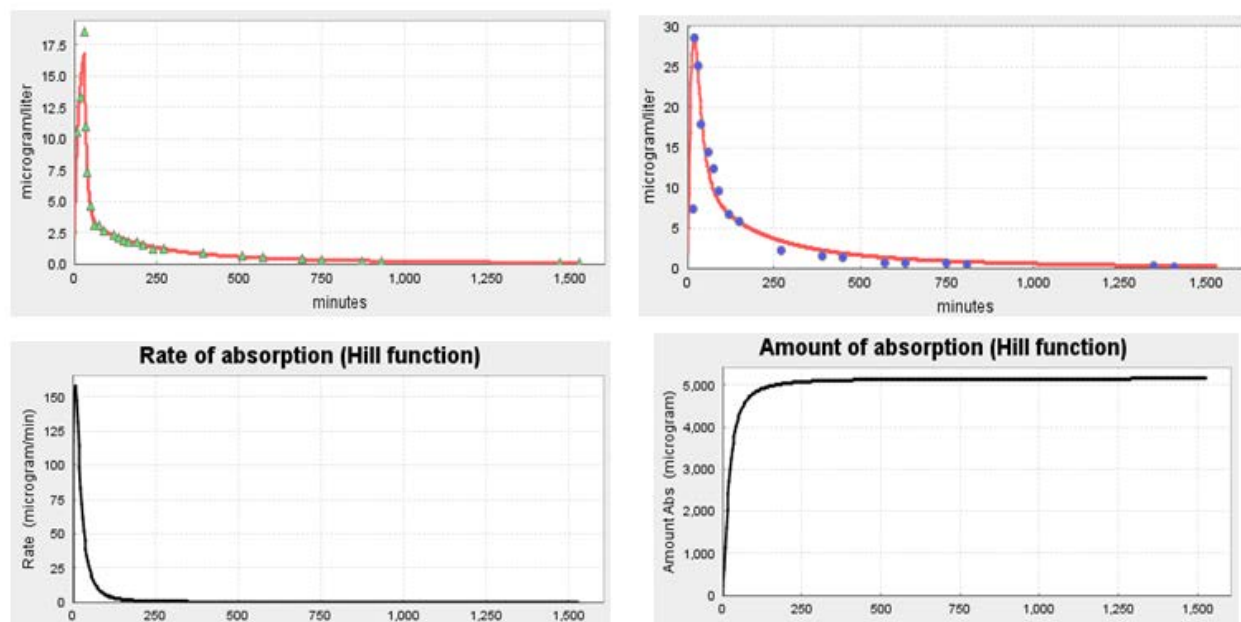


**Figure 9-1** Deconvolution estimate of nitrendipine intestinal absorption rate. Top panels: comparison of experimental (diamonds) and model plasma data (red line) for IV (left) and oral (right) input. Bottom panels: predicted intestinal absorption rate (left) and amount (right).

Nearly all the absorption occurs in the first 100 minutes, which is difficult to resolve in these plots. Run this example again, setting “Plot End” time = 150 minutes. It can be seen from Figure 9-2 that the Hill Function  $I_{\text{Int}}(t)$  provides a good fit to all of the experimental data except for the first point, which it significantly overestimates.

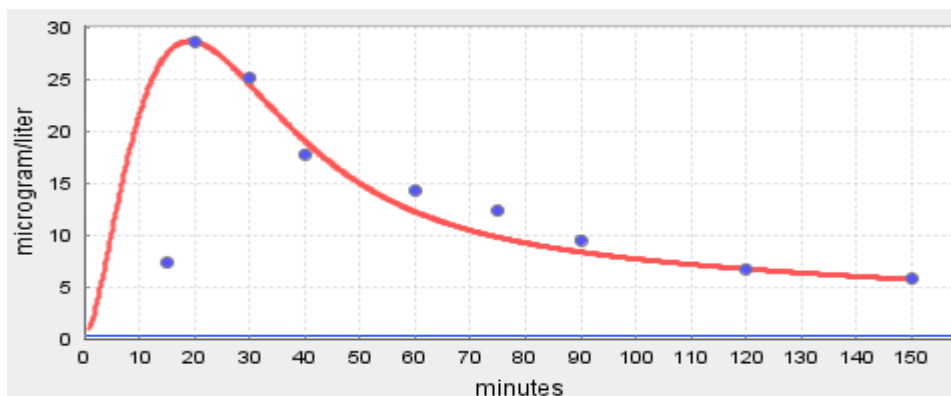


Figure 9-2 Same as upper right panel in Figure 9-1, with end plot time = 150 minutes.

The “absorption” rate determined by deconvolution is the rate that the solute enters the systemic circulation. It may be much less than the rate of intestinal absorption if a large fraction is cleared from the portal vein by hepatic metabolism before reaching the systemic circulation. This is referred to as the “First Pass Metabolism”. At the bottom of the PKQuest Output is the following (you may get slightly different results because the Powel minimization uses a random number generator):

Deconvolution - Hill Function fit to experimental data:

Absolute average error = 6.414E-1

Hill parameters: Amount reach sytemic circ =5.207E3 Time Const =2.074E1 Hill number =1.694E0

Whole blood Clearance from exp fit =1.364E0

PBPK Total Liver Blood Flow = 1.6973042686407191

Estimated First Pass Metabolism fraction = Clearance/PBPK liver flow =8.038E-1 Total amount absorbed = 2.654E4

It can see from this output (and from lower left panel in Figure 9-1), that the total amount reaching the systemic circulation 5,207 micrograms, 26% of the 20,000 microgram oral dose. As seen in the last two lines, PKQuest makes a rough estimate of the “first pass metabolism” and in this case, the estimated total amount absorbed, correcting for first pass metabolism, is 26,290 micrograms (see Section 10 for details). This is somewhat greater than the actual dose which, of course, is impossible and indicates that PKQuest overestimated the first pass metabolism because it used too large a liver blood flow. But, this estimate suggests that 100% of the nitrendipine was absorbed, and 74% of this was metabolized before reaching the systemic circulation. The assumptions involved in this estimate will be discussed in detail in the next Section 10. Open PKQuest again and “Read” the nitrendipine file. Open the “Method” section and select the “Mixed Nadj = 2” option which is another 3 parameter ( $A$ ,  $T_G$  and  $T_p$ ) absorption function:

$$(9.3) \quad \text{Absorption Rate} = A(e^{-t/T_G} - e^{t/T_p}) / (T_G - T_p)$$

where  $A$  is the total amount. This option will be the focus of the next Section on intestinal absorption. It models the stomach as a well-mixed organ whose rate of release of the drug into the small intestine is exponential and is characterized by the time constant  $T_G$ . The rate of

intestinal absorption is characterized by the time constant  $T_p$  which, as shown in Section 10, can be related to the intestinal permeability of the drug. The “Mixed Nadj = 2” fixes  $T_G$  close to the value set in the “Tgi” box. Running PKQuest with this option (with Plot End time = 150) outputs the following Figure 9-3 of the deconvolution estimate of  $C_{Int}(t)$ . It can be seen that this deconvolution method also provides only a rough fit to the first two points, and differs slightly from the Hill function method (Figure 9-2). (The details of the PKQuest Output, eg, “Permeability” will be discussed in the next Section 10).

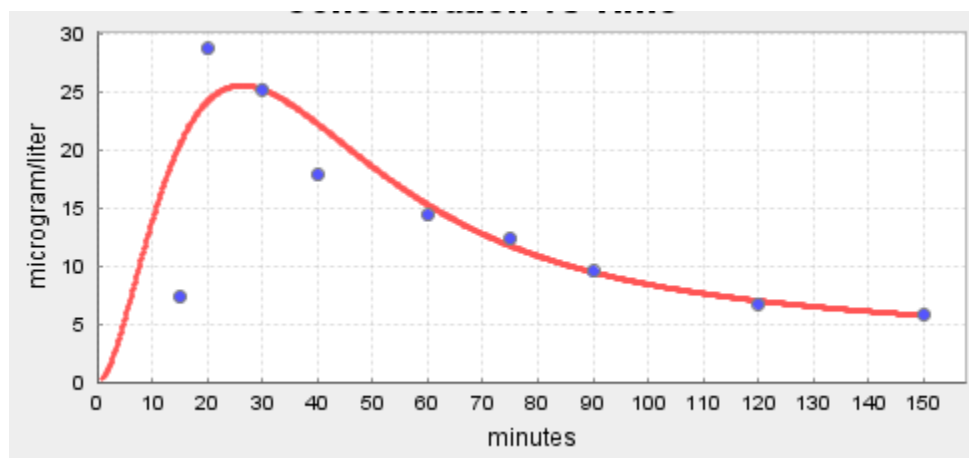


**Figure 9-3 Oral nitrendipine input. Comparison of the experimental versus deconvolution plasma concentration (red line) following oral input using the “Mixed Nadj = 2” deconvolution method.**

Open PKQuest again, “Read” the nitrendipine file, and select the “Veng-Pedersen” deconvolution method. As discussed above, when the “Smoothing” parameter is 0 (as it is by default), this method finds an exact spline function fit to the experimental  $C_{Int}(t)$  data. Running PKQuest outputs the following Figure 9-4:

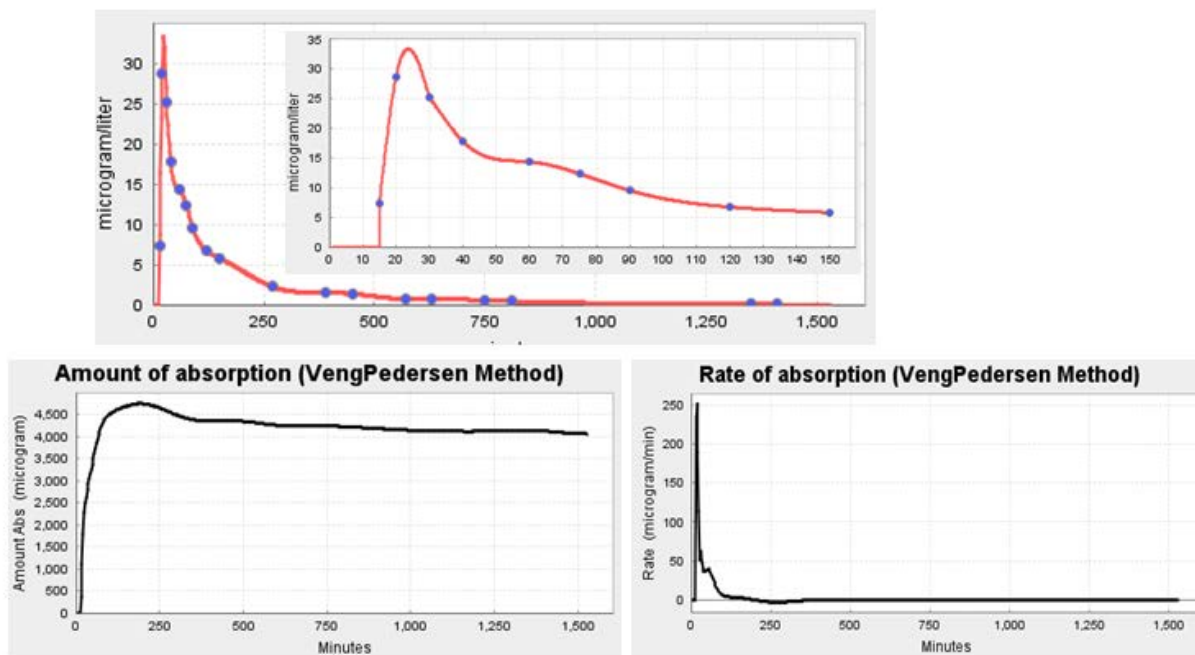


**Figure 9-4 Veng-Pedersen deconvolution for nitrendipine (Smoothing = 0).** The top figure is the experimental versus deconvolution plasma concentration (red line) (Inset: 0 to 150 minutes) for the oral input. The bottom two panels are the prediction amount and rate of systemic absorption.

It can be seen in the top panel that this approach exactly fits the experimental oral plasma data. However, this comes with the handicap of non-physiological oscillations in the absorption rate. Note that there is a physiologically impossible negative absorption rate around 200 -300 minutes that decreases the total Amount absorbed. Running the Veng-Pedersen method again with the “Smoothing” parameter set = 0.1, eliminates the sharp oscillations in the absorption rate but the non-physiological negative absorption is still present.

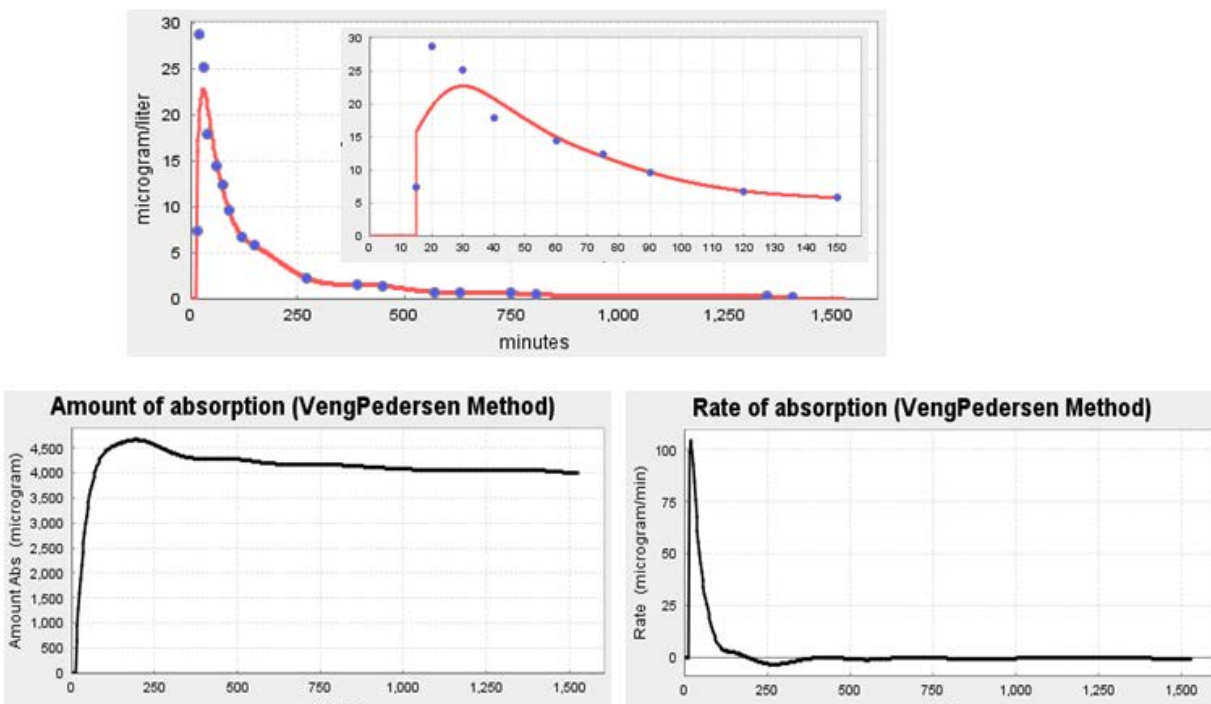
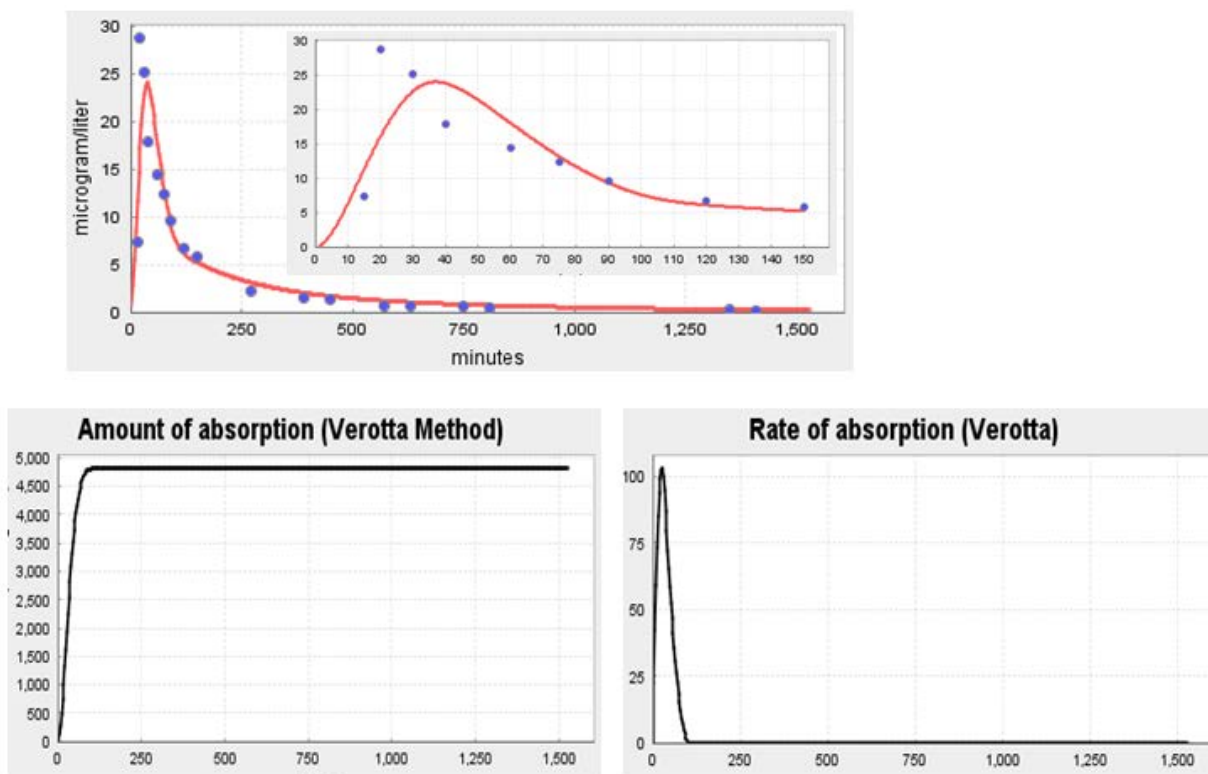


Figure 9-5 Same as Figure 9-4 with Smoothing = 0.1.

Finally, open PKQuest again, “Read” the nitrendipine file, and select the “Verotta” deconvolution method. This is a more mathematically complex spline fitting program that is usually superior to the Veng-Pedersen method. It has the major advantage in that it restricts the absorption rate to non-negative values. A crucial aspect of this method is the set of “Breakpoints” for the splines. Clicking on the “Verotta Breakpoints” button opens the Breakpoints table. The default is 5 breakpoints, spread over the experimental data (at 0, 35, 105, 330, 690, 1,380 and 1,410 minutes). **Note that there are actually 7 time points entered. The initial and final time points are not counted as breakpoints.** Run PKQuest yields the following shown in Figure 9-6.



**Figure 9-6 Verotta deconvolution for nitrendipine using the 5 default breakpoints. The top figure is the experimental versus deconvolution plasma concentration (red line) (Inset: 0 to 150 minutes). The bottom two panels are the prediction amount and rate of systemic absorption.**

It clearly does a poor job of fitting the early time points. One can improve the fit by manually entering breakpoints that closely match the early time data. Rerun the nitrendipine Verotta deconvolution, open the Breakpoints table, input “9” for “# Breakpoints”, and click on the top of table. Note that a default set of 11 points is entered. Replace these by the following list, chosen to fit the important early time data: 0,10,20,30,60,100,420,600,780,1380,1410, and run again, getting the output in Figure 9-7 which provides a better fit to the early time experimental  $C_{Int}(t)$  data. These breakpoints are just one trial set. Presumably, a better fit could be obtained with more fine tuning. This ability to precisely model  $C_{Int}(t)$  through the careful selection of the breakpoints is one of the strengths of the Verotta method. It is also one of its weaknesses since it increases the subjective input in the method. Note that both the Veng-Pedersen and Verotta methods are not quantitatively characterized in the “PKQuest Output” data panel. The rate and amount of the intestinal absorption are summarized in the output plots. The detailed numerical data in these plots is output to Excel files in the PKQuest home directory.



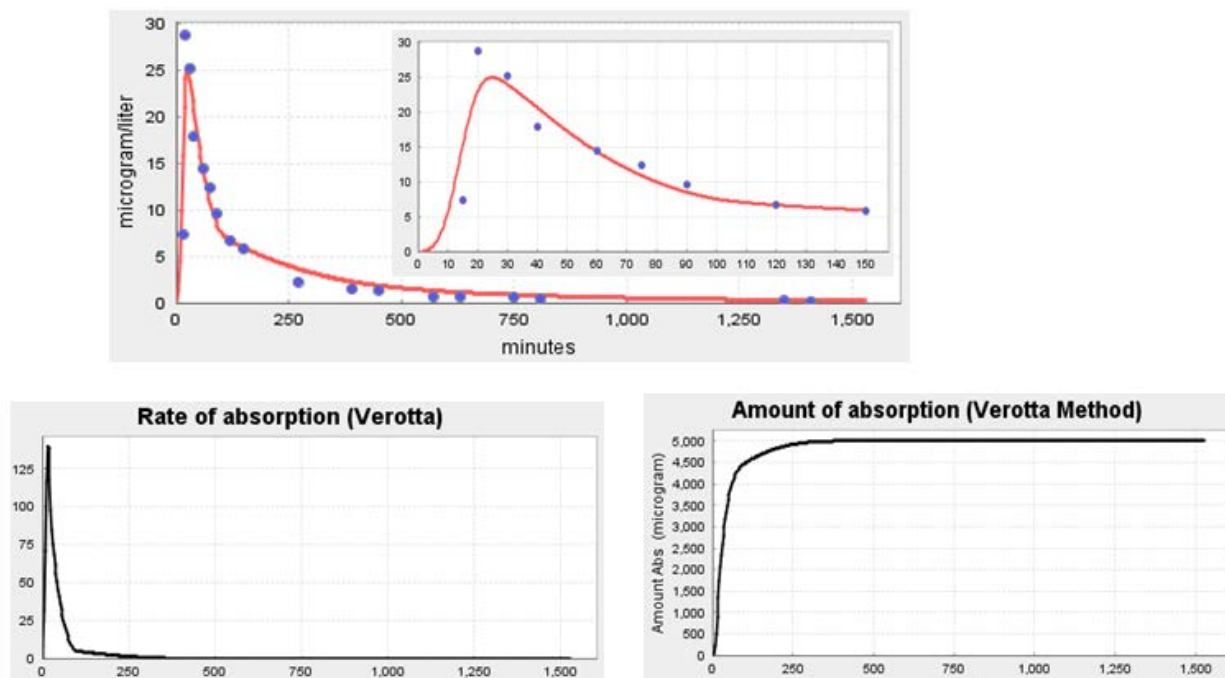


Figure 9-7 Same as Figure 9-6, except with 9 breakpoints.

This 9 parameter Verotta result is the “best” of the 6 deconvolution solutions (Figure 9-1 to Figure 9-7) for intestinal nitrendipine absorption, if “best” is defined in terms of the quality of the fit to the experimental  $C_{Int}(t)$  data. If one wants to force the data to have the form of, eg, a typical intestinal absorption curve, then either the 3 parameter Hill function or 2 parameter Mixed Nadj =2 solution would be regarded as superior. This example has been covered in detail because it illustrates how the different deconvolution methods are implemented in PKQuest and their strengths and weaknesses. All the methods have similar predictions for the absorption rate  $I_{Int}(t)$ , with a rate that goes to 0 after about 100 minutes and a total amount of absorption of about 5100 micrograms. The detailed shape of  $I_{Int}(t)$  depends on the deconvolution method chosen, which is somewhat subjective.

## 9.2 PKQuest Example: Fentanyl dermal patch.

In the previous nitrendipine example, one could make a good guess for the function form of the oral absorption rate. This example looks at the rate of absorption of fentanyl from a dermal patch with a more complicated and uncertain absorption function. It uses the experimental data of Varvel et. al. [8] in which the constant 5 minute IV infusion of 750 mg was used to determine the patch absorption rate by deconvolution. Since the patch was removed at 24 hours, this would be expected to produce a discontinuity in the absorption function.

Starting PKQuest, “Read” and “Select” the “Fentanyl patch deconv.xls” file. The general Verotta deconvolution method is used because one would not expect either the Hill or Mixed Nadj functions to fit the discontinuity produced by removing the patch at 24 hours. There

are 6 Verotta break points, two of which are close to the time the patch is removed (1440 (24 hours) and 1600 minutes). Running PKQuest, one gets the following output (Figure 9-8):

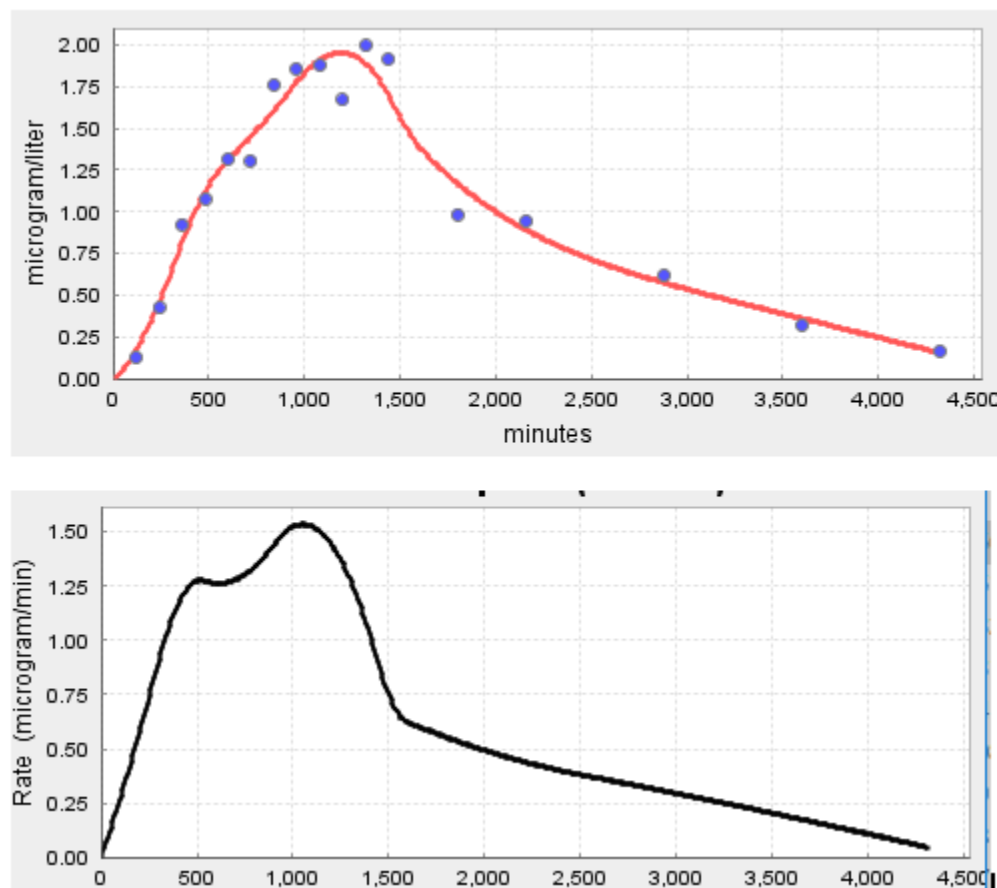


**Figure 9-8** Fentanyl patch absorption rate. Top panel: Verotta deconvolution fit (red line) to the experimental dermal patch data. Bottom panel: Rate of fentanyl absorption from dermal patch. The patch was removed at 24 hours.

It can be seen that the Verotta method provides a good fit to the patch data, with a steep decrease in absorption rate at the time of patch removal (1440 minutes). Note that absorption continues for up to 2 days after removal of the patch. This is thought to represent slow absorption from the skin that equilibrated with the patch in the first 12 hours. Run PKQuest again using either the Hill function or the Veng-Pedersen deconvolution methods and compare the results with the Verotta method.

### 9.3 PKQuest Example: Amoxicillin.

This uses the same serum antecubital PK data of Arancibia et. al. following 500 mg IV amoxicillin as a bolus input (10 second constant infusion) or as an oral 500 mg capsule (after overnight fast) that was used previously in Examples 3.3 and 4.6. Start PKQuest, “Read” and “Select” the “Amoxicillin Example Deconvolution.xls” file. Note that “N Exp” has been set = 2 (2 exponential response function) and the “Hill Function” deconvolution method has been selected. Running PKQuest, we get the following output:

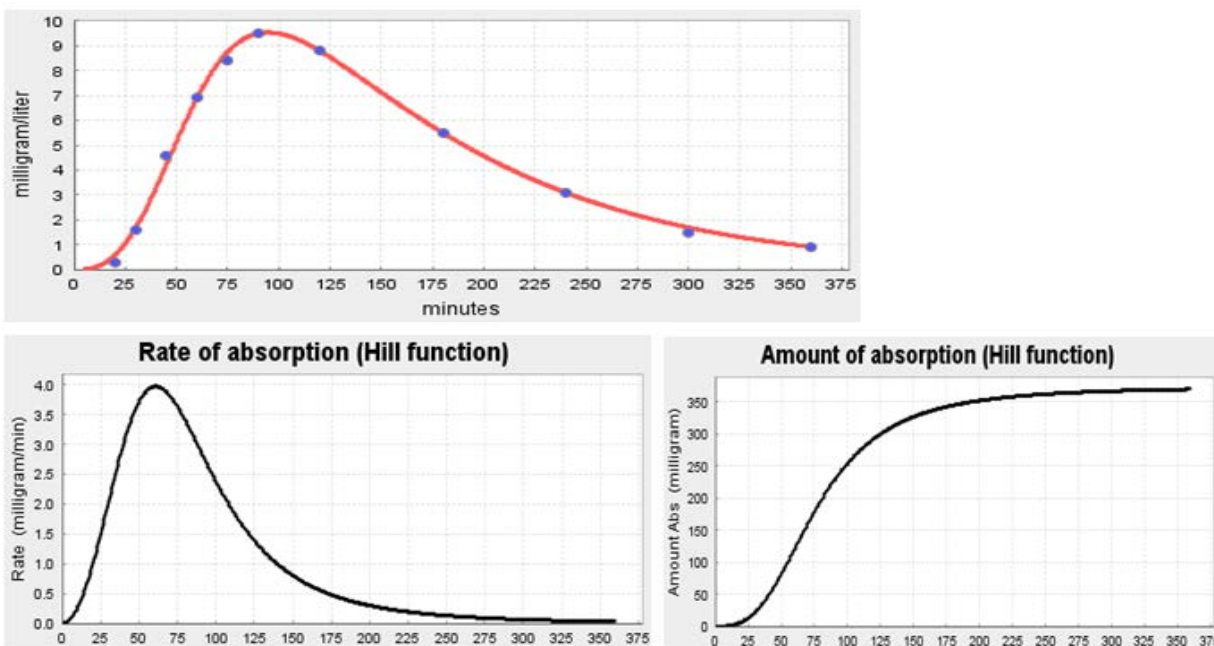


**Figure 9-9** Deconvolution solution for oral absorption of amoxicillin (500 mg capsule) using the Hill Function method. The top figure is the experimental versus deconvolution plasma concentration (red line) for the oral input. The bottom two panels are the predicted amount and rate of systemic absorption.

It can be seen that the Hill Function provides a nearly perfect fit to the plasma concentration data following the oral input.

Extracellular solutes such as amoxicillin, by definition, have very low cell membrane permeability, are highly polar, and, in general, would be expected to have negligible intestinal permeability. However, the  $\beta$ -lactam antibiotics are exceptions to this rule because they can be intestinally absorbed by the small intestinal mucosal peptide transporter. [9] The quantitative PKQuest output is:

Deconvolution - Hill Function fit to experimental data:

Absolute average error = 1.037E-1

Hill parameters: Amount reach sytemic circ = 3.739E2 Time Const = 7.745E1 Hill number = 2.925E0

Whole blood Clearance from exp fit = 2.244E-1

PBPK Total Liver Blood Flow = 1.5563471903307473

Estimated First Pass Metabolism fraction = Clearance/PBPK liver flow = 1.442E-1 Total amount absorbed = 4.369E2

The total amount that reaches the systemic circulation is 374 mg, 75% of the 500 mg oral dose. Remember, this is the amount reaching the systemic circulation and it might be less than the amount absorbed if there is significant first pass metabolism. Note that at the bottom of the above output, there is the line:

Estimated First Pass Metabolism fraction = Clearance/PBPK liver flow = 1.442E-1 Total amount absorbed = 4.369E2

PKQuest uses the  $CL_{ss}$  determined from the IV input and estimates what the total absorption would be **assuming that this  $CL_{ss}$  is hepatic**. However, amoxicillin, like most other extracellular solutes, is cleared primarily by renal clearance and has negligible hepatic clearance. Thus, this estimate is not applicable and the total amount absorbed should be equal to the amount that reaches the systemic circulation (= 374 mg). It is because of the peptide transported that amoxicillin (and other  $\beta$ -lactam antibiotics) have clinically effective oral absorption (75% for amoxicillin).

#### 9.4 Exercise: Propranolol.

Use the experimental IV and oral absorption data of Olanoff et. al. [10] to determine the rate of systemic absorption of propranolol by deconvolution. The average subject weight was 82 kg. The oral dose (80 mg = 80,000 microgram gelatin capsule, dideuterium-labeled) and the IV dose (7 minute constant infusion of 0.1 mg/kg or 8,200 microgram/82 kg) were given simultaneously, using a labeled propranolol for the oral dose. The average plasma concentration (microgram/liter) vs time (min) data for the IV and oral inputs are listed below:

IV		Oral	
Time	Conc	Time	Conc
17	30.5039	30	9.145374
37	22.08921	60	44.62332
67	18.90583	90	55.87069
97	17.33999	120	50.94879
127	14.41945	180	36.05339
187	10.44175	300	22.86646
307	7.872635	480	12.99847
487	4.29825	720	7.137842
727	2.485961		

To set up the deconvolution routine, you need to do the following steps after starting PKQuest: 1) Click the “Deconvolution”, “NonPK” and “Fit Vein” check boxes; 2) Input the IV dose into the “Regimen” table (set “Amount” = 8200; “End” = 7, “Site” = 0, “Type” = 1, and also set “Weight” = 82); 3) Copy (Ctrl c) and paste (Ctrl v) the above data into “Vein Conc 1” and “Vein Conc 2” tables, respectively; 4) Set the “Plot/End” = 730; 5) Set the “Amount unit” = microgram.

Start with the “Hill Function” deconvolution method and answer the following questions:

- 1) What is the total amount that enters the systemic circulation for the oral dose?
- 2) It is known from different experiments that propranolol is 100% absorbed. Using this information, what is the percent “First pass metabolism” of propranolol. (Hint, if you did not get a value close to 77%, you did something wrong).

Try playing around with the other deconvolution methods. In the next Section, we will discuss the intestinal absorption and first pass metabolism of propranolol in more detail.

## 9.5 References.

1. Levitt DG: **The use of a physiologically based pharmacokinetic model to evaluate deconvolution measurements of systemic absorption.** *BMC Clin Pharmacol* 2003, **3**:1.
2. Gillespie WR, Veng-Pedersen P: **A polyexponential deconvolution method. Evaluation of the "gastrointestinal bioavailability" and mean in vivo dissolution time of some ibuprofen dosage forms.** *J Pharmacokinet Biopharm* 1985, **13**(3):289-307.
3. Pedersen PV: **Model-independent method of analyzing input in linear pharmacokinetic systems having polyexponential impulse response II: Numerical evaluation.** *J Pharm Sci* 1980, **69**(3):305-312.
4. Pedersen PV: **Model-independent method of analyzing input in linear pharmacokinetic systems having polyexponential impulse response I: Theoretical analysis.** *J Pharm Sci* 1980, **69**(3):298-305.
5. Verotta D: **Estimation and model selection in constrained deconvolution.** *Ann Biomed Eng* 1993, **21**(6):605-620.
6. Verotta D: **Concepts, properties, and applications of linear systems to describe distribution, identify input, and control endogenous substances and drugs in biological systems.** *Crit Rev Biomed Eng* 1996, **24**(2-3):73-139.
7. Mikus G, Fischer C, Heuer B, Langen C, Eichelbaum M: **Application of stable isotope methodology to study the pharmacokinetics, bioavailability and metabolism of nitrendipine after i.v. and p.o. administration.** *Br J Clin Pharmacol* 1987, **24**(5):561-569.
8. Varvel JR, Shafer SL, Hwang SS, Coen PA, Stanski DR: **Absorption characteristics of transdermally administered fentanyl.** *Anesthesiology* 1989, **70**(6):928-934.
9. Brandsch M: **Transport of drugs by proton-coupled peptide transporters: pearls and pitfalls.** *Expert Opin Drug Metab Toxicol* 2009, **5**(8):887-905.
10. Olanoff LS, Walle T, Cowart TD, Walle UK, Oexmann MJ, Conradi EC: **Food effects on propranolol systemic and oral clearance: support for a blood flow hypothesis.** *Clin Pharmacol Ther* 1986, **40**(4):408-414.

## 10. Intestinal absorption rate and permeability, the “Averaged Model” and first pass metabolism.

In the preceding section, the deconvolution method was introduced and illustrated by using it to determine the rate of intestinal absorption. This section will focus specifically on intestinal absorption and discuss a new approach that provides an estimate of the small intestinal mucosal permeability of drugs. In addition, the “first pass metabolism” will be discussed in more detail, including its dependence on liver blood flow and how it can be estimated using deconvolution.

In previous sections we have predicted a drug's PK based on its molecular structure – in particular if it is highly polar than it has the characteristic PK of extracellular solutes (Section 5) and, if it is highly lipid soluble, then it has the characteristic lipid soluble PK (Section 7). There is a large research effort devoted to extending these qualitative results to detailed quantitative predictions of a drug's PK and pharmacodynamic properties based just on its structure, ie, “Quantitative Structure-Activity Relationship” (QSAR) modeling. This is obviously of particular importance in the field of medicinal chemistry where it plays an important role in the selection of drug candidates. One subset of QSAR is directed to predicting the rate of intestinal absorption of a drug based on its structure. The rate limiting factor in this absorption is the permeability of the small intestinal epithelial cell layer. There are currently two different quantitative measurements that are used to characterize this permeability: 1) the in-vitro permeability of cultured “Caco-2” monolayers, or 2) the fraction of the drug that is orally absorbed in humans. As discussed below, both of these approaches have their limitations. We saw in the previous section that, using deconvolution, one could determine the rate of systemic absorption of a drug. One might expect that one could use this absorption rate to determine the permeability. Surprisingly, this approach has not been previously used. In this section, we will discuss a new approach, referred to as the “Averaged Model” (AM), developed by Levitt [1] for using deconvolution measurements to determine a drug's intestinal permeability.

Since the derivation is somewhat involved and it is not necessary to know these details in order to use this technique, a brief summary of all the steps that are required to determine P using the AM model will be provided here, with the detailed derivation in the following section. Step 1) Assume that the rate of systemic absorption ( $R_s$ ) of an orally administered drug can be described by the following function and determine the 3 parameters  $M_s$ ,  $T_p$ ,  $T_g$  by deconvolution:

$$(10.1) \quad R_s(t) = M_s [e^{-t/T_g} - e^{-t/T_p}] / (T_g - T_p)$$

where  $M_s$  is the total amount absorbed into the systemic circulation, and  $T_g$  and  $T_p$  are the time constants for gastric emptying and intestinal permeability, respectively. Step 2)  $M_s$  is the

amount that reaches the systemic circulation. For the permeability estimate, we need to know the total amount absorbed, which will be greater than  $M_s$  because of first pass intestinal and hepatic metabolism. From the plasma concentration data for the IV input (used in the deconvolution), determine  $Cl_{ss}$  (eq. (3.1)) and combine this with the PBPK liver blood flow ( $F_L$ ) to estimate  $E_H$ , the amount of drug extracted by the liver in one pass (ie, first pass hepatic metabolism):

$$(10.2) \quad E_H = Cl_{ss} / F_L$$

Step 3) Estimate the fraction of the oral dose that is absorbed from the small intestine ( $F_A$ ) using the relation (see eq. (3.6):

$$(10.3) \quad F_A = M_s / [(1 - E_H)(1 - E_I) \text{Dose}]$$

where Dose is the oral dose and  $E_I$  is the intestinal extraction which is usually assumed to be zero. Step 4) Finally, estimate the small intestinal permeability ( $P$ ) using the following:

$$(10.4) \quad P = r F_A / (2T_p)$$

where  $r$  is the small intestinal radius and a value of 1 cm is usually assumed.

### 10.1 Derivation of the “Averaged Model” (AM).

This section provides a detailed derivation of the AM model and can be skipped if the reader is willing to accept the validity of the above relation between  $T_p$  and intestinal permeability ( $P$ ) (eq. (10.4)). In order to relate the absorption rate to the permeability, one needs a physical model of the factors involved in small intestinal transit and absorption. This is a complex process that will be represented by the following simplified model. Most drug absorption studies are under fasting conditions, when there are only small fluid volumes in the small intestine which is relatively collapsed along its entire length. It is assumed that, for these conditions, there is a constant cross sectional area ( $= \pi r^2$ ), convective flow  $F$ , dispersion  $D$  and mucosal permeability  $P$  along the entire length of the small intestine. For this assumption, the mass balance for the small intestinal drug concentration at a distance  $x$  from the stomach at time  $t$  ( $c(x,t)$ ) is described by the following partial differential equation:

$$(10.5) \quad \pi r^2 \frac{\partial c(x,t)}{\partial t} = \pi r^2 D \frac{\partial^2 c(x,t)}{\partial x^2} - F \frac{\partial c(x,t)}{\partial x} - 2\pi r P c(x,t)$$

As a boundary condition ( $x=0$  and  $x=L$ ) for eq. (10.5), it is assumed that there is a one way convective inflow from the stomach ( $=I_G(t)$ ) and outflow to the large intestine ( $=F_c(L,t)$ ) and that the dispersive transport at the boundary is zero. This is consistent with the one-way property of the pyloric and ileocecal sphincters.  $I_G(t)$  is the rate of gastric emptying and it will be assumed that it can be described by a well stirred compartment drained by a constant convective flow  $F$ :

$$(10.6) \quad I_G(t) = F C_0 e^{-t/T_G}$$

where  $T_G$  is the gastric emptying time constant.  $C_0$  is the initial gastric concentration, which is equal to:

$$(10.7) \quad C_0 = \frac{\text{Oral Dose}}{F T_G}$$

Surprisingly, although eq (10.5) is a complicated partial differential equation that is a function of 3 parameters (D, F, P), one can use it to derive a simple, approximate analytic relationship between the absorption rate and the permeability P. Integrating both sides of eq. (10.5) from 0 to L (the small intestine length):

$$(10.8) \quad \pi r^2 \frac{d}{dt} \int_0^L c(x,t) dx = \pi r^2 L \frac{dC(t)}{dt} = I_0(t) - I_L(t) - 2\pi r L P C(t)$$

$$C(t) = (1/L) \int_0^L c(x,t) dx \quad I_0(t) = I_G(t) \quad I_L(t) = F c(L,t)$$

where the boundary conditions for eq. (10.5) have been used for  $I_0(t)$  and  $I_L(t)$ . The function  $C(t)$  is the “averaged” concentration over the length of the intestine and  $I_0(t)$  and  $I_L(t)$  are the rate of entering the small intestine from the stomach and leaving to the large intestine, respectively. First, consider the limiting case where the drug is completely absorbed, i.e.  $I_L(t) = 0$ . For this case, eq. (10.8) reduces to:

$$(10.9) \quad V \frac{dC(t)}{dt} = I_0(t) - P S C \quad V = \pi r^2 L \quad S = 2\pi r L$$

where V and S are the small intestinal volume and surface area, respectively. This is identical to the case of a well-mixed compartment of volume V with arbitrary input  $I_0(t)$  and concentration dependent exit  $=PSC$ . Assuming  $I_0(t) = I_G(t)$  (eq. (10.6) and solving eq. (10.9), one obtains the AM equation for the case of 100% absorption:

$$(10.10) \quad C(t) = (\text{Dose}/V) T_p [e^{-t/T_G} - e^{-t/T_p}] / (T_G - T_p) \quad T_p = r / (2P)$$

where  $T_p$  is the “permeability time constant”. The rate of small intestinal absorption ( $R_D(t)$ ) is:

$$(10.11) \quad R_D(t) = P S C(t) = \text{Dose} [e^{-t/T_G} - e^{-t/T_p}] / (T_G - T_p)$$

where the subscript “D” indicates that the entire dose is absorbed. This is an exact result for the limiting case where the solute is completely absorbed.



Now consider another limiting case where the solute is not completely absorbed, but the dispersion  $D$  is so fast that the concentration  $c(x,t)$  is uniform over its entire length, ie, is independent of  $x$  ( $c(x,t) \rightarrow C(t)$ ). In this limit, eq.(10.8) reduces to:

$$(10.12) \quad \begin{aligned} V \frac{dC(t)}{dt} &= I_0(t) - F C(t) - PS C(t) = I_0(t) - \left[ \frac{F + PS}{PS} \right] PS C(t) \\ &= I_0(t) - (PS / F_A) C(t) \end{aligned}$$

using the relation that  $PS/(PS + F)$  is the fraction absorbed ( $=F_A$ ). This is because  $PS C(t)$  is the amount absorbed and  $F C(t)$  is the remainder that is not absorbed and passes into the large intestine. It can be seen that eq. (10.12) is equivalent to eq.(10.9), with the  $P$  replaced by  $P/F_A$ . Thus, it has the same solution (eq.(10.10)), with  $P$  replaced by  $P/F_A$ :

$$(10.13) \quad C(t) = (\text{Dose}/V) T_p [e^{-t/T_G} - e^{-t/T_p}] / (T_G - T_p) \quad T_p = rF_A / (2P)$$

The rate of absorption ( $R_M(t)$ ) is:

$$(10.14) \quad R_M(t) = PSC(t) = M [e^{-t/T_G} - e^{-t/T_p}] / (T_G - T_p) \quad M = F_A \text{ Dose}$$

where  $M$  is the total amount absorbed. Note that eq. (10.14) is also applicable to the case where there is complete absorption ( $R_D(t)$ , eq. (10.11)) and  $F_A = 1$ .

As shown above, eq. (10.14), with  $T_p = rF_A/(2P)$ , provides an exact description of the intestinal absorption rate for two limiting cases: 1) complete drug absorption; and 2) rapid luminal dispersion. It will be assumed that eq. (10.14) is a good approximation for  $R_M(t)$ , in general, under all conditions. The will be referred to as the ‘‘Averaged Model’’ (AM) assumption. The accuracy of this assumption was checked by comparing its predictions with the exact numerical solution to the partial differential eq. (10.5). It was shown that for the normal human small intestinal dispersion rate, eq. (10.14) is surprisingly accurate, with the permeability  $P$  determined from the AM model differing from the exact  $P$  by at most 20%, over the entire range of experimental interest where from 1% to 100% of the dose is absorbed.[1]

There is still one more step involved in relating the deconvolution absorption rate ( $I_{\text{Int}}(t)$ ) to the intestinal permeability. The rate  $R_M(t)$  is the rate that solute crosses the intestinal luminal membrane while  $I_{\text{Int}}(t)$  is the rate that the solute enters the systemic circulation which may be less than  $R_M(t)$  if there is significant hepatic metabolism (ie, ‘‘first pass metabolism’’) that occurs before reaching the systemic circulation. Assuming a linear system, the amount entering the systemic circulation ( $M_S$ ) is related to the  $M$  of eq. (10.14) by (see eq. (3.6)):

$$(10.15) \quad M_S = (1 - E_I)(1 - E_H)M = (1 - E_I)(1 - E_H)F_A \text{ Dose}$$

where  $E_I$  and  $E_H$  are the intestinal and hepatic fractional extraction, respectively and  $F_A$  is the fraction absorbed. Although the intestinal extraction ( $E_I$ ) is usually assumed to be negligible,

there are some drugs where it has been reported to be significant.[1]  $E_I$  is difficult to measure and is usually neglected. In contrast, the hepatic extraction ( $E_H$ ) can approach 100% and must be accounted for in determining  $P$ . Fortunately, it is possible to estimate  $E_H$  directly during the deconvolution procedure. Deconvolution uses the plasma concentration following a known IV input to determine the system response function. This same concentration data can be used to determine the clearance ( $Cl_{ss}$ , eq.(3.1)). Using the definition of clearance (eq. (3.20)) and assuming that it is entirely hepatic (see eq. (3.10)):

$$(10.16) \quad E_H = \frac{Cl_{ss} C_A(t)}{F_L C_A(t)} = Cl_{ss} / F_L$$

where  $F_L$  is the liver blood flow (portal plus hepatic).

This completes the derivation of the AM approach for determining the intestinal permeability  $P$  from the deconvolution absorption rate for an oral drug ( $I_{int}(t)$ ). To summarize the steps involved: 1) Assume that  $I_{int}(t)$  is of the form of eq. (10.14) with  $M$  replaced by  $M_S$ , the total amount absorbed into the systemic circulation and determine the 3 parameters  $M_S$ ,  $T_P$  and  $T_G$  by deconvolution. 2) Determine  $Cl_{ss}$  from the IV input and estimate  $E_H$  from eq. (10.16). 3) Using  $M_S$ ,  $E_H$  and the known oral Dose and assuming  $E_I = 0$ , determine the fraction absorbed,  $F_A$ , from eq. (10.15). Finally, using  $T_P$  and  $F_A$ , estimate  $P$  from eq. (10.13):

$$(10.17) \quad P = r F_A / (2T_P)$$

This last step requires an estimate of  $r$ , the small intestinal radius. This is the effective radius that was used in the derivation to determine the intestinal cross section and surface area. A value of 1 cm was assumed by Levitt [1] for the fasting conditions under which most drug studies are carried out. The other parameter required is  $F_L$ , the liver blood flow used in eq. (10.16). PKQuest uses the default PBPK hepatic flow of 1.575 liters/min for the standard 70 kg, 21% fat subject. (This is the sum of the PKQuest “portal” plus “hepatic” flow). However, this is just approximate and liver blood is variable, increasing after meals, and is decreased by some drugs, such as beta blockers (see propranolol example below).

There is one additional complication. Since eq (10.14) is symmetrical in  $T_P$  and  $T_G$ , there is no way, a priori, to distinguish them. For the large series of drugs investigated by Levitt, only drugs that were administered in oral solutions that would not have any dissolution time delay were used. Since it known that the gastric time constant  $T_G$  for these drugs should be about 10-15 minutes, the time constant in this range can be assigned to  $T_G$ . In more general cases one will have to make some assumption about the rate of gastric emptying in order to be able to assign a value to  $T_P$ .

## 10.2 Small intestinal permeability: correlation with $P_{\text{oct/w}}$ , Caco-2 monolayer permeability and fraction absorbed.

Levitt [1] used this AM method to catalog the small intestinal permeability ( $P$ ) and fraction absorbed ( $F_A$ ) during normal human drug absorption of 90 drugs with varying physical-chemical properties. This section will present a brief survey of these results. The most accurate measurements of human small intestinal permeability are the single-pass jejunal perfusion results of Lennernas and colleagues.[2] These provide direct measurements of  $P$  in a perfused jejunal segment in conscious humans. Currently, they have published the jejunal permeability for 28 drugs.

Figure 10-1 shows a log-log plot of the AM versus the perfused jejunal  $P$  for the 8 drugs that were studied by both methods. The dashed line is the line of identity. The black and red points are weak bases and acids, respectively, and the green point is the uncharged solute antipyrine. It can be seen that for most solutes the AM permeability is in good absolute agreement with the direct perfusion permeability. This is surprising, given the many simplifying assumptions in the AM model. It suggests that the AM model provides quantitatively valid estimates of human small intestinal  $P$ . The major exception is the weak acid furosemide (red point) whose AM permeability is 30 times greater than the perfusion permeability. This is probably because, as discussed below, the weak acid has an increased AM model  $P$  in the first section of the intestine (duodenum and proximal jejunum) which has a pH that is more acid than the pH of 6.5 used in the perfusion studies.

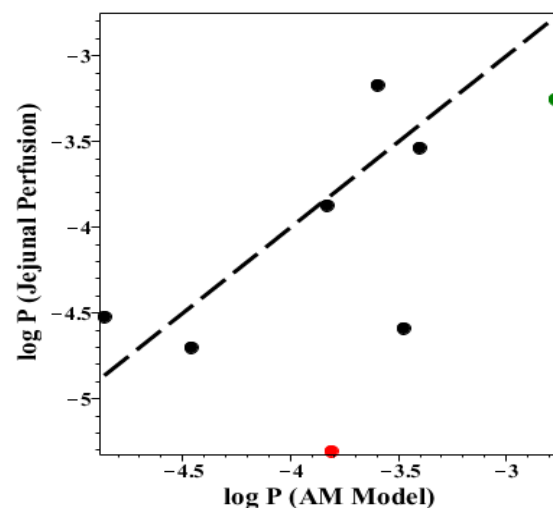


Figure 10-1 Comparison of “Averaged Model”  $P$  versus direct measurement by human jejunal perfusion.

The physical-chemical drug property that is most widely used to predict  $P$  is the octanol/water partition coefficient ( $P_{\text{oct/w}}$ ). The permeability of a drug depends on the rate that it can dissolve into and diffuse through the cellular bilayer membrane. Figure 10-2 shows a diagram of a bilayer lipid membrane of thickness  $L$  separating two well stirred compartments with aqueous concentration  $C_1$  on the left and  $C_2$  on the right. The concentration just inside the lipid membrane is equal to:

$$(10.18) \quad C_1^m = P_{M/W} C_1 \quad C_2^m = P_{M/W} C_2$$

where  $P_{M/W}$  is the membrane/water partition coefficient. The flux  $J$  across the membrane is proportional to the concentration gradient in the lipid region:

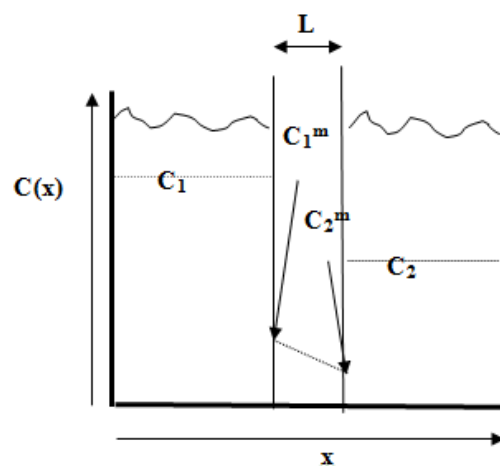


Figure 10-2 Diagram of cell membrane (thickness  $L$ ) separating two well-stirred compartments.

$$\begin{aligned}
 (10.19) \quad J &= D_M (C_1^M - C_2^M) / L = (P_{M/L} D_M / L) (C_1 - C_2) \\
 &= P (C_1 - C_2) \quad \Rightarrow \quad P = P_{M/L} D_M / L
 \end{aligned}$$

where  $D_M$  is the diffusion coefficient in the membrane, and  $P$  is the overall membrane permeability, defined in terms of the aqueous concentration. Since  $D_M$  varies by only a factor of 2 or 3 for most drugs, while  $P_{M/L}$  varies by a factor of thousands or more,  $P$  is primarily determined by  $P_{M/W}$ . Although there is some debate about what lipid is the best representative of the interior of the bilayer cell membrane, octanol seems as good as any [3] and, because of its experimental convenience, has become the standard. Although more complicated approaches that combine  $P_{oct/W}$  with estimates of polar surface area and hydrogen bond donors can improve permeability estimates [4],  $P_{oct/W}$  captures the main features and will be focused on here.

There are some exceptions to this general model. Drugs that mimic biologically active compounds can be either absorbed or secreted by specific membrane transport systems. The most notable is the peptide transporter (PepT) that is a carrier for small peptides (2 or 3 amino acids) and is important for normal protein absorption. Drugs that are designed to mimic peptides, such as the  $\beta$ -lactam antibiotics, can be absorbed at relatively high rates by this system.[5] The other exception is very small molecules (mol. wt < 250) that can be transported through the aqueous intercellular tight junctions. [6] However, these exceptions are rare and  $P_{M/L}$  ( $\approx P_{oct/W}$ ) is the predominate determinant of intestinal permeability.

If a drug is ionizable (acid or base), it is only the neutral, unionized form that partitions in the membrane (or octanol) and  $P_{oct/W}$  depends on the pH. For monoprotic acids (HA), the fraction of the drug that is unionized ( $F_U$ ) in the aqueous phase as of function of pH is described by:

$$\begin{aligned}
 (10.20) \quad HA &\rightleftharpoons H^+ + A^- \quad K_A = \frac{[H^+][A^-]}{[HA]} \\
 F_U &= \frac{[HA]}{[HA] + [A^-]} = (1 + [A^-]/[HA])^{-1} = (1 + K_A/[H^+])^{-1} = (1 + 10^{pH - pK_A})^{-1}
 \end{aligned}$$

where  $K_A$  is the aqueous dissociation constant. Previously in this book, “ $P_{oct/W}$ ” has been used to indicate the “partition” coefficient without distinguishing how it is defined for ionizable solutes. The convention in the PK literature is that  $\log P$  refers to the unionized partition, and  $\log D$  (“distribution”) refers to the total drug partition:

$$\begin{aligned}
 (10.21) \quad \log P_{oct/W} &= \log \left( \frac{[HA]_{oct}}{[HA]_w} \right) \\
 \log D_{oct/W} &= \log \left( \frac{[HA]_{oct} + [A^-]_{oct}}{[HA]_w + [A^-]_w} \right) \approx \log \left( \frac{[HA]_{oct}}{[HA]_w + [A^-]_w} \right) = \log(F_U \frac{[HA]_{oct}}{[HA]_w})
 \end{aligned}$$

where it has been assumed that the octanol concentration of the charged form ( $[A^-]_{\text{oct}}$ ) is zero. One must be careful when looking at literature values of the octanol partition to distinguish which of these is being measured. Substituting eq.(10.20) for  $F_U$ , into eq. (10.21) for  $\log D$ :

$$(10.22) \quad \log D = \log F_U + \log P = \log P - \log(1 + 10^{pH - pK_A})$$

The equivalent relation for monoprotic bases is:

$$(10.23) \quad BH^+ \rightleftharpoons H^+ + B \quad K_A = \frac{[H^+][B]}{[BH^+]}$$

$$F_U = \frac{[B]}{[B] + [BH^+]} = (1 + [BH^+]/[B])^{-1} = (1 + [H^+]/K_A)^{-1} = (1 + 10^{pK_A - pH})^{-1}$$

$$\log D = \log P - \log(1 + 10^{pK_A - pH})$$

The pH varies along the length of the small intestine, from 4.4 in proximal duodenum, to 5.4 in first part of jejunum, to 6.4 in mid intestine and 7.4 in terminal ileum.[1] For weak acids, the unionized fraction, and therefore permeability  $P$ , will be greater in the first part of the small intestine, increasing their rate of absorption. Weak bases will have the opposite, with lower  $P$  in the first part of the small intestine and decreased absorption rate. This means that the AM model assumption of a constant  $P$  is incorrect, and must be accounted for when interpreting the results.

Figure 10-3 show a plot of the  $\log D_{\text{oct/W}}$  at pH 7.4 versus the AM  $\log P$  (permeability) for weak acids (red), weak bases (black), charged (green) and uncharged (blue). Although  $P$  is roughly proportional to  $D_{\text{oct/W}}$ , the correlation is weak, indicating that factors other than octanol partition influence the permeability. At high values of  $\log D$ ,  $P$  levels off because the absorption rate becomes limited by the diffusion rate through the unstirred water and cell layer and is no longer membrane limited. This is illustrated below in the PKQuest Example for acetaminophen. Also, as predicted, the weak acids (red) have a higher  $P$  than the weak bases (black) for the same  $\log D$ .

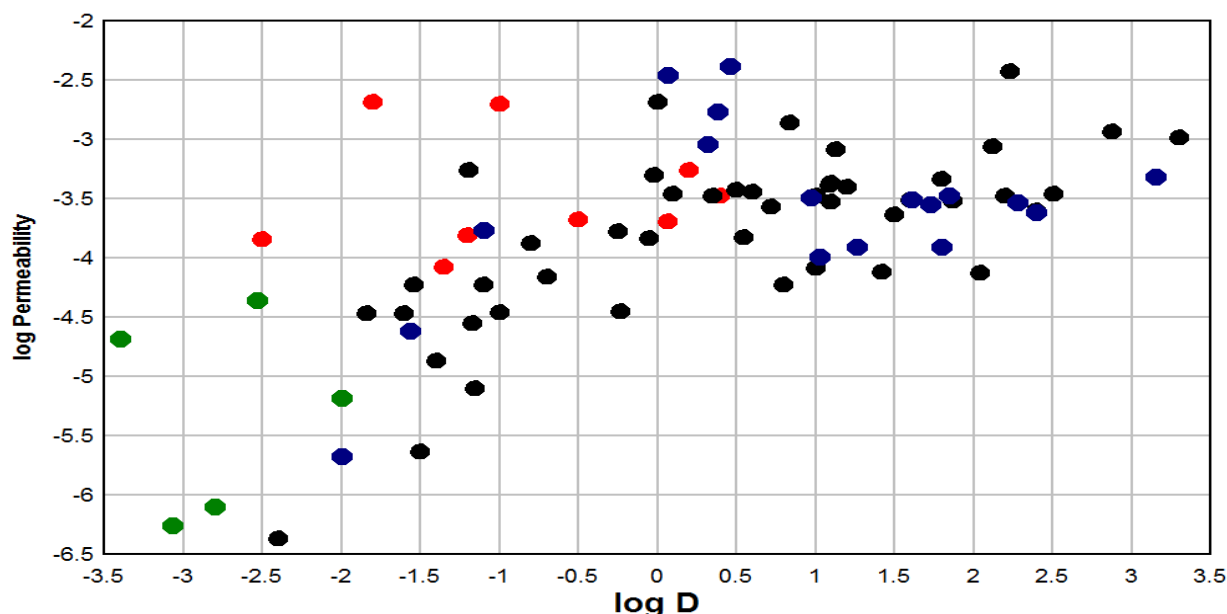


Figure 10-3 Plot of  $\log D$  at pH 7.4 versus  $\log$  the Averaged Method permeability: Weak acids (red); weak bases (black); uncharged (blue) and charged (green).

As discussed in the introduction, the only previously available methods for screening the permeability of a large series of drugs are either the Caco-2 monolayer permeability or the fraction absorbed ( $F_A$ ). As will be shown here, both of these methods have important limitations. The Caco-2 cell line is derived from colorectal cells and, in culture, forms intact monolayers that resemble small intestinal enterocytes with, supposedly, similar permeability properties. The standard procedure is to culture the cells on semipermeable supports fitted into multi-well culture plates, allowing screening of large numbers of compounds. [7] A major limitation of this technique is that there are very large unstirred fluid layers, varying from 564 to 2500 microns, depending on the stirring rate. This is from 12 to 55 times greater than the physiological unstirred layer (see below). This means that the Caco-2 method cannot discriminate between the  $P$  values of solutes with a large membrane permeability because they become diffusion limited.

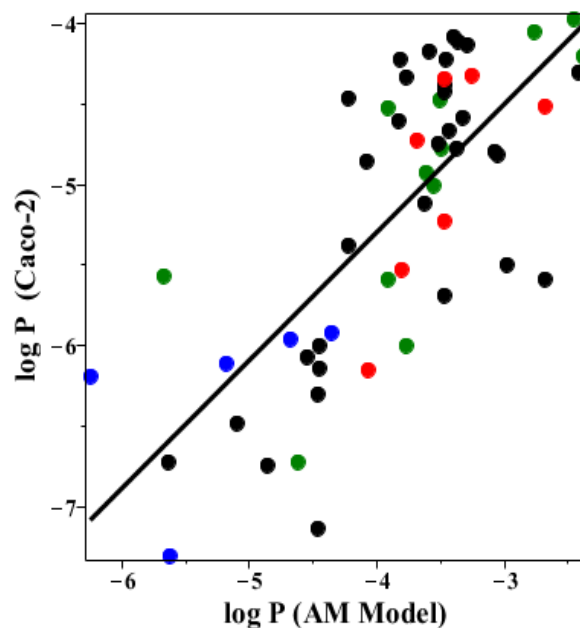


Figure 10-4 Comparison of the log of the permeability determined by AM method versus Caco-2 monolayer. Weak acids (red); weak bases (black); charged (blue) and uncharged (green).

Figure 10-4 compares the log of the Caco-2 permeability ( $P$ ) versus the AM  $P$ . Although there is a strong correlation between the two  $P$  measurements, the absolute values differ markedly. At the high  $P$  end of the plot, the AM  $P$  is 40 times greater than Caco-2  $P$ . This is just what one would predict since these high  $P$  solutes are unstirred layer limited and the Caco-2 unstirred layer is about 40 times greater than the AM layer. The low  $P$  end of the plot is for solutes that are highly polar or charged and, presumably are limited by paracellular tight junction transport. The low Caco-2  $P$  is 6.8 times less than the AM  $P$ , suggesting that the Caco-2 tight junction  $P$  underestimates the physiological  $P$ .

The other QSAR screening procedure is to compare the fraction of the drug absorbed ( $F_U$ ) in humans with the drug structure. Figure 10-5 shows a plot of the AM  $F_U$  as a function of the AM  $P$ . For values of the AM  $P$  greater than about  $10^{-4}$  cm/sec, the drugs are 100% absorbed and, for  $P$  less than about  $10^{-5}$ , absorption drops to 10% or less. Thus,  $F_U$  is a poor marker of permeability because it cannot distinguish different permeability in either the high  $P$  ( $>10^{-5}$  cm/sec) or low  $P$  ( $<10^{-4}$  cm/sec) range. One could argue that  $F_U$  is the only clinically important drug property, so that this is not a serious limitation. However for QSAR

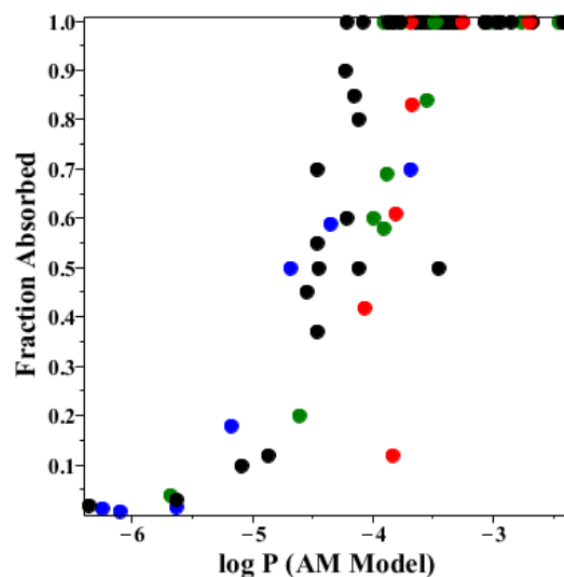


Figure 10-5 Fraction of drug absorbed as function of AM model permeability.

studies it is clearly advantageous to have as wide a range as possible.

The different factors reviewed in this section are discussed in more detail in the following four examples of the PKQuest calculation of the AM absorption rate for a specific drug:

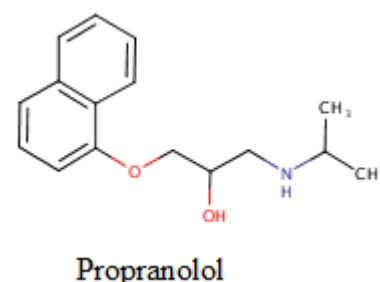
Example 1) Propranolol, a weakly basic drug that is a 100% absorbed and has a high first pass metabolism. Example 2) Acetaminophen, a small uncharged drug with a very high permeability that is limited by diffusion through the aqueous unstirred layer. Example 3) Risedronate, a charged drug with a very low permeability whose absorption curve provides a quantitative measure of small intestinal transit time. Example 4) Acetylcysteine, a weak acid that is absorbed only in the proximal, more acidic section of the small intestine.

### 10.3 PKQuest Example: Propranolol intestinal permeability.

This example will use the same experimental Olanoff et. al.[8] data as in Exercise 9.4. Start PKQuest and “Read” and “Select” the “Propranolol

permeability.xls” file. There are two different versions of the “Averaged Model” deconvolution method implemented in PKQuest: Method 1) “Mixed Nadj =3”: Varies the 3 “Averaged Model” parameters ( $M_S$ ,  $T_P$ , and  $T_G$ , eq. (10.1)) and uses deconvolution to find the set that provides the best fit to the fit to the experimental  $C_{Int}(t)$  data (input in the “Vein Conc2” table). The initial estimates of  $T_P$  and  $T_G$  are determined by the value input into the “Tgi” box. ( Try some different initial values if the fit is poor.) Method 2) “Mixed Nadj =2”:

Use this if you think you roughly know the gastric emptying time constant  $T_G$  and want to force  $T_G$  into this range. Input this value of  $T_G$  into the “Tgi” box. PKQuest will try 3 different value of  $T_G$  ( $T_{gi}$ ,  $1.2 T_{gi}$ , and  $1.4 T_{gi}$ ) and find the values of the 2 parameters  $M_S$  and  $T_P$  that gives the best fit to the experimental  $C_{Int}(t)$  data. For this propranolol case, the 80 mg of propranolol was given in “gelatin” capsules which should dissolve rapidly and one would expect  $T_G$  to be about 15 minutes. Thus, for this example, the “Mixed Nadj=2” option has been selected and  $T_{gi}$  has been set = 15. All the other settings are identical to those used for the Deconvolution method.



Run PKQuest, getting the output in Figure 10-6. The deconvolution fit to the  $C_{Int}(t)$  data using the “Averaged Model” is quite good (red line), (although not as good as the Hill function fit obtained in Exercise 9.4). It can be seen, qualitatively, that the oral absorption rate is rapid, peaking at about 30 minutes, and completed by about 150 minutes, indicating a relatively high intestinal permeability ( $P$ ). The information needed to quantitatively determine  $P$  is listed in the PKQuest output:

Deconvolution - Well Mixed Function fit to experimental data:

Average error = 1.681E0

Well Mixed parameters: Amount reach systemic circ =2.116E4  $T_1$  (min) =2.1E1  $T_2$  = 3.098E1

Whole blood Clearance from exponential fit (liters/min) =1.141E0

PBPK Total Liver Blood Flow (liters/min) = 1.8444649711778518 Hepatic Extraction = 0.6186290710079922  
 Intestinal radius(r) = 1.0 Permeability if completely absorbed (cm/sec)=  $r/(2 \cdot T \cdot 60)$  for T1 =3.968E-4 for T2 =2.69E-4

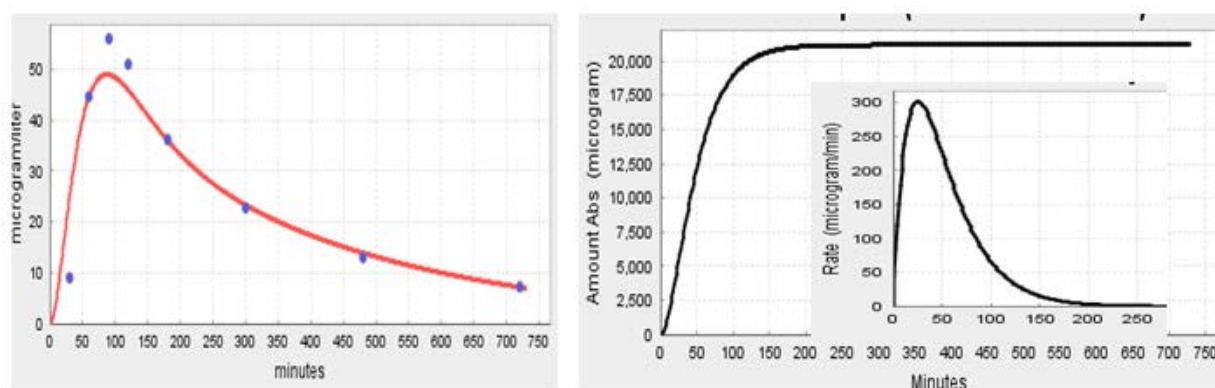


**Figure 10-6** PKQuest “Averaged Model” (Nadj=2) deconvolution output for propranolol. **Left panel:** The deconvolution fit (red line) to the experimental propranolol plasma concentration following the oral 80 mg dose. **Right panel:** Time dependence of the Amount and Rate (inset) of intestinal absorption.

The “Averaged Model” parameters for this plot are:  $M_S$  = “Amount reach systemic circ” = 21,160 micrograms, and the two time constants are  $T_1 = 21$  min and  $T_2 = 31$  minute. (Note that 21 is 1.4  $T_{gi}$ , which is one of the initial trial values). As discussed above, one must guess which of the two time constants corresponds to  $T_P$ . In this case one would expect relatively fast dissolution and gastric emptying of the gelatin capsule, so the  $T_2 = 30.1$  min probably corresponds to  $T_P$ , but this is uncertain. The “Whole blood Clearance from the exponential fit” to the IV input ( $=Cl_{SS}$ ) is 1.141 liter/min. Using the “TBPK total Liver Blood Flow” = 1.84 liters/min for these subjects (average weight = 82 kg), the “Hepatic Extraction” =  $E_H = Cl_{SS}/F_L = 0.618$  (eq. (10.16)). Finally, the small intestinal “Permeability if completely absorbed” (ie,  $F_A = 1$ , eq.(10.3)) using  $T_1$  and  $T_2$  for  $T_P$  is  $39.7 \times 10^{-4}$  cm/sec and  $26.9 \times 10^{-4}$  cm/sec, respectively. Note that PKQuest only outputs  $P$  assuming  $F_A = 1$ . The user must do some independent calculations, as illustrated below, if  $F_A < 1$ .

It can be seen from Figure 10-6 that, although the absorption is rapid and completed by 100 minutes, only a total of 21,160 micrograms reaches the systemic circulation, 27% of the total 80,000 microgram oral dose. Since the absorption is completed before the propranolol should be leaving the small intestine (transit time  $\approx 200$  minutes [1]) one would expect it to be completely absorbed. Assuming complete absorption, there must be a first pass fractional metabolism of 0.73 of the absorbed dose before it reaches the systemic circulation. However, from the PKQuest output, the estimated  $E_H$  is 0.618 (less than 0.73) and, assuming  $E_I = 0$ , the  $F_A$  (eq. (10.3)) is:

$$(10.24) \quad F_A = M_S / [(1 - E_H)(1 - E_I) \text{Dose}] = 21,160 / [(1 - 0.618) * 80,000] = 0.69$$



Quantitative recovery of urine metabolites also indicates that propranolol is completely absorbed [9], ie,  $F_A$  actually equals 1.0 and something is wrong with eq. (10.24).

One possibility is that there is a significant intestinal mucosal extraction ( $E_I$ ), but there is no evidence for this. As can be seen in Table 10-1,  $F_A$  is very sensitive to the assumed liver blood flow ( $F_L$ ) for solutes with large clearances (propranolol  $Cl_{SS} = 1.141$  liters/min for these subjects with average weight = 82 kg). The PBPK value  $F_L$  of 1.84 liters/min is just approximate, and reported values have a large variability. Olanoff et. al. [8] measured the liver blood flow using indocyanine green in

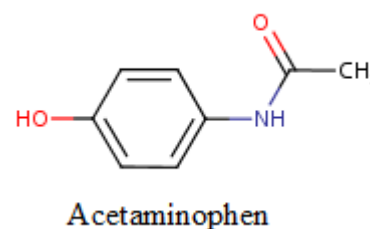
**Table 10-1 Dependence of propranolol hepatic extraction (= first pass metabolism) and fraction absorbed on liver flow.**

Liver Flow	Hepatic Extraction	Fraction Absorbed
1.84	0.62	0.69
1.7	0.65	0.64
1.6	0.71	0.92
1.5	0.76	1.1

the same subjects used for the propranolol absorption studies before the propranolol dose and found an average  $F_L$  of 1.61 liters/min/82 kg. In addition, propranolol has been reported to reduce liver blood by as much as 25%. [10] Thus, the true liver flow in the propranolol absorption studies may be 1.5 liters/min, which, from Table 10-1, would be consistent with complete absorption. Assuming that  $T_P = T_2 = 30.98$  min,  $P = 2.69 \times 10^{-4}$  cm/sec (eq. (10.4)). As this example illustrates, some subjective decisions are needed when deciding on what value of  $F_A$  should be used in the  $P$  estimation. In this case it was easy because there were independent direct measurements showing 100% absorption.

#### 10.4 PKQuest Example: Acetaminophen - very rapid, unstirred layer limited, intestinal permeability.

Acetaminophen has a very high membrane permeability because it is a small (mol. Wt= 151) nonpolar molecule, that is uncharged at pH=7.4 (very weak acid,  $pK_a=9.5$ ) and  $\log P_{oct/W} = 0.46$ . Start PKQuest and Read the “Acetaminophen permeability.xls” file. This uses the data of Ameer et. al. [11] for the plasma concentration following a 5 minute constant IV infusion of 650 mg, or an oral dose (elixir) of 650 mg. Note that the “Mixed Nadj=3” deconvolution method has been selected with a initial guess for “Tgi” = 10 minutes. Run PKQuest, getting the output in Figure 10-7. Qualitatively, the absorption is extremely fast, with the absorption completed in only 50 minutes.



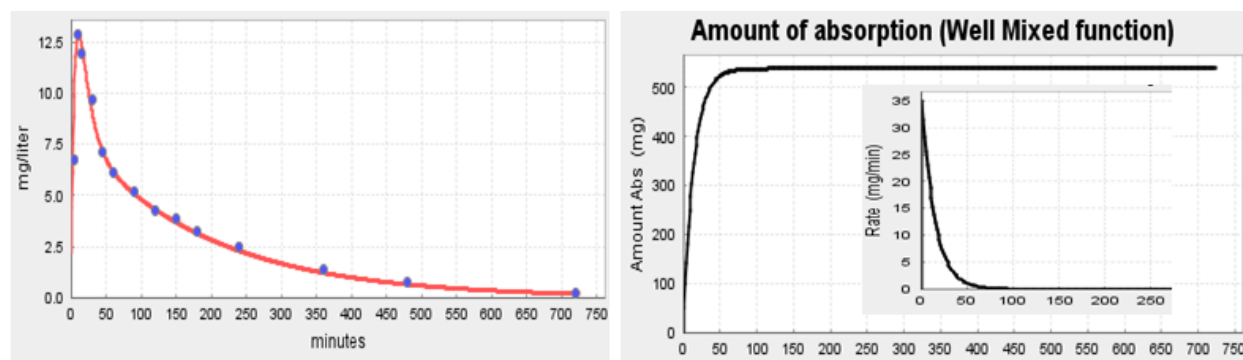


**Figure 10-7** PKQuest “Averaged Model” (Nadj=2) deconvolution output for acetaminophen. Left panel: The deconvolution fit (red line) to the experimental plasma concentration following the oral 650 mg dose. Right panel: Time dependence of the Amount and Rate (inset) of intestinal absorption.

The quantitative results are listed in the PKQuest Output panel:

Deconvolution - Well Mixed Function fit to experimental data:

Average error = 1.496E-1

Well Mixed parameters: Amount reach systemic circ = 5.47E2 T1 (min) = 8.533E-1 T2 = 1.409E1

Whole blood Clearance from exponential fit (liters/min) = 3.246E-1

PBPK Total Liver Blood Flow (liters/min) = 1.6012304421138859 Hepatic Extraction = 0.20271298161697604

Intestinal radius( $r$ ) = 1.0 Permeability if completely absorbed (cm/sec) =  $r/(2 \cdot T \cdot 60)$  for T1 = 9.765E-3 for T2 = 5.913E-4

The “Amount reaching systemic circulation” = 547 mg, which when corrected for the  $E_H$  of 0.2 corresponds to an  $F_A$  (eq. (10.3) of 683 mg, indicating complete absorption of the 650 mg oral dose. Assuming that  $T_1 = 14$  min =  $T_G$ ,  $T_P = T_2 = 0.85$  minutes The small intestinal absorption is so fast that it is essentially limited by the rate of gastric emptying, limiting the accuracy of the intestinal permeability measurement. Using a  $T_P$  of 1 minute,  $P = 8.3 \times 10^{-3}$  cm/sec, 30 times greater than the propranolol permeability. Although this “Averaged Model” result is the first quantitative measurement of the acetaminophen permeability, its rapid absorption is well known and its gastric emptying limitation is the basis of the method that is routinely used to quantitate gastric emptying.[12]

One can use the acetaminophen permeability to estimate the thickness of the “unstirred fluid layer” separating mucosal capillaries from the luminal drug. In the derivation of the “Averaged Model” there is an inherent assumption that the intestinal and villus contractions mix the luminal contents producing a radially uniform concentration  $c(x,t)$ . However, no matter how good the mixing, the hydrodynamics require that there must be a thin unstirred boundary layer next to the mucosal cell surface.[13] This layer become rate limiting for drugs with very high cell membrane permeability. Based on the rate of disaccharide hydrolysis in the human jejunum, Levitt et. al. [14] estimated a thickness of about 35 microns. If one assume acetaminophen absorption is limited by diffusion through this unstirred layer then the permeability  $P$  can be related to the thickness ( $L$ ) of this layer:

$$(10.25) \quad P = D_{UL} / L$$

where  $D_{UL}$  is the diffusion coefficient in the unstirred water layer. Using a  $D_{UL} = 9.1 \times 10^{-6} \text{ cm}^2/\text{sec}$  (the antipyrine water diffusion coefficient at  $37^\circ\text{C}$  [15]) and the acetaminophen  $P = 8.3 \times 10^{-3} \text{ cm/sec}$ ,  $L = 1.1 \times 10^{-3} \text{ cm} = 11 \text{ microns}$ . Since this  $L$  should correspond to the distance between the intestinal blood capillary and the lumen, it should be greater than the mucosal cell thickness of about 25 microns [16]. Thus, this  $L$  seems improbably small. Because the absorption of acetaminophen is limited primarily by gastric emptying ( $T_G = 14 \text{ min}$ ), it is difficult to accurately determine the  $T_P$  and the value of  $T_P = 1 \text{ min}$  may be too small, leading to an overestimate of  $P$ .

### 10.5 PKQuest Example: Risedronate – very low permeability drug, absorption limited by small intestinal transit time.

Risedronate (Figure 10-8) is a small (mol. Wt = 283), highly polar ( $\log P_{\text{oct/W}} = -3.6$ ), relatively strong acid ( $\text{pK}_a \approx 2.0$  [17]) that is charged at intestinal pH (4.4 to 7.4). It is cell membrane impermeable and has a very low intestinal permeability that, presumably, is via the epithelial tight junction aqueous pores. This example uses the experimental data of Mitchell, et. al. [18] for the plasma concentrations following a 0.3 mg, 60 minute constant IV infusion and a 30 mg oral solution. Start PKQuest and Read the “Risedronate permeability.xls” file. Run PKQuest, getting the output in Figure 10-9.

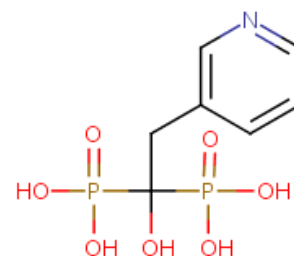


Figure 10-8 Risedronate

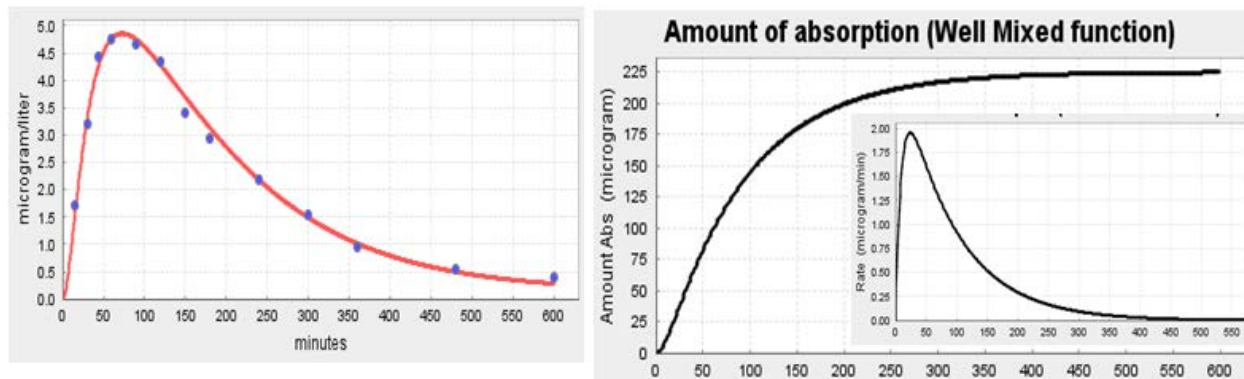


Figure 10-9 PKQuest “Averaged Model” (Nadj=2) deconvolution output for risedronate. Left panel: The deconvolution fit (red line) to the experimental plasma concentration following the oral 30 mg dose. Right panel: Time dependence of the Amount and Rate (inset) of intestinal absorption.

The “Averaged Model” deconvolution of the oral input provides a nearly perfect fit to the experimental plasma concentration (red line). The quantitative results are listed in the PKQuest Output panel:

Deconvolution - Well Mixed Function fit to experimental data:

Average error = 9.198E-2

Well Mixed parameters: Amount reach systemic circ = 2.247E2  $T_1$  (min) = 9.6E0  $T_2$  = 8.751E1

Whole blood Clearance from exponential fit (liters/min) = 1.679E-1  
 PBPK Total Liver Blood Flow (liters/min) = 1.5783557215122588 Hepatic Extraction = 0.1063747854411533  
 Intestinal radius( $r$ ) = 1.0 Permeability if completely absorbed (cm/sec) =  $r/(2 \cdot T \cdot 60)$  for  $T_1 = 8.681E-4$  for  $T_2 = 9.523E-5$

The “Amount reaching systemic circulation” is 225 micrograms, just 0.75% of the 30 mg oral dose. **Also, since risedronate is cleared by renal excretion [18] and is not metabolized, there is no first pass metabolism.** It is important that one be aware that not all the clearance is necessarily hepatic. (For the previous examples, nearly all the clearance was hepatic.) Thus, only 0.75% of the oral dose was absorbed ( $F_A = 0.0075$ ). The gastric emptying time constant =  $T_G = 9.6$  minutes and the  $T_P = 87.5$  minutes. The estimated small intestinal permeability =  $P = rF_A/(2 \cdot 60 \cdot T_P) = 7.1 \times 10^{-7}$  cm/sec. This is 10,000 fold less than the acetaminophen permeability and illustrates the dramatic range in  $P$  that can be determined by this “Averaged Model” approach.

The risedronate absorption rate provides an interesting and novel method to estimate the small intestinal transit time. Since the amount absorbed is negligible, the amount in the small intestine ( $=VC(t)$ ) at any time is simply a balance between the amount that has entered the small intestine by gastric emptying (the integral of eq. (10.6)) and the amount that has entered the large intestine ( $=A_L(t)$ ):

(10.26)

$$VC(t) = \text{Dose}[1 - e^{-t/T_G}] - A_L(t)$$

$$\Rightarrow A_L(t) / \text{Dose} = [1 - e^{-t/T_G}] - T_P [e^{-t/T_G} - e^{-t/T_P}] / (T_G - T_P)$$

where eq. (10.13) has been used for  $C(t)$ . A plot of  $A_L(t)/\text{Dose}$  (the fraction of dose that has passed into the small intestine) versus time for risedronate is shown in Figure 10-10. The small intestinal transit is quite fast, with 50% of the dose entering the large intestine by 70 minutes, and 90% by 216 minutes. This is at the rapid end of the range of transit times reviewed by Davis et.al. [19] The fact that the absorption is complete by 300 minutes also indicates that there is no significant absorption during the 24 hour passage through the large intestine.

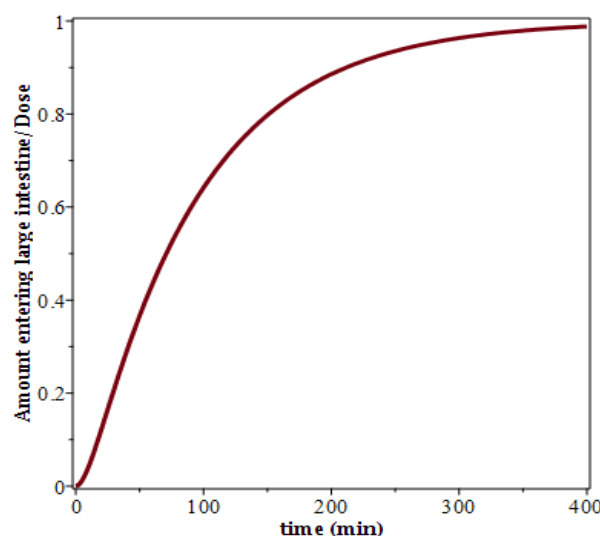


Figure 10-10 Plot of  $A_L(t)/\text{Dose}$  for risedronate

## 10.6 PKQuest Example: Acetylcysteine – weak acid absorbed only in the proximal region of small intestine.

Acetylcysteine (Figure 10-11) is a small (mol. wt. = 163), acid ( $pK_a = 3.25$ ) which is more than 99.99% ionized at pH 7.4. As seen in the

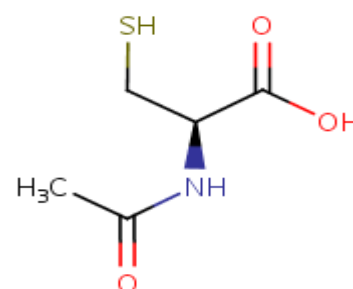
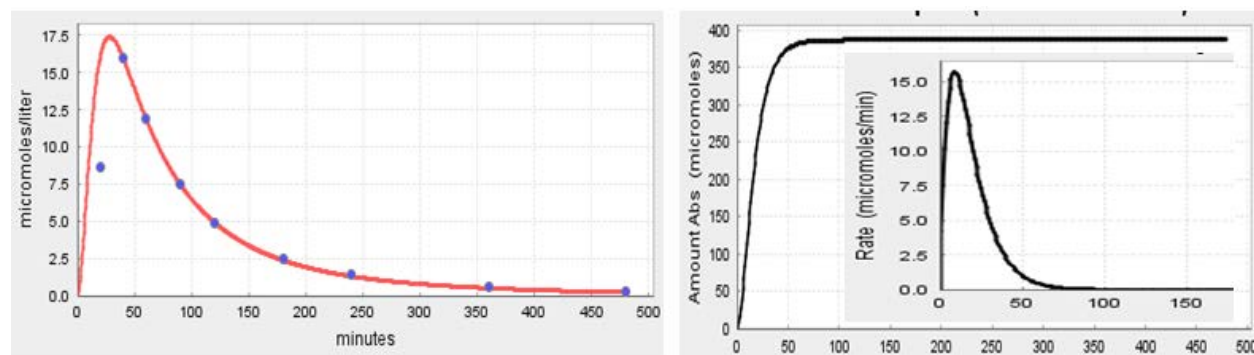


Figure 10-11 Acetylcysteine

above risedronate example in which less than 1% was absorbed, charged solutes should not be absorbed. However, about 10% of acetylcysteine is absorbed and it has a peculiar absorption rate. Start PKQuest, Read “Acetylcysteine permeability.xls”. This file uses the data from Borgstrom et. al. [20] for the N-acetylcysteine following either a 600 mg (=3,676 micromoles), 5 minute IV infusion or a 600 mg oral dose. Figure 10-12 shows the PKQuest output.



**Figure 10-12** PKQuest “Averaged Model” (Nadj=3) deconvolution output for acetylcysteine. **Left panel:** The deconvolution fit (red line) to the experimental plasma concentration following the oral 600 mg dose. **Right panel:** Time dependence of the Amount and Rate (inset) of intestinal absorption.

The quantitative output is:

Deconvolution - Well Mixed Function fit to experimental data:

Average error = 4.364E-2

Well Mixed parameters: Amount reach systemic circ = 3.862E2 T1 (min) = 1.131E1 T2 = 6.947E0

Whole blood Clearance from exponential fit (liters/min) = 2.206E-1

PBPK Total Liver Blood Flow (liters/min) = 1.5745432680786544 Hepatic Extraction = 0.1401181457519654

Intestinal radius(r) = 1.0 Permeability if completely absorbed (cm/sec) =  $r/(2 \cdot T \cdot 60)$  for T1 = 7.37E-4 for T2 = 1.199E-3

The amount reaching the systemic circulation is 386 micromoles, 10.5% of the oral dose. This is also the total amount absorbed since acetylcysteine, like risedronate, is cleared entirely renally so that there is no first pass metabolism.

How does one explain this 10% absorption of an, apparently, charged drug? Table 10-2 lists the fraction of the weak acid acetylcysteine that is in the neutral, non-ionized form as a function of pH (eq. (10.20)). The pH in the small intestine varies over its length, from 4.4 in proximal duodenum, to 5.4 in first part of jejunum, to 6.4 in mid intestine and 7.4 in terminal ileum.[1] Thus, for the first 25 to 35 cm of the intestine, from 1% to 5% of the acetylcysteine will be in its unionized form. Given the high P of similar small unionized molecules such as acetaminophen (see above), this is probably sufficient to account for the 10.5% absorption. It also explains why the absorption is complete by 50 minutes (Figure 10-12) since it only occurs in the first 5 to 10% of the small intestine. This same process is probably involved in the absorption of aspirin (acetylsalicylic acid). It is a slightly weaker acid ( $pK_a = 3.5$ ) and more lipid soluble molecule, allowing it to be about 60% absorbed in the first part of the intestine. [1]

**Table 10-2**

pH	Fraction unionized
3.5	0.359935
4	0.15098
4.5	0.05324
5	0.017472
5.5	0.005592
6	0.001775
6.5	0.000562

## 10.7 References.

1. Levitt DG: **Quantitation of small intestinal permeability during normal human drug absorption.** *BMC Pharmacol Toxicol* 2013, **14**:34.
2. Lennernas H: **Intestinal permeability and its relevance for absorption and elimination.** *Xenobiotica* 2007, **37**(10-11):1015-1051.
3. Diamond JM, Katz Y: **Interpretation of nonelectrolyte partition coefficients between dimyristoyl lecithin and water.** *J Membr Biol* 1974, **17**(2):121-154.
4. Kramer SD: **Absorption prediction from physicochemical parameters.** *Pharm Sci Technolo Today* 1999, **2**(9):373-380.
5. Brandsch M: **Transport of drugs by proton-coupled peptide transporters: pearls and pitfalls.** *Expert Opin Drug Metab Toxicol* 2009, **5**(8):887-905.
6. Levitt DG, Hakim AA, Lifson N: **Evaluation of components of transport of sugars by dog jejunum in vivo.** *Am J Physiol* 1969, **217**(3):777-783.
7. van Breemen RB, Li Y: **Caco-2 cell permeability assays to measure drug absorption.** *Expert Opin Drug Metab Toxicol* 2005, **1**(2):175-185.
8. Olanoff LS, Walle T, Cowart TD, Walle UK, Oexmann MJ, Conradi EC: **Food effects on propranolol systemic and oral clearance: support for a blood flow hypothesis.** *Clin Pharmacol Ther* 1986, **40**(4):408-414.
9. Walle T, Walle UK, Olanoff LS: **Quantitative account of propranolol metabolism in urine of normal man.** *Drug Metab Dispos* 1985, **13**(2):204-209.
10. Lebrech D, Nouel O, Corbic M, Benhamou JP: **Propranolol--a medical treatment for portal hypertension?** *Lancet* 1980, **2**(8187):180-182.
11. Ameer B, Divoll M, Abernethy DR, Greenblatt DJ, Shargel L: **Absolute and relative bioavailability of oral acetaminophen preparations.** *J Pharm Sci* 1983, **72**(8):955-958.
12. Willems M, Quartero AO, Numans ME: **How useful is paracetamol absorption as a marker of gastric emptying? A systematic literature study.** *Dig Dis Sci* 2001, **46**(10):2256-2262.
13. Sugano K: **Aqueous boundary layers related to oral absorption of a drug: from dissolution of a drug to carrier mediated transport and intestinal wall metabolism.** *Mol Pharm* 2010, **7**(5):1362-1373.
14. Levitt MD, Strocchi A, Levitt DG: **Human jejunal unstirred layer: evidence for extremely efficient luminal stirring.** *Am J Physiol* 1992, **262**(3 Pt 1):G593-596.
15. Fagerholm U, Lennernas H: **Experimental estimation of the effective unstirred water layer thickness in the human jejunum, and its importance in oral drug absorption.** *Eur J Pharm Sci* 1995, **3**:247-253.
16. Mackenzie NM: **Comparison of the metabolic activities of enterocytes isolated from different regions of the small intestine of the neonate.** *Biol Neonate* 1985, **48**(5):257-268.
17. Meloun M, Ferencikova Z, Malkova H, Pekarek T: **Thermodynamic dissociation constants of risedronate using spectrophotometric and potentiometric pH-titration.** *Cent Eur J Chem* 2012, **10**(2):338-353.
18. Mitchell DY, Barr WH, Eusebio RA, Stevens KA, Duke FP, Russell DA, Nesbitt JD, Powell JH, Thompson GA: **Risedronate pharmacokinetics and intra- and inter-**

- subject variability upon single-dose intravenous and oral administration.** *Pharm Res* 2001, **18**(2):166-170.
19. Davis SS, Illum L, Hinchcliffe M: **Gastrointestinal transit of dosage forms in the pig.** *J Pharm Pharmacol* 2001, **53**(1):33-39.
  20. Borgstrom L, Kagedal B, Paulsen O: **Pharmacokinetics of N-acetylcysteine in man.** *Eur J Clin Pharmacol* 1986, **31**(2):217-222.

## 11. Non-linear pharmacokinetics - Ethanol first pass metabolism.

A fundamental assumption underlying all the previous sections was that the pharmacokinetics are linear. The experimental definition of linear PK is that, eg, the blood concentration  $C(t)$  is directly proportional to the input  $I(t)$ . If the input is changed to  $2 \cdot I(t)$ , then the blood concentration should be  $2 \cdot C(t)$ . If the system is non-linear, most of the PK concepts discussed previously are no longer valid. The standard compartmental and non-compartment analysis discussed in Sections 2 and 3 are not valid and concepts such as clearance and, possibly, volume of distribution become concentration dependent. The most common reason for non-linearity is that the concentrations become high enough to saturate either the liver metabolic systems or the blood binding sites. The great majority of drugs have linear PK because they are active at very low concentrations (micromolar or less) that are far below the blood protein binding or metabolic enzyme (eg, cytochrome P450) capacity. It is only for drugs that are present at high concentrations that non-linearity becomes apparent. This section will focus on the PK of ethanol where human blood concentrations of 17 millimolar (the legal limit for driving) or greater are routine.

Researchers are so used to linear PK that they can become unaware of the assumptions that they are using when interpreting their results. The most dramatic illustration of this is the large series of publications by Lieber and colleagues [1-5] that, supposedly, documented a large first pass human gastric ethanol metabolism. These studies culminated with an article published in the New England Journal of Medicine (one of the most prestigious clinical journals in the world) entitled "High blood alcohol levels in women – the role of decreased gastric alcohol dehydrogenase activity and first-pass metabolism".[3] The idea that women were more susceptible to alcohol than men because of their lower rates of stomach ethanol metabolism was major news. It was taken up by the New York Times and spread to the evening news. However, in fact, as shown by Levitt and Levitt [6], Levitt et. al. [7] and Wagner [8], gastric first pass metabolism is negligible and these conclusions are entirely an artifact of assuming that ethanol has linear PK. Norberg, et. al. [9] have reviewed the ethanol PK, with a focus on one or 2-compartment modelling.

We have previously discussed how the "Bioavailability" of an oral dose can be determined by comparing the "area under the curve" (AUC) following an oral and IV dose (eq. (3.9)). This result follows directly from the fact that, for a linear system, the AUC is proportional to the dose reaching the systemic circulation. The basic error of Lieber and colleagues was to assume the validity of this for ethanol, with its non-linear metabolism. For example, they compared the AUC following an ethanol dose of 256 millimoles (amount in 1 bottle of beer) given either as a constant 20 minute IV infusion or orally 1 hour after a large meal.[4] They found that the AUC for the oral dose was 28% of that of the IV dose and concluded that the bioavailability was 28%, ie, there was 72% first pass metabolism. It will be



shown that a large fraction of this 28% lower AUC following the oral dose is primarily the result of the difference in input times for this non-linear system.

Before going to the full non-linear PBPK model, it is helpful to start with a simple 1-compartment model which captures the essentials of this non-linearity. Figure 11-1 shows the 1-compartment model modified for a solute that has non-linear metabolism, eg, Michaelis-Menton kinetics characterized by a  $V_M$  and  $K_M$ :

$$(11.1) \quad Q(t) = \frac{V_M C(t)}{K_M + C(t)}$$

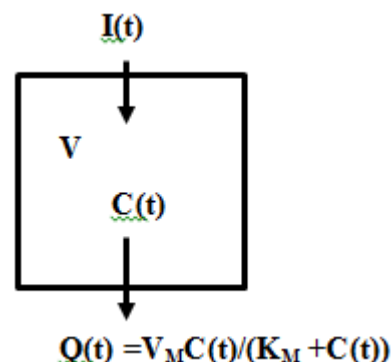


Figure 11-1

(This simple model is only a rough approximation because in the whole animal the rate of metabolism is limited by both  $Q(t)$  and the rate of liver blood flow.) For human ethanol metabolism, the  $V_M \approx 2$  mmol/min/70 kg and the  $K_M \approx 0.5 - 0.1$  mM. [6, 10] Ethanol behaves like a tracer of water, distributing in all the body water with a volume of distribution ( $V$ ) of about 40 liter/70 kg. Using these 1-compartment parameters, Figure 11-2 shows the concentration that results from the 228 millimolar dosage used by Lieber and colleagues given as a constant infusion over either 20 minutes (black), corresponding to the IV input, or 120 minutes (red), corresponding to the input following the oral dose following a meal. It can be clearly seen that, although the identical total dose was used, there is a marked difference in the AUCs which are 286 and 101 for the 20 minute and 120 minute infusions, respectively. That is, because of the non-linear PK, the AUC for a 120 minute infusion (oral dose) is 35% of that for the 20 minute infusion (IV dose) even when there is zero first pass metabolism! That is, with this crude model, of the 72% “first pass metabolism” found by Lieber and colleagues, 65% can be explained simply as a result of the non-linear PK.

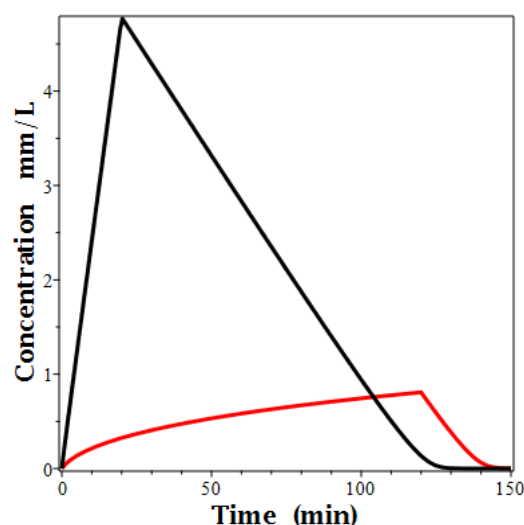


Figure 11-2 One compartment concentration for a constant infusion of 228 mm of ethanol over either 20 minutes (black) or 120 minutes (red)

Lieber and colleagues concluded that the first pass metabolism was gastric, not hepatic, based on experiments in humans comparing the AUC after IV, oral and duodenal infusions. [2] They found that the AUC following the oral dose was 19% of the IV AUC, while duodenal AUC was 75% to the IV AUC (nearly equal), and, therefore, the first pass metabolism must be gastric, and not intestinal or hepatic. These experiments suffer from the same problem as the previous ones. Ethanol should be nearly instantaneously absorbed from the small intestine duodenal infusions while it should be delayed by gastric emptying for the oral dose. (A similar solute, acetaminophen, has a small intestinal absorption time constant of 1 minute, see Section

10.4 ). Thus, duodenal infusion should be equivalent to portal vein infusion. Since the duodenal and IV infusion were both at a constant rate for 20 minutes, one would expect the duodenal AUC to be only slightly less than IV AUC if there was only small first pass hepatic metabolism.

The above results using the 1-compartment model are only a crude approximation to the human PK. Levitt has developed, using PKQuest, the only PBPK model that provides a detailed analysis of the non-linearity of ethanol PK.[10] The rest of this section will focus on these results. An important clinical question is what is the “true” first pass ethanol metabolism (= 1 – bioavailability). The liver clearly can produce significant first pass metabolism. At very low, non-saturating concentrations ( $\ll K_M \approx 0.1$  mM), about 50- 60% of the ethanol entering the liver is cleared. However, as seen in Figure 11-2, even with low doses of ethanol (1 bottle of beer), blood ethanol levels quickly rise to saturating levels ( $>K_M \approx 0.1$  mM). When the blood ethanol levels are saturated, even defining “first pass metabolism” becomes difficult. The usual definition is “the fraction of the absorbed ethanol that is metabolized by the liver before it enters the systemic circulation.” However, this breaks down if there is non-linear metabolism. If the liver metabolism is saturated, any absorbed ethanol that is metabolized will simply displace the metabolism of an equivalent amount of systemic ethanol and the change in total systemic ethanol will be the same as if there was no first pass metabolism. That is, if the blood concentration is high enough to completely saturate the liver enzyme ( $>1$  mM, 10 times  $K_M$ ), first pass hepatic metabolism is close to zero.

The following analysis will use the notation described previously in eq. (3.6) defining the relation between the oral dose ( $D_{oral}$ ) and the amount entering the systemic circulation ( $D_{oral\_sys}$ ):

$$(11.2) \quad D_{oral\_sys} = D_{oral} F_A (1 - E_I)(1 - E_H)$$

where  $F_A$  is the fraction absorbed and  $E_I$  is the intestinal (including gastric) extraction (= intestinal first pass metabolism) and  $E_H$  is hepatic extraction (= hepatic first pass metabolism). For the rapidly absorbed ethanol,  $F_A = 1$ . The procedure used in PKQuest to define and measure both  $E_I$  and  $E_H$  involves the following 3 steps: 1) Develop a PBPK model with the ethanol metabolism described eq. (11.1) with  $C(t)$  equal to the liver tissue concentration and calibrate the model using a known IV infusion. Except for the non-linear metabolism, this is a very simple well characterized PBPK model because ethanol is basically a tracer of water and there is no significant blood or tissue binding or partition. 2) Using this PBPK model, determine the rate and amount ( $=D_{Abs}$ ) of ethanol absorption (amount entering portal vein) following an oral input using the Hill function absorption rate method used previously in PKQuest Example 4.6. This provides a measurement of  $E_I$ , since  $F_A = 1$  and from eq. (11.2):

$$(11.3) \quad D_{Abs} = D_{oral} (1 - E_I) \quad \Rightarrow \quad E_I = 1 - D_{Abs} / D_{oral}$$

3) Using the blood ethanol concentrations following the oral input, find the IV input function and amount ( $D_{oral\_sys}$ ) that would produce these oral blood concentrations. This provides a direct

measure of the rate that the oral dose entered the systemic blood and a definition of the hepatic extraction ( $E_H$ ):

$$(11.4) \quad D_{oral\_sys} = D_{Abs}(1 - E_H) \Rightarrow E_H = 1 - D_{oral\_sys} / D_{Abs}$$

Note that this approach of finding the equivalent IV input that produces the oral blood concentration provides a rigorous definition of  $E_H$  that avoids the difficulties discussed above.

These procedures for characterizing ethanol metabolism and oral absorption are described in detail in the following PKQuest Examples. A brief summary of the results will be provided here. The first set of data that was modeled was that of Jones et. al. [11] who determined the blood ethanol concentration under 3 different conditions in the same subjects, all receiving a total dose of 456 mm ethanol: 1) Following a 30 minute constant IV infusion after an overnight fast; 2) oral dose after an overnight fast; 3) oral dose after a meal. Figure 11-3 shows the PKQuest PBPK model fits to the data for the different inputs. The AUCs for the 3 inputs are 1,200 (IV), 781 (oral fasting), and 411 (oral meal) mM\*min. If one assumed that ethanol had linear PK (and it was 100% absorbed,  $F_A=1$ ), then one would conclude from eqs. (3.9) and (3.10) that the first pass metabolism of ethanol after a meal was 65% ( $1-411/1200$ ).

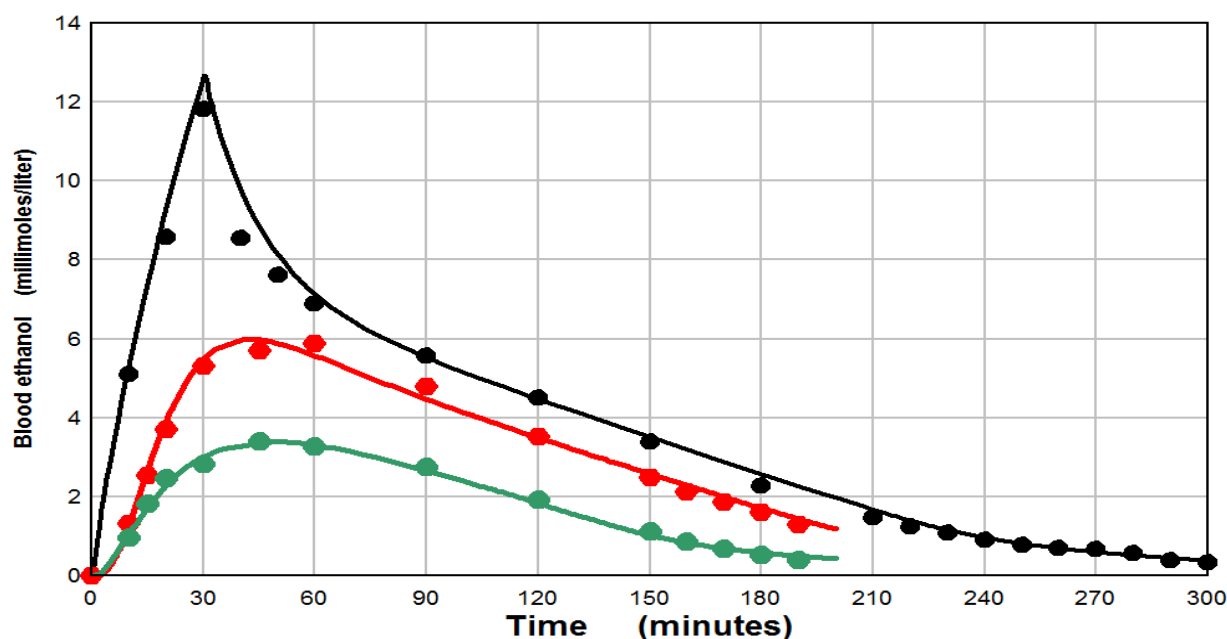
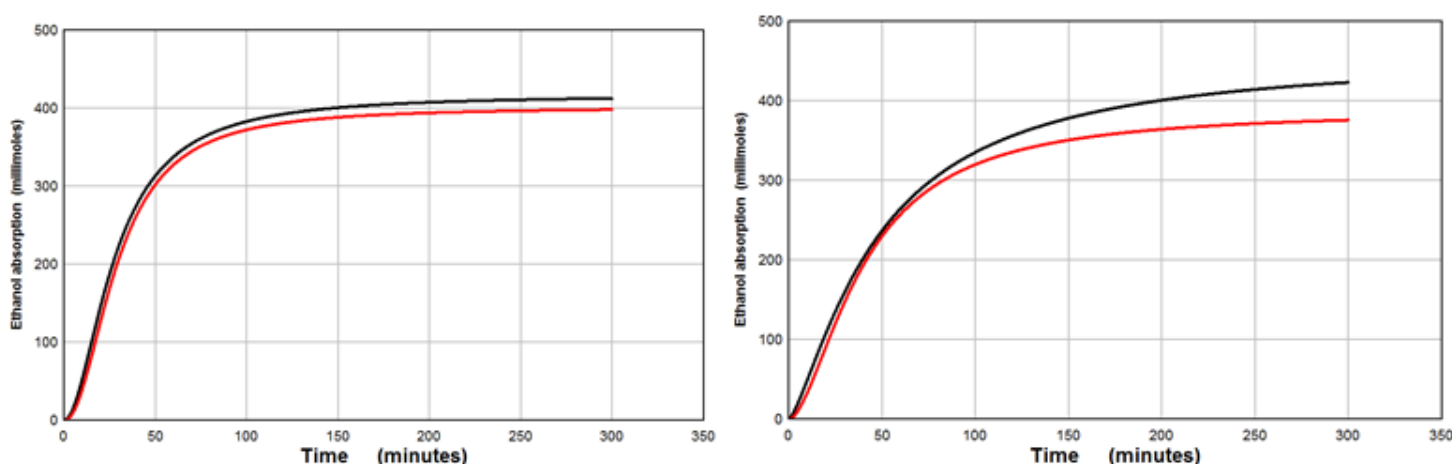


Figure 11-3 Blood ethanol following a 456 mm ethanol dose either IV in fasting subjects (black), oral in fasting subjects (red) or oral after a meal (green). The solid lines are the PBPK model fits to the experimental data.

Figure 11-4 shows the time course of the rate of ethanol absorption from the intestinal (ie, amount reaching portal vein) (Black) and the rate that the ethanol reaches the systemic circulation (ie, after first pass hepatic metabolism) (Red) using the PKQuest non-linear PBPK model. The right panel is for the case where the oral ethanol was in fasting subjects and the left

panel after a meal. The total amount absorbed in the fasting subjects was 417 mm, 8% less than the oral dose of 456 mm. Although this might indicate a small amount of intestinal extraction ( $E_I$ , gastric or small intestine), it may be artefactual. For the fasting case, 401 mm enters the systemic circulation, ie, the first pass hepatic metabolism is only 4%. The absorption is delayed after a meal (right panel) because of delay in gastric emptying. This slower absorption allows more time for metabolism leading to lower blood ethanol concentration (see Figure 11-3), less saturation, and higher first pass metabolism with 388 mm of ethanol reaching systemic circulation (Red) out of the 458 mm ethanol that are absorbed. Thus, the first pass metabolism is 15%, much less than the 65% based on the AUC assuming linear PK.



**Figure 11-4** Time course of amount of ethanol absorbed from intestine (Black) and amount reaching systemic circulation (Red). Left panel: After 456 mm oral ethanol in fasting subjects. Right panel: After 456 mm oral ethanol after a meal.

The second set of data analyzed is that of Dipadova et. al. [12] for the administration of a smaller dose of 228 mm ethanol, half that of Jones et. al. in the above analysis. The ethanol was administered either IV or orally, both of which were after a meal. Figure 11-5 shows the IV (black) and oral blood ethanol concentration experimental data and PKQuest PBPK model fits. The AUCs are 280 (IV) and 93 (oral), which would correspond to a 67% first pass metabolism if the PK were linear. Figure 11-6 shows the corresponding amount of ethanol that is absorbed (black) and reaches the systemic circulation (red) using the non-linear PBPK model. For this lower dose and the slow rate of absorption following a meal because of delayed gastric emptying, there is a larger hepatic first pass metabolism because the blood concentration is lower and the metabolism is not as saturated. The total amount absorbed is 228 mm, which is identical to the oral dose, indicating that there is no gastric or intestinal metabolism, in contrast to the conclusion of Lieber and colleagues. The total amount reaching the systemic circulation is 141 mm, corresponding to 38% hepatic first pass metabolism. In summary, using the data that Dipadova et. al. [12] interpreted as indicating that there was 67% first pass metabolism by gastric mucosa (assuming linear PK), actually corresponds to 38% first pass hepatic metabolism with no gastric metabolism when using the correct non-linear PBPK model.

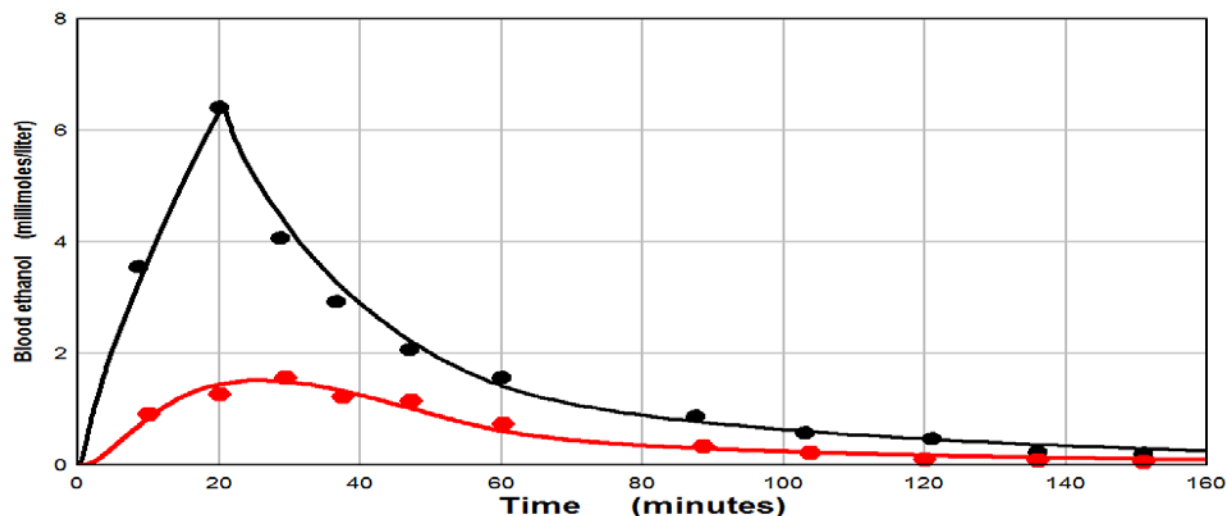


Figure 11-5 Blood ethanol following a 228 mm ethanol dose either IV (black) or oral, both of which were after a meal.

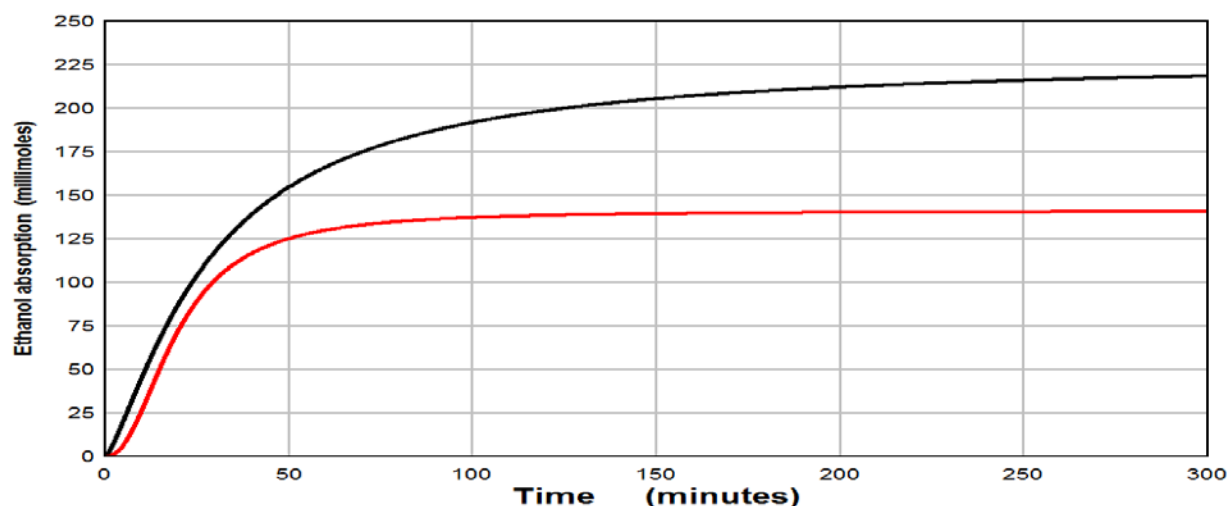


Figure 11-6 Time course of amount of ethanol absorbed from intestine (Black) and amount reaching systemic circulation (Red).

As discussed above, there are three separate steps involved in determining the ethanol first pass metabolism: 1) Use a known ethanol IV input to calibrate the non-linear PBPK. 2) Using the blood concentration following an oral dose, use this PBPK model to determine the rate and total amount or the oral ethanol that enters the systemic circulation. 3) Using this same blood concentration following an oral dose, determine the equivalent rate and amount of an IV infusion that would produce this blood concentration. The differences in the amounts between (2) and (3) correspond to the first pass hepatic metabolism. These 3 steps will be illustrated in the following three PKQuest examples.

### 11.1 PKQuest Example: PBPK model of IV ethanol input.

Start PKQuest and Read the “ethanol IV Example.xls”. This uses the data from Jones et. al. [11] comparing the blood ethanol concentration following an IV dose of 456 mm/70 kg given as a constant 30 minute infusion in fasting subjects versus the blood ethanol following the same oral dose in fasting and fed subjects. There are several things to note about the ethanol PKQuest parameters. Ethanol is basically a tracer of water, so that there is no specific tissue binding. There is a minor difference between water and ethanol in that ethanol has a very small olive oil/water partition of 0.074 [13] and, thus, has a slightly higher (about 2%)  $V_{ss}$ . This is input in PKQuest by checking the “Fat/water partition” box and setting “Kfwat” = 0.074 (the “free plasma fr” and “Blood fat fr” are default values). The ethanol metabolism is input by checking the “Liver Fr. Clear” box. This is the fraction of blood ethanol that is cleared in one pass through the liver **in the limit of zero concentration** (i.e. no saturation). In this case it is 0.52. Finally, checking the “Km” box turns on the non-linear metabolism and the Km is set to 0.05 mM. The 456 IV 30 min dose is input in the “Regimen” table. Note that in the “Plot” “Organs table, the “antecubital” box is checked and the “Conc. Unit” = 2, indicating that the ethanol “blood” (not plasma) concentration is determined, which is typical in ethanol measurements.

Click the “Semilog” option and Run, getting the output in Figure 11-7.

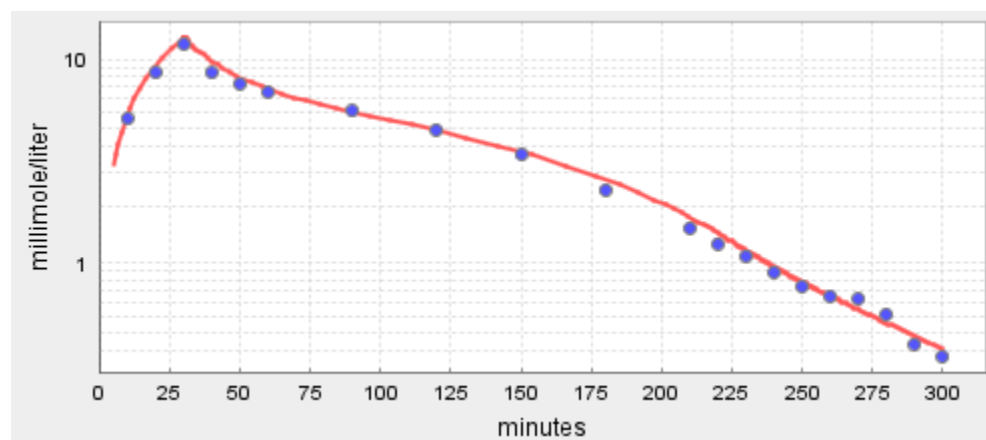


Figure 11-7 Semilog fit of PBPK model to 30 min constant IV ethanol infusion.

It can be seen the standard PKQuest PBPK model provides an excellent fit to the IV data using only two adjustable parameters (the zero concentration fractional clearance and the  $K_M$ ). Near the end of the “PKQuest Output” is the line:

liver Saturating Metabolism:  $V_m c/(c+K_m)$ :  $c$  = free water tissue conc.  $V_m = 1.636E0$   $K_m = 5E-2$ ; Fraction whole blood clearance in limit of 0 conc: = 5.2E-1

This provides a conversion between the “Fraction whole blood clearance in limit of 0 conc” that was input and the more standard liver “ $V_M$ ” in units of mm/min for the subject (in this case, 70 kg). You can check this by unchecking the “Liver Fr. Clear” box and checking “ $V_m$  or intrinsic clr” and entering 1.636. You should get an identical output. Cytosolic liver alcohol

dehydrogenase is the rate-limiting enzyme in ethanol metabolism. This enzyme has marked polymorphism which may account for ethnic variations in ethanol PK. There is some confusion in the literature about the value of  $K_M$ . One sees reports in reviews of about 1 mM [9]. These are based on the use of 1-compartment models.[14] This large a  $K_M$  is clearly not compatible with either the PBPK model used here or a 2-compartment model (liver and rest of body) [6, 7] where the liver cytosolic activity is directly modeled, both of which require a  $K_M$  in the 0.1 mM range. One can visualize the sensitivity of this PBPK model by rerunning PKQuest with varying values of  $K_M$ . Although the data cannot clearly distinguish between a  $K_M$  of 0.05 versus 0.1, values of 0.15 or larger provide significantly poorer fits. The value of  $K_M = 0.05$  was selected here because it provided a better fit than 0.1 for the Dipodova ethanol PKQuest examples (which are more sensitive to  $K_M$  because they use lower ethanol doses).

## 11.2 PKQuest Example: PBPK model of oral ethanol in fasting subject.

Start PKQuest and Read the “ethanol GI fasting example.xls” file. This is for the same subjects used for the IV input, given the same dose (of 456 mm/70 kg) orally after an overnight fast. Everything is identical to the previous file except that the “Regimen” table has been set for a Hill function (“Type = 3”) GI input (“Site = 2). Initially, set the “Amount = 456” (the total dose) and T (=20, Time constant) and N=2 (Hill number). Then check the “Find In..” box. This will run a Powel minimization routine to find the best Hill function parameters (takes about 30 seconds). One gets the output in Figure 11-8. The optimal Hill function Amount (=  $D_{Abs}$ ) is about 417 mm. This is the amount that enters the portal vein, ie, the total amount of intestinal absorption. Since it is about 10% less than the oral dose (456 mm), this would correspond to an  $E_I$  (intestinal extraction) of about 10% (eq. (11.3)). However, given the uncertainty in the model, it is probably not significant.

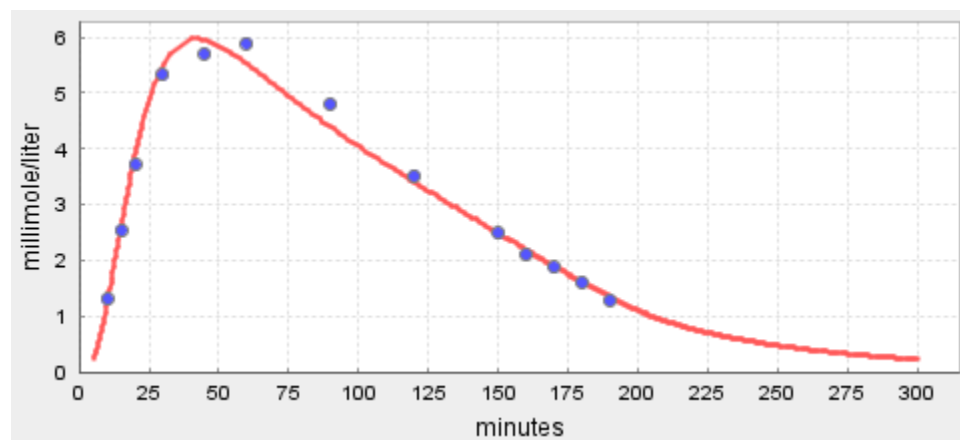


Figure 11-8 PBPK model fit for ethanol oral, Hill function input after overnight fast.

The next step is to find  $E_H$  by finding the IV input that would reproduce the blood ethanol values after the oral input. Start PKQuest and Read the “ethanol GI fasting example.xls” file again. Change the input “Site” to venus (Site = 0) check the “Find In...” box and rerun, getting the output in Figure 11-9. The IV Hill function input amount ( $D_{oral\_sys}$ ) is 401 mm, only slightly less than orally absorbed amount (ie, input to portal vein) determined above of 417 mm. Using eq. (11.4), this would correspond to an  $E_H$  (hepatic extraction) =  $1 - D_{oral\_sys}/D_{abs} = 1 - 401/417 = 0.04$ .

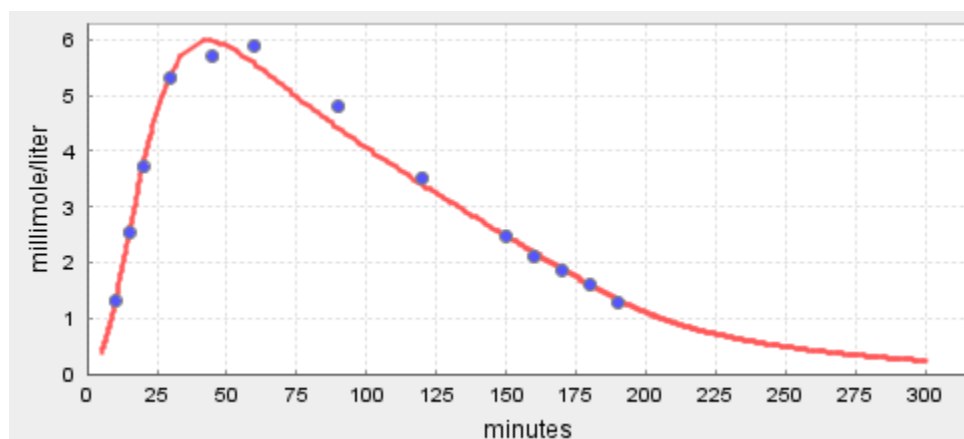


Figure 11-9 PBPK model fit for ethanol Hill function IV input for fasting oral blood data in Figure 11-8.

### 11.3 PKQuest Example: PBPK model of oral ethanol with a meal.

Start PKQuest and Read the “ethanol GI meal example.xls” file. Everything is identical to the IV file, with one major change. It has been shown directly using an “IV ethanol clamp” procedure that the presence of a meal increases hepatic ethanol metabolism by about 25%. [15] Thus, the “Liver Fr. Clear” (in the limit of zero concentration) has been increased from the 0.52 obtained from the IV input in fasting subjects to 0.58. Again, in the “Regimen” table set the “Amount = 456” (the total dose) and T (=20, Time constant) and N=2 (Hill number) and check the “Find In...” box, and “Run”, to find the optimal Hill Function input parameters (it will take about 30 seconds. One gets the output in Figure 11-10. There is an excellent fit to the oral data for input “Amount” of 458 mm (=  $D_{Abs}$ ). This is nearly identical to the total dose of 456 mm and indicates that  $E_I$  (eq. (11.3) is negligible. There is a bit of a fudge factor in this result because the increase in the hepatic metabolism from 0.52 to 0.58 was done with knowledge of the desired end result. However, there is incontrovertible evidence that the meal does raise the metabolism by at least this much. In the analysis of the Dipadova et. al. [12] data discussed above (see Figure 11-5 and Figure 11-6), this fudging is avoided by using the IV infusion after a meal to directly determine this increased hepatic metabolism.



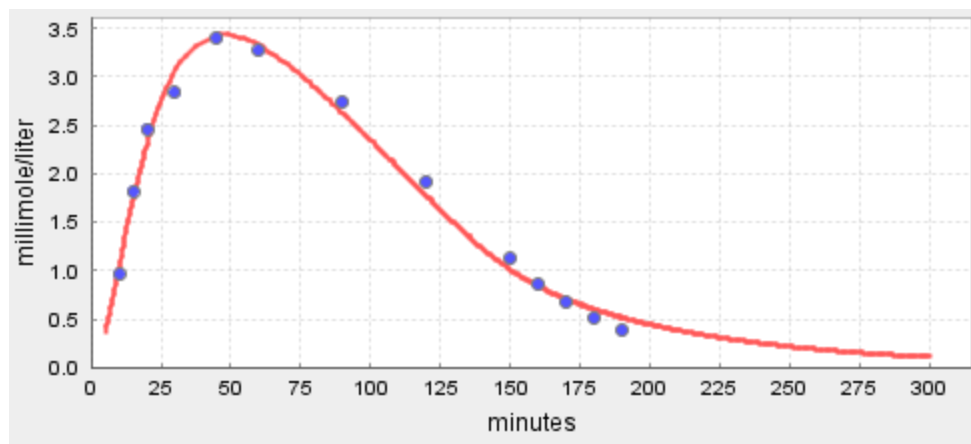


Figure 11-10 PBPK model fit for ethanol oral, Hill function input following a meal.

Start PKQuest and “Read” this same file. Change the input “Site” to IV (site = 0), check the “Find In..” box and rerun. This finds and outputs the IV Hill input function that would produce the blood ethanol concentrations following on oral dose – i.e. the oral ethanol that reached the systemic circulation =  $D_{\text{oral\_sys}}$ . The  $D_{\text{oral\_sys}}$  384 mm, and thus, from eq. (11.4), the first pass hepatic metabolism =  $E_H = 1 - D_{\text{oral\_sys}}/D_{\text{Abs}} = 0.16$ . This  $E_H$  is 4 times larger than the  $E_H$  of 0.04 found above for the same dose of oral ethanol in fasting subjects. This is primarily because the meal slows the gastric emptying and the absorption rate of ethanol, so that the blood ethanol concentration is lower and the metabolism is less saturated. There is also a small secondary effect resulting from the 11% increase in hepatic metabolism following the meal.

## 11.4 References

1. Caballeria J, Baraona E, Rodamilans M, Lieber CS: **Effects of cimetidine on gastric alcohol dehydrogenase activity and blood ethanol levels.** *Gastroenterology* 1989, **96**(2 Pt 1):388-392.
2. Caballeria J, Frezza M, Hernandez-Munoz R, DiPadova C, Korsten MA, Baraona E, Lieber CS: **Gastric origin of the first-pass metabolism of ethanol in humans: effect of gastrectomy.** *Gastroenterology* 1989, **97**(5):1205-1209.
3. Frezza M, di Padova C, Pozzato G, Terpin M, Baraona E, Lieber CS: **High blood alcohol levels in women. The role of decreased gastric alcohol dehydrogenase activity and first-pass metabolism.** *N Engl J Med* 1990, **322**(2):95-99.
4. Julkunen RJ, Di Padova C, Lieber CS: **First pass metabolism of ethanol--a gastrointestinal barrier against the systemic toxicity of ethanol.** *Life Sci* 1985, **37**(6):567-573.
5. Julkunen RJ, Tannenbaum L, Baraona E, Lieber CS: **First pass metabolism of ethanol: an important determinant of blood levels after alcohol consumption.** *Alcohol* 1985, **2**(3):437-441.
6. Levitt MD, Levitt DG: **The critical role of the rate of ethanol absorption in the interpretation of studies purporting to demonstrate gastric metabolism of ethanol.** *J Pharmacol Exp Ther* 1994, **269**(1):297-304.

7. Levitt MD, Li R, DeMaster EG, Elson M, Furne J, Levitt DG: **Use of measurements of ethanol absorption from stomach and intestine to assess human ethanol metabolism.** *Am J Physiol* 1997, **273**(4 Pt 1):G951-957.
8. Wagner JG: **Lack of first-pass metabolism of ethanol at blood concentrations in the social drinking range.** *Life Sci* 1986, **39**(5):407-414.
9. Norberg A, Jones AW, Hahn RG, Gabrielsson JL: **Role of variability in explaining ethanol pharmacokinetics: research and forensic applications.** *Clin Pharmacokinet* 2003, **42**(1):1-31.
10. Levitt DG: **PKQuest: measurement of intestinal absorption and first pass metabolism - application to human ethanol pharmacokinetics.** *BMC Clin Pharmacol* 2002, **2**:4.
11. Jones AW, Jonsson KA, Kechagias S: **Effect of high-fat, high-protein, and high-carbohydrate meals on the pharmacokinetics of a small dose of ethanol.** *Br J Clin Pharmacol* 1997, **44**(6):521-526.
12. DiPadova C, Worner TM, Julkunen RJ, Lieber CS: **Effects of fasting and chronic alcohol consumption on the first-pass metabolism of ethanol.** *Gastroenterology* 1987, **92**(5 Pt 1):1169-1173.
13. Chinard FP, Thaw CN, Delea AC, Perl W: **Intrarenal volumes of distribution and relative diffusion coefficients of monohydric alcohols.** *Circ Res* 1969, **25**(3):343-357.
14. Lee BY, Yoon HK, Baek IH, Kwon KI: **Population pharmacokinetics of multiple alcohol intake in humans.** *Alcohol* 2013, **47**(2):159-165.
15. Ramchandani VA, Kwo PY, Li TK: **Effect of food and food composition on alcohol elimination rates in healthy men and women.** *J Clin Pharmacol* 2001, **41**(12):1345-1350.